Using Autonomous Recording Units for Estimating Detectability in Animal Populations

by

Daniel A. Yip

A thesis submitted in partial fulfillment of the requirements for the degree of

Doctor of Philosophy

in

Ecology

Department of Biological Sciences

University of Alberta

Abstract

Accurate assessment of how animals distribute themselves across the landscape is an essential component of ecological research. Ecologists often conduct surveys to subsample a representative portion of an area of interest and extrapolate their findings to a larger region. Acoustic surveys are frequently used to study a variety of organisms including birds, which rely on acoustic communication and vocalize regularly. The development of autonomous recording units (ARUs) has greatly increased the popularity of acoustic surveys, due to the ability to record surveys and leave recording equipment unattended for extended periods of time. However, variation in the detectability of wildlife is difficult to quantify, and can be strongly influenced by the focal species, the surrounding environment, and method of recording and processing data. Furthermore, count data from ARUs are typically considered to be indices of abundance, and obtaining density requires significantly more effort and data. My objectives were to investigate and quantify variables that influence detectability, determine how variation in detectability influences estimates of relative abundance, describe methods to address and correct for variation in detectability, and develop methods to efficiently estimate animal density using ARUs. I found that detectability is greatly influenced by the surrounding environment and that detectability greatly differs between open and closed vegetation types. Ignoring variation in detectability can lead to estimates of relative abundance in open vegetation types that are more than double that of closed vegetation types, due to increases in the area sampled by ARUs. Furthermore, detectability is influenced by the type of recorder used, and while sometimes equivalent to the detectability of human observers, standardization of detectability is required to properly integrate data from multiple sources. Finally, I presented methods to predict correction factors for different species and vegetation types based on the generalized sound characteristics of their vocalizations or songs. These correction factors should offset differences in detectability between different environmental conditions without the need for calibration studies. I also present a new method for estimating animal density from ARUs by estimating the distance of a vocalizing individual from the sound level measured on an audio recording. I show that these estimates are more accurate and objective than distance estimation in human observers and can provide estimates of animal density through conventional distance sampling. Integrating and standardizing data from ARUs and other sources is important when looking at large-scale ecological patterns. My research contributes to the growing number of studies that investigate variation in detectability of acoustic signals in different environments and the implication on wildlife surveys. I also provide innovative methods which should increase the versatility, quality and accuracy of data obtained from audio recordings and allow ecologists to integrate data from multiple sources to answer questions at different ecological scales.

Preface

This thesis is an original work by Daniel A. Yip. Research methods comply with all ethics and permitting requirements associated with the University of Alberta and the Province of Alberta, Canada (permit no. GP-54843).

Chapter 2 of this thesis was published in 2017 as D. Yip, E. Bayne, P. Sólymos, J. Campbell, and D. Proppe, "Sound attenuation in forest and roadside environments: implication for avian point count surveys", *The Condor: Ornithological Applications*, vol. 119, issue 1, 73-84. I was responsible for idea conception, data collection, analysis, and writing of the manuscript. E. Bayne, J. Campbell, and D. Proppe provided significant input on the conception of the idea and along with P. Sólymos provided feedback during writing of the manuscript.

Chapter 3 of this thesis was published in 2017 as D. Yip, L. Leston, E. Bayne, P. Sólymos, and A. Grover, "Experimentally derived detection distances from audio recordings and human observers enable integrated analysis of point count data", *Avian Conservation and Ecology*, vol. 12, issue 1, article 12. I was responsible for idea conception, data collection, analysis, and writing of the manuscript. L. Leston provided support for data processing and feedback during manuscript preparation. E. Bayne and P. Sólymos provided feedback on idea conception and the writing of the manuscript. A. Grover was an undergraduate student completing a BIOL 499 independent research project which I supervised in 2014-15. She contributed to data collection and analysis.

Chapter 4 of this thesis has been submitted to *Bioacoustics* as D. Yip and E. Bayne, "Correcting for environmental variation in avian detectability using playback experiments" and is currently under review. I was responsible for idea conception, data collection, analysis, and writing of the manuscript. E. Bayne provided feedback on idea conception and writing of the manuscript.

Chapter 5 of this thesis was published in 2019 as D. Yip, E. Knight, E. Haave-Audet, S. Wilson, C. Charchuk, C. Scott, P. Sólymos, and E. Bayne, "Sound level measurements from audio recordings provide objective distance estimates for distance sampling wildlife populations", *Remote Sensing in Ecology and Conservation*, vol. 5, issue 3. Elly Knight and I were jointly responsible for idea conception, data collection, analysis, and writing of the manuscript. E. Haave-Audet was an undergraduate student completing a BIOL 499 independent research project which I supervised in 2017-18. She contributed to data collection and processing, and writing of the manuscript. S. Wilson collected and processed localization data and provided feedback on the writing of the manuscript. C. Scott developed convolutional neural networks used in the analysis and provided input during the writing of the manuscript. C. Charchuk, P. Sólymos, and E. Bayne provided feedback during the writing of the manuscript.

Additionally, methods developed over the course of this project were used to collect data included in manuscripts submitted as R. Hedley, S. Wilson, D. Yip, K. Li, and E. Bayne, "Distance truncation via sound level for bioacoustics surveys in patch habitat", which is currently under review at *Bioacoustics*, R. Hedley, L. McLeod, D. Yip, D. Farr, P. Knaga, K. Drake, and E. Bayne, "Modelling the occurrence of the Yellow Rail (*Coturnicops noveboracensis*) in the context of ongoing resource development in the oil sands region of

Alberta", which is currently under review at *Avian Conservation and Ecology*, J. Congdon, A. Hahn, K. Campbell, E. Scully, D. Yip, E. Bayne, and C. Sturdy, "Acoustic discrimination of predators by black-capped chickadees", which is currently under review at *Animal Cognition*, and J. Congdon, A. Hahn, K. Campbell, E. Scully, D. Yip, E. Bayne, and C. Sturdy, "Can you hear me now? The effect of signal degradation on perceived predator threat in black-capped chickadees", which is under review at *Behavioural Processes*.

Acknowledgements

Thank you to my supervisor, Dr. Erin Bayne, for taking me on as a graduate student and giving me the opportunity to explore ecology as a passion and as a career path. Your ideas, perspective, and guidance have pushed me to become a better scientist than I ever imagined. I would also like to thank my committee members Dr. Peter Sólymos and Dr. Christopher Sturdy for all your input, suggestions, and feedback from which my thesis benefitted greatly. My undergraduate research advisors, Dr. Michael Stock and Dr. Shannon Digweed, were important influences in my decision to pursue a graduate program.

Funding and in-kind support for the development of biodiversity monitoring methods was provided by the National Science and Engineering Research Council of Canada, the Government of Alberta, the Alberta Biodiversity Monitoring Institute, the Alberta Conservation Association, the Northern Scientific Training Program, UAlberta North, Suncor Energy Inc, the Ecological Monitoring Committee for the Lower Athabasca, and the Oilsands Monitoring Program, a collaboration between Environment and Climate Change Canada and Alberta Environment and Parks.

Thank you to Alex MacPhail, Michelle Knaggs, Logan McLeod, Natasha Annich, Jillian Cameron, Cassandra Hardie, Elizabeth Beck, Hedwig Lankau, Darcy Doran-Myers, and all the members of the Bayne and Boutin Labs for helping me haul what seemed to be an infinite number of acoustic recorders through bogs, fens, swamps, and many other equally challenging environments in the name of science. Thank you to Scott Wilson, Jessie Watson, Anjolene Hunt, Justin Johnson, and Jeremiah Kennedy for the lively office banter, Elène Haave-Audet, Lionel Leston, Chris Scott, and Alison Grover for the great collaborations, and a huge thank you in

particular to Elly Knight, Julia Shonfield, Janet Ng, Clayton Lamb, and Eric Nielsen for taking the time to help me with my questions, joining me for impromptu brainstorming sessions, and struggling through thesis-related problems with me over yet another pot of coffee.

Having a well-rounded lifestyle was critical to my success during graduate school. Thank you to Scott Williamson, Hilary Cameron, Nakita Rubuliak, Janet Ng, and countless others for being there during the unplanned overnight bivouacs, suffering through the 15-hour mountain bike rides, summiting mountains with me at midnight in blowing snow and rain, and for accompanying me on all the adventures that turned into more type two fun than we could have thought possible.

Finally, thank you to my family for believing in me over the past six years. Your continued support kept me going through the ups and downs of graduate school and for that I am extremely grateful.

Table of Contents

List of Tables

List of Figures

Chapter 1. Introduction

ACOUSTIC COMMUNICATION IN BIRDS

Acoustic communication, particularly bird song, has a variety of functions including territorial defence, species recognition, mate attraction, and sexual selection. One of the most important functions of bird song is for establishing and maintaining territories. Individuals use bird song to signal that an area is occupied, which has shown to significantly decrease territorial intrusion (Peek 1972). This serves as a deterrence to reduce physical conflict, allowing individuals to conserve energy and resources instead of chasing intruding individuals (Catchpole and Slater 2008). Bird song also plays an important role in species recognition, both for identifying conspecifics and sympatric individuals that may occupy a similar niche. This allows individuals to defend territories from competitors of the same species, or closely related species that may compete for the same resources (Matyjasiak 2004). Species recognition also allows females to identify potential mates of the same species (Clayton 1990).

Bird song also plays an important role in mate attraction and sexual selection. Song is a reliable indicator of male quality, which females use during mate selection in many species. Trade-offs between the time spent singing and foraging means that males in higher quality territories can spend more time singing (Reid 1987). Frequent singing also means higher metabolic costs to an individual as well (Ward et al. 2004). The quality of the actual song is also an honest indicator of mate quality; certain syllables and traits such as frequency range and trill rates can be more costly to perform (Podos 1996). Females respond preferentially to males that consistently perform at physical and physiological limits (Ballentine et al. 2004) as high quality mates can afford the energy expenditure and costs relative to lower quality individuals.

Emphasis on acoustic communication, at frequently and regular intervals, means that bird song can be used as reliable index of presence, abundance, and diversity. In temperate regions, singing patterns follow regular cycles, both daily (i.e. dawn chorus) and seasonally (i.e. breeding cycle in migratory species). Thus, ecologists routinely use bird song as a proxy for population status to answer a multitude of questions related to ecological themes.

ACOUSTIC MONITORING IN ECOLOGY

Making ecological inferences requires accurate assessment of how animals distribute themselves across the landscape. Censusing large areas is logistically and financially unrealistic in most cases, therefore ecologists often conduct surveys to subsample locations believed to be representative of the entire area and extrapolate the results to make inferences about the entire population. Surveys are also used when contrasting animal distribution across different variables or treatments by examining differences in animal occupancy, abundance, density or diversity. Therefore, data that are inaccurate or not representative of the treatment or region of interest could result in masking of biological patterns and inaccurate assessment of abundance and population.

Acoustic surveys are used extensively in ecological research to successfully study a variety of organisms in terrestrial, freshwater, and marine ecosystems. In particular, acoustic surveys targeting avian species are frequently used because many species rely on acoustic communication and will vocalize consistently and at regular intervals (Catchpole and Slater 2008). One of the most widely used methods to sample avian populations is through the use of point counts. Traditionally, human observers travel to predetermined locations and record detections of each species for a specific duration of time. While there are instances where individuals may be detected visually, the majority of avian detections from point counts are often aural, particularly in vegetated environments where visibility is poor (Rosenstock et al. 2002). Therefore, acoustic surveys are a particularly attractive substitute to traditional counts. Data obtained through acoustic surveys can be used to estimate the abundance, density, occupancy, or diversity of local populations and communities.

While the basic requirement for acoustic monitoring is the use of an acoustic sensor and the ability to record the surrounding acoustic environment, one of the biggest technological advances that has popularized its use is the development of autonomous recording units (ARUs). ARUs are acoustic sensors that can be programed to record at set intervals, or on a specific schedule, and can therefore be left unattended in the field for extended durations. Concerns over observers not detecting individuals that are present during field surveys has led to repeated visit approaches to account for variable detection probability (Kéry et al. 2005). ARUs allow for an unlimited number of repeated visits without an increase in labor due to the ability to schedule surveys, while still only having to visit a site twice (once to deploy, and once to pick-up the ARU). ARUs can also be used to sample multiple locations simultaneously, when an insufficient number of field observers are available to cover the same area. Another major benefit is the ability to sample locations that are logistically difficult without requiring an observer be present. For example, ARUs can be deployed during the day in wetlands and scheduled to record at night for nocturnal species when access would be unfeasible.

Finally, the ability to record surveys and store them as a permanent record can reduce observer effects on data collection in two ways. First, the presence of observers in the field can influence animal behavior (Gutzwiller and Marcum 1997). The use of ARUs means an observer will not be present during the survey and any effect of observer presence can be avoided. Second, transcription of audio recordings can reduce observer bias compared to identification of species and individuals in the field. Recordings can be reviewed by multiple observers and as many times as necessary. Unknown or uncommon species can also be checked against reference recordings to ensure accurate identification.

One of the largest disadvantages to using acoustic surveys is storage and processing of audio recordings (Shonfield and Bayne 2017). High quality audio recordings require a relatively high amount of storage space and finding a physical or virtual location to back up and maintain data that is also easily accessible for data processing can be logistically or financially difficult. Processing of audio recordings also takes up considerable time and effort. While acoustic surveys can decrease field effort considerably, raw recordings often require manual interpretation, although methods for computer-based recognition are increasing in use. Finally, the up-front cost along with long-term maintenance (i.e. repairs, microphones, batteries, etc.) for audio recording equipment is significantly more than surveys conducted by human observers. Equipment failure in the field can also go unnoticed for extended periods of time, particularly with ARUs and could lead to extensive loss of data (Shonfield and Bayne 2017).

ACOUSTIC TECHNOLOGY

Early acoustic recording technology consisted of all-purpose field recorders or repurposed commercial audio equipment. These early iterations typically had trade-offs between battery life, on-board data storage, portability, cost, and durability. More recently, commercial wildlife recorders have become readily available such as SongMeter recorders from Wildlife

Acoustics (www.wildlifeacoustics.com) and Swift recorders from the Cornell Lab of Ornithology (www.birds.cornell.edu/brp/swift/). Improvements to these devices have resulted in recording units that are more customizable, have longer battery life, more data storage capabilities, are lighter, more durable, and more affordable, increasing their accessibility and popularity in monitoring programs and in wildlife research. Open-source options such as AudioMoth (Hill et al. 2018) have further increased customizability and affordability.

One of the biggest challenges in dealing with bioacoustic datasets is efficient processing of field recordings. ARUs can generate large volumes of data which must be processed before answering ecological questions. Automated recognition is an approach that involves training a computer algorithm to classify acoustic signals. Each classified signal is assigned a probability value, a measure of how likely a signal is to be the focal or target species. Users can set a pre-defined probability threshold so that only signals of a certain quality are classified for further review. There are several approaches used for automated recognition and species detection, some of the most common including spectrogram cross-correlation (Katz et al. 2016), band-pass filtering (Charif et al. 2010), and convolutional neural networks (Abadi et al. 2015). The increase in processing efficiency relative to manual transcription of acoustic recordings, combined with ease of collecting data using ARUs, makes acoustic monitoring an appealing option for ecological research.

DETECTABILITY

For birds and many other taxonomic groups, imperfect detectability means that only a portion of the target species are counted and can be defined as:

$$p = \frac{c}{N}$$

where c is the number of individuals counted, N is the number of individuals present during a survey, and p is the probability of detection, or detectability (Johnson 2008). When detectability is consistent or variation in detectability is low, count data is strongly correlated the number of animals present and can provide a reliable index of abundance. However, when variation in detectability is high, the value of count data decreases because the relationship between abundance and the number of individuals counted becomes unclear (Johnson 2008, Rigby 2016). Variation in detectability is complicated to account for because variation in the number of counted individuals can covary with the number of animals present and their detectability (Johnson 2008). Therefore, one of the biggest challenges is to separate variation in detectability from changes in abundance, and failing to account for variation in detectability can lead to inaccurate assessment of animal populations.

A variety of methods are used to address variation in detectability such as repeated visits to the same location (Kéry et al. 2005), double observer approaches (Nichols et al. 2000), and modelling the decrease in number of detections with distance from an observer (Buckland et al. 1993). However, a major hurdle when conducting acoustic surveys is controlling for variation in detectability due to differential attenuation of sound signals. Under free field conditions, sound amplitude is expected to attenuate at approximately 6dB for every doubling of distance between the signaler and receiver (Wiley and Richards 1982). However, environmental conditions cause attenuation in excess of what is predicted from free field conditions and is directly related to the environment sound signals travel through. Free field conditions are rarely met outside of laboratory settings and can influence detectability and the resulting estimates of abundance, density, occupancy, or diversity of the target species or community.

Many factors can influence detectability of a signal including the surrounding vegetation characteristics, local atmospheric conditions, species-specific vocalization traits, recording technology used to conduct surveys, and the method used to process audio recordings. Vegetated environments increase scattering, reverberation, and absorption of acoustic signals (Padgham 2004, Pacifici et al. 2008) and local atmospheric conditions change the density of air through which signals propagate (Harris 1966). Vocalization structure also has a large influence on signal propagation and can vary greatly between species. Certain vocalization characteristics can also interact with the surrounding environment, adding further complexity when trying to account for variation. For example, high frequency signals attenuate at a higher rate, and are absorbed more in vegetation environments than open environments relative to low frequency signals (Forrest 1994). Vocalizations resembling pure sine waves can propagate further in vegetated environments (Morton 1975, Brumm and Naguib 2009), but trills are used by species in open environments to maximize signal transmission (Wiley 1991, Brumm and Naguib 2009).

The equipment and settings used for recording can greatly affect detectability during processing of audio recordings. Different combinations of microphones and audio recorders will vary in frequency response, dynamic range, sensitivity, and signal-to-noise ratio. Sampling rate, bit depth, and compression format also influences sound quality and are programable on many different devices. Audio processing can also introduce variation in detectability whether through human observers or automated recognition. Detectability between observers can be influenced by age, skill level, and experience (Pearson et al. 1995, Helzner et al. 2005) and automated recognition software can produce different results depending on the training dataset, the method or type of recognizer, and probability threshold used (Knight et al. 2017). Variation due to equipment and processing procedures are less problematic because they can easily be addressed by standardizing equipment and interpretation of audio recordings. However, variation in detectability due to the surrounding environment can be much more problematic due to the complexity and number of factors present.

CURRENT METHODS

Bioacoustic datasets most commonly provide information on the presence or absence of species or are used as an index for relative abundance (Johnson 2008). This requires careful consideration and control of factors that may influence detectability between treatments of interest at the experimental design or analysis phases. Previous studies have suggested quantifying differences in detectability or detection area to create statistical offsets for correcting variable detectability (Solymos et al. 2013, Darras et al. 2016, MacLaren et al. 2018). Others have suggested using a cost-weighed approach to model sound attenuation in heterogenous habitats based on measurable parameters associated with factors that may influence sound attenuation (Royle 2018).

Estimates of animal density are often desirable because it converts count data to a common standard that can be used to compare animal numbers between different datasets, research programs, or regions (Solymos et al. 2013). This requires accounting for availability (individuals that are present but don’t vocalize) and declining detectability with increasing distance (Buckland et al. 1993). Availability can be addressed using removal modelling (Farnsworth et al. 2002), however determining the distance over which sound travels and the area covered by a survey is an essential part of density estimation which is problematic due to issues with variable detectability described previously. Established methods to estimate animal density from bioacoustic datasets are typically labor-intensive or statistically complex and require the use of time-synchronized ARUs to localize individuals and estimate density through spatially-explicit capture-recapture models (Dawson and Efford 2009, Efford et al. 2009). More recently, signal strength has been used as a proxy for distance in combination with conventional distance sampling models as a less labor-intensive alternative (Darras et al. 2018*b*, Sebastian-Gonzalez et al. 2018).

THESIS OBJECTIVES

One of the main issues with acoustic surveys is controlling for variation in detectability due to the surrounding environment, between species, and across different recording devices. As a result, these surveys often yield estimates of relative animal abundance because detectability is hard to quantify and detection distances for different species in different environments are often unknown. Methods for estimating true animal abundance or density often use grids of ARUs or require substantial preliminary analysis. My thesis aims to investigate and quantify sources of environmental and species related variation in detectability and detection distance, determine how these sources of bias influence the results of point counts if not accounted for, and provide recommendations and methods for addressing variable detectability and estimating the abundance and density of acoustic animals using ARUs.

In chapter 2, I investigate the influence of roads on sound attenuation and discuss potential biases in survey results for roadside sampling programs such as the North American

Breeding Bird Survey. In chapter 3, I test the performance of four different acoustic recorders to determine how much variation is associated with the recording technology used during an acoustic survey. I also compare the performance of these acoustic recorders to human observers and discuss methods to integrate data from multiple point count sources for analysis. In chapter 4, I study the effect of vegetation type and species-specific sound characteristics on detection probability and detection distance. I also propose a method of correcting for variable detectability using sound playback experiments and model predictions to estimate correction factors based on the sound parameters for a given species. In chapter 5, I propose a method for estimating the density of wildlife populations using conventional distance sampling by predicting the distance of a vocalizing individual based on the relative sound level calculated by automated recognition software. I present case studies of two different species, the Ovenbird (*Seiurus aurocapilla*) and the Common Nighthawk (*Chordeiles minor*) and run simulations to compare the accuracy of density estimates from this method, estimates where distance estimation error from human observers is considered, and the true density from the simulation. In chapter 6, I summarize my findings from the aforementioned chapters, discuss the current state of the field and the implications for survey and monitoring programs, and provide recommendations and suggestions for future research on this topic.

Chapter 2. Sound attenuation in forest and roadside environments: implication for avian point count surveys

INTRODUCTION

One of the largest datasets available to ornithologists in North America is the Breeding Bird Survey (hereafter BBS). Many advances in our knowledge of birds have come from the BBS (U.S. Geological Survey 2009). However, there is concern that the road-side nature of this survey may provide biased estimates of bird abundance and trends relative to non-BBS monitoring and research done off-road (Bart et al. 1995, Keller and Scallan 1999, Lawler and O'Connor 2004), particularly when combining both types of data for analysis. Roadside habitats differ from forest interior habitats in a number of ways that could alter our understanding of avian abundance and diversity patterns. It is known that roadside habitats often have differences in vegetation composition and structure (Keller and Scallan 1999), physical characteristics (road salts, sediments, etc.; Trombulak and Frissell 2000), and levels of ambient noise (Parris and Schneider 2008) relative to the forest interior. Traffic volume can also vary and to control for this, BBS surveys are often conducted along relatively low use and secondary roads where alterations to the environment by traffic are minimized (Droege 1990). However, studies of sound transmission suggest that the distance at which sounds can be detected will vary between open and closed (more dense) environments (Fricke 1984). If this is the case, roadside surveys, such as those utilized by the BBS, may be confounded by the open linear environments that necessarily define roads if compared to off-road surveys.

Attenuation and degradation of acoustic signals are directly related to the distance the signal must travel. Wiley and Richards (1982) state that under free field conditions, all sounds are expected to attenuate at ~6dB each time the distance between the source and the observer is doubled (inverse distance law). Free field conditions are rarely met outside of the laboratory as the composition of the sound path can result in attenuation in excess of what is predicted by the inverse distance law. Several factors can affect excess attenuation. Scattering and reverberation effects are higher when vegetation is present and thus could increase the attenuation of sound (Wiener and Keast 1959, Richards and Wiley 1980, Yang et al. 2013). Although scattering can reduce the transmitting energy of any frequency, this effect is especially significant for higher frequency sounds, since shorter wavelengths are less able to pass around obstructing objects than sounds produced at lower frequencies (Piercy et al. 1977). Roadsides are more open along their path, so the acoustic environment could differ greatly from that of the forest interior. In addition to lower vegetation density along transmission paths, roadsides differ in surface composition characteristics. Decreased porosity on roads can decrease attenuation by lowering the impedance characteristics of the road surface (Aylor 1972). Finally, local atmospheric conditions can vary when comparing roadside to interior locations. Environmental gradients such as wind and temperature can differ between roadsides and interior areas and are often stronger in open areas which can result in higher attenuation (Wiener and Keast 1959, Morton 1975, Trombulak and Frissell 2000). Overall, differences between roadside and forest areas suggest the distance bird vocalizations transmit could differ from the forest interior considerably, potentially leading to biased estimation of avian abundance for studies combining roadside and non-roadside data.

To evaluate whether the distance over which sounds could be detected differed between sounds produced along open transmission paths parallel to the road, forest edge, and forested transmission paths perpendicular to roads, we played back and re-recorded a series of pure tones and different bird songs along forestry roads in boreal conifer and deciduous forests stands.

These roads were selected because they are relatively free of confounding variables found along most roads (e.g., noise, traffic, surrounding development). Differing vegetation structure can influence sound (Aylor 1972), thus we chose two of the main forest types in the boreal forest. A common assumption is that the detection area is circular. If transmission is altered along roadways in comparison to interior areas, we predicted directionally dependent differences in detectability between the forest interior, forest edge, and road transects would be observed. We had three objectives. First, measure how sound attenuation is influenced by roads and forest type by calculating excess attenuation for each type of transmission path. Second, determine if sound transmission of bird song is differentially affected by roads and forest type by determining the distances at which sounds can be detected by observers listening to sound playbacks and the environmental factors that influence them. Finally, calculate the effective area surveyed and develop statistical correction factors to standardize count data obtained from on and off-road sites.

METHODS

Field Playbacks

We conducted 600 playback trials at 30 different distances between the recorder and the playback unit (hereafter stations) between July 22 and August 24, 2014. Ten transects each were placed along forestry roads, forest edges, and within the forest interior at least 50m from the road (Fig. 2.1). Forest transects were located perpendicular to roads in sites where the vegetation path was representative of a single forest class. In this region, tree diversity is low and forest stands are often composed of a single species. Half of transects were in deciduous dominated forest (defined as at least 65% deciduous, with the dominant species being Trembling Aspen, *Populus* *tremuloides*) and half in coniferous dominated forest (defined as at least 65% coniferous, with the dominant species being White Spruce, *Picea glauca,* or Black Spruce, *Picea mariana*). Dominance was determined by estimating forest composition at four points per transect every 250m. The research was done near Calling Lake, Alberta, Canada (55.21°, -113.19°). Each playback was done between 08:00 – 20:00 MST during late summer to reduce the chance of recording actual bird sounds. Average wind speed, temperature, and humidity were recorded using a handheld weather monitor (Kestrel 4000) for the duration of each playback. Wind levels at the start of each trial were less than or equal to Beaufort scale of 2 and averaged 1.3 ± 1.4 km (SD) per hour. Temperature averaged 24.7 ± 5.1 degrees Celsius. Relative humidity was 58.3 ± 14.1%. The date and order (forest vs road) of playback at each site was selected by alternating between forested and road transects. Roads were low-use (<1 vehicle per hour) dirt or gravel forestry roads. Recordings were done in absence of vehicle traffic.

We broadcast 36 known sounds from an Alpine digital CD Receiver (CDE-122) connected to an Alpine 6.5-inch speaker and tweeter set (SPR-60) contained within a wooden box (25x29x38cm) at 30 standardized distances ranging from 12 to 1312 meters measured using GPS (GARMIN GPSmap 78, accuracy ± 3m) at each transect. The speaker was placed so it faced directly at the recorder at a height of 1.5 metres, a height similar to other avian playback studies (Maynard et al. 2012, Koloff and Mennill 2013, Sandoval et al. 2015). At each site, a Song Meter SM2+ Automated Audio Recorder (Wildlife Acoustics, Maynard, MA, USA) was set to continuously record (sampling rate 44.1 kHz, bit depth 16, .wav format). Recording units were located at the forest edge and road and the speaker was moved to each distance interval for playback. Forest edge was defined as the transition between the mature trees and the ditch of the road where the forest ends with a distinct edge. The road was defined as the transition between the ditch and the actual road surface. For the road and forest edge transect, the playback unit was placed at the forest edge and broadcast to both road and forest edge recorders simultaneously. For forest transects, the recording and playback unit were located separately within a continuous stand of deciduous or coniferous forest to best simulate a bird calling from within an interior forest environment.

Playbacks at each station consisted of a 5:10 minute sequence beginning with an escalating series of one second pure (sine wave) tones following ½ octave intervals (1000, 1414, 2000, 2828, 4000, 5656, 8000 hertz). We used Adobe Audition CS6 (Adobe Systems Inc.) to generate these sounds. These tones were followed by a series of vocalizations of boreal bird and amphibian species selected to represent a range of frequencies and song complexities including (in no particular order): Clay-coloured Sparrow (*Spizella pallida*, CCSP), Black and White Warbler (*Mniotilta varia*, BAWW), Lincoln's Sparrow (*Melospiza lincolnii*, LISP), Brown-headed Cowbird (*Molothrus ater*, BHCO), Red-breasted Nuthatch (*Sitta canadensis*, RBNU), Bay-breasted Warbler (*Setophaga castanea*, BBWA), Dark-eyed Junco (*Junco hyemalis*, DEJU), White-throated Sparrow (*Zonotrichia albicollis*, WTSP), Cape May Warbler (*Setophaga tigrina*, CMWA), Common Raven (*Corvus corax*, CORA), Belted Kingfisher (*Megaceryle alcyon*, BEKI), Olive-sided Flycatcher (*Contopus cooperi*, OSFL), Pine Siskin (*Carduelis pinus*, PISI), Tennessee Warbler (*Leiothlypis peregrina*, TEWA), Warbling Vireo (*Vireo gilvus*, WAVI), Rose-breasted Grosbeak (*Pheucticus ludovicianus*, RBGR), Ovenbird (*Seiurus aurocapilla*, OVEN), Yellow Rail (*Coturnicops noveboracensis*, YERA), Western Toad (*Anaxyrus boreas*, WETO), Canadian Toad (*Bufo hemiophrys*, CATO), Northern Saw-whet Owl (*Aegolius acadicus*, NSWO), Boreal Owl (*Aegolius funereus*, BOOW), Great Gray Owl (*Strix nebulosa*, GGOW), Long-eared Owl (*Asio otus*, LEOW), and Barred Owl (*Strix varia*, BADO). We used a two second interval between calls to avoid signal overlap. This sequence was broadcast at an SPL of 90dB (re 20 µPa) which we normalized using the peak amplitude (maximum volume) of each sound in Adobe Audition CS6 and calibrated using a handheld sound level meter (Sper Scientific 840018) measuring the 1000Hz tone one meter from the speaker (based on fast-time A-weighting).

Sound Processing

Recorded playbacks were isolated from continuous recordings using Audition and individual sounds from each sequence were clipped into individual sound files (n=27143) using an automated script and the 'textgrid' function in Praat V5.4.06 (Boersma and Weenik 2015). These clips were randomized and joined together in sets of 10 sounds with 2 second spacing to create a single sequence of randomized sounds using an automated batch script. These sequences were given to six observers who identified any detectable sounds by sight, using visual scanning of spectrograms in Adobe Audition (window type: Blackman-Harris; window length: 2048), and by sound, using standardized volume levels and headphones, simultaneously. Volume levels were selected to maximize amplitude and detections while avoiding any risk of hearing damage. Fifteen percent of sounds were blank ambient background sound consisting of low levels of wind and vegetation noise normally present in recordings to control for false positive identifications. Randomization of sounds removed an observer's ability to predict which sounds would occur in what order although observers were aware of all possible species that could be presented.

The inverse distance law predicts sound pressure levels will attenuate at a specific rate (Berg and Stork 2004). However, vegetation can alter attenuation rate. We measured relative sound pressure level (SPL) of the pure tones (n=5656) using a batch process selection table function in Raven Pro version 1.4 (Charif et al. 2010). We calculated averaged background noise levels within the same bandwidth of each measured tone at hourly intervals for each site (n=5) to determine baseline power level of each transect. We removed data at distances where the SPL of pure tones dropped to the levels of ambient background noise. While it is still possible to detect sounds below this level, it is no longer possible to measure SPL. Measurements were conducted on a selection of 0.4s duration and 100Hz bandwidth for each clip (i.e. for 1000Hz – 950 to 1050Hz selection) by calculating power spectral density summed over the frequency range of the selection (window type: Hann; window length: 256). We chose a shorter section of each pure tone and avoided doing measurements at the onset or end to avoid acoustic distortion. We then calculated excess attenuation from what would be predicted based on the inverse distance law using:

$$\text{Eq. 1. } EXCESS_{SPL} = (SPL_{12.5} - SPL_i) - \left(20 * \log10\left(\frac{d_i}{12.5}\right)\right)$$

Here, $SPL_{12.5}$ is the SPL at 12.5m, SPL_i is the SPL for 'i' distance, and d_i is the distance 'i' in metres at which each tone was recorded. We used SPL at 12.5m as a reference value because it was the closest distance measured and calculated excess attenuation for each distance beyond 12.5m for each individual transect.

Sound Attenuation and Excess Attenuation

We used Akaike's Information Criterion (Burnham and Anderson 2002) to rank linear mixed models (lmer function, lme4 package, in program R - Bates et al. 2015) that predicted the effect of distance, frequency, transect and vegetation type, and weather on sound attenuation and excess attenuation. We ranked models with all tones pooled together to investigate the effect of frequency between different tones. We also tested models for each individual tone to investigate effects on sound by the environment for each frequency separately. Site was included as a random effect. The best model for each tone was selected using the lowest AICc and ΔAIC values (Appendix 1.1.2). For model selection where ΔAICc <2, we selected the most parsimonious model as our best model (Arnold 2010). We found a strong negative correlation between humidity and temperature (r = -0.77). Humidity was weighted higher during preliminary model selection, so temperature was dropped from our full models to avoid issues with collinearity as both variables influence attenuation (Harris 1966). Log transformed distance had higher model weight in preliminary analyses and was included over untransformed distance in subsequent analyses. We reported marginal (R^2_m) R^2 values to provide information on variation due to fixed effects, and conditional (R^2_c) R^2 values to provide information on variation due to fixed and random effects for each final model (Nakagawa and Schielzeth 2013, r.squaredGLMM function, MuMIn package, Barton 2015).

Effect on Observer Detection

Generalized linear models were ranked using AICc for each species and tone to predict observer detection probability (Appendix 1.1.4). We randomly partitioned data into 70% training data and 30% testing data and performed cross-validation on our models. These models predicted the probability of an observer detecting a given species or tone as a function of weather, distance, and transect type (road, forest edge, or forest) in each forest type (deciduous or coniferous). Similarly, we modelled detection data with all species pooled and included the minimum frequency of each species to investigate a species-specific frequency effect. Minimum frequency is defined as the lowest frequency measured over the duration of each species-specific sound.

Finally, we validated our best model for each species and tone by determining AUC statistics and receiver-operator curves using our testing data (roc function, pROC package, Robin et al. 2011; Appendix 1.1.4).

We performed a Monte Carlo simulation to determine if statistical differences existed between detection distance in forests, forest edge, and roads as well as for deciduous and coniferous forest types. This was done to determine the scale of effective detection radius (hereafter EDR) correction required between different combinations of transect and forest types (see below). We generated coefficients (n=1000) using maximum likelihood estimates and variance covariance matrix from the original model and calculated 90% confidence intervals of the predicted values for each species when making comparisons. If statistical differences did not exist between certain combinations of transect and forest, we assumed correction was not necessary.

We investigated differences in wind speed, relative humidity, and temperature at forest interior and roadside sites using a linear mixed model in R (R Core Team 2015, lmer function, lme4 package, Bates et al. 2015) to account for variation in site, date, and time. We used ordinal date and time on a continuous scale of minutes relative to average sunrise time for the days of sampling. We included site as a random effect.

Calculating correction factors to standardize count data

We developed correction factors for each species and tone by calculating a ratio of the effective area sampled when in the forest, on roads, and at forest edges ($A_{Forest} : A_{Road} : A_{ForestEdge}$). To do this, we followed a half-normal detection function often used in the distance sampling literature to calculate effective detection radius (EDR: Solymos et al. 2013). EDR is the parameter, τ, in the half-normal detection function: $p(d) = \exp(-d^2/\tau^2)$. EDR is defined as the distance at which number of individual birds detected outside τ is equal to the number of missed individuals within τ. We ran our GLMs with a fixed intercept at 0, complimentary log-log link ("cloglog") function, and binomial distribution. Interaction with distance was included in models for all parameters of interest but main effects were excluded to accommodate a fixed intercept. This allowed us to calculate EDR using a linear modelling framework. We transformed distance to $x = -d^2$ before modelling so that distance was a linear predictor. We estimated EDR for all species and tones on roads, forest edges, and within forests by summing the beta coefficients of variables related to distance in our best models (β). We calculated EDR using: $\tau = (1/\beta)^{0.5}$. Finally, we determined the effective area sampled for the forest using the formula for area of a circle ($A_{Forest} = \pi\, \tau_{Forest}^2$). We presented two scenarios for effective area sampled on a road, a simple ellipse ($A_{Road/ForestEdge} = \pi\, \tau_{Forest}\, \tau_{Road/ForestEdge}$) and a more complicated equation (Appendix 1.3.1) taking into account the angle of detection and proportion of distance travelled through forest versus road. The ratio of $A_{Forest} / A_{Road/ForestEdge}$ is the correction factor for a given species or tone which can be used to multiply roadside or forest count data to allow for standardization (Appendix 1.3.2).

RESULTS

Estimating Sound Attenuation and Excess Attenuation for Pure Tones of Different Frequencies

Relative SPL attenuated at a higher rate with increasing frequency when all tones were pooled together (Fig. 2.2). Relative SPL was also negatively influenced by distance for all tones. The top performing model for each individual tone included log(Distance) and transect while omitting weather variables with the exception of the 8000Hz tone. Tones that were transmitted through forests attenuated at a higher rate than along forest edges or roads in both coniferous and deciduous vegetation types (Fig 2.2). For 8000Hz tones, wind negatively influenced relative SPL. For all models assessing influences on relative SPL the R^2_m was >0.71 and R^2_c >0.77 (Appendix 1.1.2).

Excess attenuation increased with distance at all frequencies and at higher frequencies with all tones pooled together. The top performing model for each individual tone was the same as for relative SPL and included log(Distance) and transect while omitting weather variables. At 8000Hz, the top performing model included wind. Tones had higher excess attenuation when transmitted through the forest interior for both vegetation types (Fig. 2.2). All tones transmitted along roads and forest edges initially had lower attenuation than expected from free field environments. At 8000Hz, wind increased rates of excess attenuation. For all models assessing influences on excess attenuation the R^2_m was >0.39 and R^2_c >0.52 (Appendix 1.1.3).

Estimating Effects of Transect Type and Weather on Detectability

Detectability declined with distance at different rates for different transect and forest type combinations. Detectability decreased with increasing frequency (Fig. 2.3). The top performing model for each species varied. A global model including distance, transect type, humidity, and wind was the top performing model for 13 species and two pure tones. A model excluding wind and humidity was selected for 12 species and six pure tones (BEKI, PISI, BBWA, TEWA, CMWA, LISP, YERA, WTSP, OSFL, RBGR, WAVI, DEJU, 1000Hz, 1414Hz, 4000Hz, 5656Hz, 8000Hz). Wind had a variable effect on detectability where four species appeared to be positively influenced (CCSP, BAWW, OVEN, BHCO) and eleven negatively influenced (BOOW, NSWO, LEOW, BADO, WETO, CORA, RBNU, GGOW, CATO, 2000Hz, 2828Hz). Humidity had a positive effect on detectability for 15 species (BOOW, NSWO, LEOW, BADO, WETO, CORA, RBNU, BAWW, CATO, OVEN, BHCO, 2000Hz, 2828Hz). The top model for 8000Hz included observer as an important parameter for detection probability.

Environmental gradients differed between roads and the forest interior. Wind speed was lower within the forest (mean ± SD; 0.9 ± 1.1 km per hour) than on roads (1.8 ± 3.4 km per hour; Fig. 2.4). Humidity decreased with time on roads and in forests but decreased faster on roads than in forests over the day (forest: 56.4 ± 12.5%, road: 60.2 ± 15.4%; Fig. 2.4). We did not find strong support for a transect effect on temperature (forest: 26.3 ± 3.4 degrees Celsius, road: 23.1 ± 6.0 degrees Celsius) but observed a positive relationship with time of day (Fig. 2.4).

We compared Monte Carlo 90% confidence intervals to investigate differences between each combination of transect/forest type. We found probability of detection was higher on road compared to interior forest for every combination of forest type for almost all species (Fig. 2.5). Similarly, we found detection to be higher for roads compared to interior forest with the exception of the comparison between deciduous forest edge and deciduous interior forests. Comparisons for several species showed higher detectability on roads of both forest types versus deciduous forest edges (BEKI, DEJU, LISP, OSFL, PISI, RBGR, TEWA, WAVI, YERA). Five species differed between deciduous and coniferous forest edges (BEKI, DEJU, LISP, PISI, RBGR; Appendix 1.4). We found no differences between road transects or interior forest transects of different forest types, aside from some of the pure tones. Owls (NSWO, BOOW, GGOW, LEOW, BADO) and lower frequency pure tones (1000, 1414, 2000, 2828Hz) did not differ between any combination of transect or forest type. AUC values for test data were >0.90

for most species (Appendix 1.1.4). The lowest frequency tones (1000, 1414, 2000) and four owl species (BADO, GGOW, LEOW, NSWO) were 0.90>ROC>0.80. A single tone (2000Hz) had 0.80>ROC>0.70 (AUC=0.7993).

Estimating Effective Detection Radius, Effective Survey Area, and Corrections for Roads, Forest Edges, and Forests

We combined roads and interior forests of different forest types into single categories because we found no difference between forest types for both categories. Although we found differences with five species when comparing forest edge transects of different forest types, we collapsed them into a single category as well to simplify effective area estimation, increase robustness of EDR estimates, and provide corrections for the 'broadest' group possible to make it more applicable to researchers wishing to use our data. We then estimated EDR and effective survey area for the three transect types, and calculated correction factors for comparing detections from different transects (Appendix 1.3.2). A correction factor of one indicates the transmission of vocalizations is not influenced by transect and the same effective area is surveyed regardless of whether a point count is done at a roadside or the forest interior. Deviations from one indicate increasing difference between transects. Calculated correction factors varied depending on how strongly transmission of bird calls was influenced by being in the forest interior in comparison to road and forest edge. High frequency songbirds generally had smaller EDR values than lower frequency species like owls and higher frequency sounds had greater difference in EDR between the forest and road indicating high attenuation along forest transects (Fig. 2.3). Pure tones had some of the largest EDR values but the correction varied by frequency. Correction factors for road-forest comparisons were the largest, followed by forest edge-forest, and road-forest edge, in descending order.

DISCUSSION

Sound attenuation in forests often differs from open environments due to differences in microclimate, vegetation density, and forest structure, which can cause variable scattering and absorption of sound waves (Wiener and Keast 1959, Richards and Wiley 1980). We compared sound attenuation and detection distances in roadside and forested transects. Attenuation of pure tones increased at a greater rate in forests than on roads or forest edges, and as frequency increased, suggesting that scattering or absorption by vegetation plays an important role in sound transmission. This trend in frequency is supported by past findings which suggest that higher frequencies attenuate faster for this reason (Piercy et al. 1977). Similarly, excess attenuation was higher in forests than along roads although we found no clear pattern in frequency. Sound attenuated less than what was expected from the inverse distance law when transmitted along roads at distances close to the source, possibly because the road surface and corridor reflects sound leading to less attenuation (Bullen and Fricke 1976).

Detection was mainly influenced by distance and transect type. The magnitude of this effect was much larger for forest interior transects than forest edge or road transects and most sounds had greater detection distances on roads than in forests. Monte Carlo analysis in all owl species and the four lowest frequency tones did not show a significant effect of transect type (Appendix 1.4), but during AIC model selection all species and sounds included transect as an important parameter. This suggests the overlapping confidence intervals found during Monte Carlo simulation are a result of a large degree of uncertainty and variance in detection for those species and sounds, instead of small differences in point predictions. We also found these low frequency species to have the lowest AUC values during model validation. All sounds with AUC <0.90 also had overlapping confidence intervals for all transects during Monte Carlo simulations. Due to the nature of our study design, sounds with larger detection distances had more detections and less non-detections which increases uncertainty in slope estimation for our models. We suggest that lower frequency sounds are more prone to variability in detection and statistical uncertainty resulting in larger confidence intervals and decreasing model fit during validation.

We found higher frequency sounds had lower detection probability and detection distance when calculating EDR (Fig. 2.3). When ranking species and tones in descending order of correction value required to standardize counts, we found that passerines and high frequency tones required larger corrections in comparison to owls and lower frequency tones. This suggests that low frequency sounds are less prone to attenuation in forests, which is in line with previous literature (Fricke 1984). Detection probability of high frequency sounds declined faster, but EDR for some of these species was over twice the distance on road compared to forest (Appendix 1.3.2). We propose that when surveying songbirds, the effective area sampled is almost always larger when sampling from a road leading to inflated counts of species when surveys are done from roads relative to the actual abundance in the forest interior. For the 8000Hz frequency tone, we found observer to be an important parameter. We believe this to be a result of human hearing ability as this sound approaches the upper threshold of the human hearing range. Some observers were able to identify these tones while others were unable to detect them consistently, regardless of distance. Observer hearing ability can be influenced by a variety of factors such as age or sex (Pearson et al. 1995, Helzner et al. 2005). Our observers consisted of a combination of men and women between the age of 18-25 to reduce any observer-related hearing differences.

Furthermore, the randomized nature of our study design means that observer bias towards any specific transect or distance should not be an issue.

We found mixed results for differences in attenuation between road and forest edge. Four tones (1414, 2000, 2828, 8000Hz) had no difference in relative attenuation between the two transect types while the road transect for three tones (1000, 4000, 5656Hz) had slightly higher attenuation than the forest edge. This contrasts with the patterns we see in our EDR estimates. We speculate that this results from our broadcasts at shorter distances having to travel slightly longer to the road ARU than the edge ARU due to how we set up the study design (Fig. 2.1). This can impact our reference values and influence our measures of relative SPL. At greater distances, this difference decreases and becomes less important as it becomes less than the error of the GPS units we used to measure distance. Ultimately, this should not affect our estimates of EDR as they were based on binary detection data and all sounds were detected at smaller distances.

The 4000Hz tone and some species with a minimum frequency close to 4000Hz (WTSP, WAVI, PISI) had higher than normal EDRs for what our models predicted. We have two possible explanations for this. First, the frequency sensitivity of the human ear peaks around 4000Hz meaning human observers should be able to better detect these frequencies. Second, the frequency response of our playback speaker was slightly higher when measuring SPL for the 4000Hz tone. We believe the pattern seen for observer detection of sounds near 4000Hz to result from a combination of these two factors. However, since we use the relative difference for EDR between roadside and off-road transects, this does not influence the calculation of correction factors.

Our models for lower frequency species generally include weather parameters in the top model for predicting detectability. We found models for 15 species included weather variables and of these species, only three were high frequency passerines (BAWW, OVEN, CCSP). The rest, including CORA, RBNU, all owl species, and pure tones from 2000-2828Hz, are generally lower frequency and have higher EDRs. However, our pure tone attenuation models did not include any weather variables with the exception of 8000Hz. We propose two possible explanations for this observation. First, wind and associated abiotic noise from vegetation usually occupy lower frequency bands and could influence detection by masking signals more than high frequency sounds. This affects an observer's ability to identify a sound but does not decrease SPL. Second, larger EDR estimates associated with many of these species and sounds means a greater distance between signal and receiver for weather to influence sound transmission.

Local atmospheric conditions also influenced detection probability although this effect was much weaker than distance or transect type. Patterns seen in the effect of wind on detection probability suggest a decrease in detection probability is influenced primarily by the interaction of wind and vegetation. We found no negative effect of wind when playback was done on roads but a significant effect on forest edges where vegetation was present for species models containing weather. This suggests increasing wind causes vegetation noise which reduces detection probability at the lower frequency range due to signal overlap with sounds like rustling vegetation. Detection modelling associated wind with an increased detection probability for four species (BAWW, CCSP, OVEN, and BHCO). We can think of no logical reason for this result and may be caused by some error in our measurements of wind speed. We did not find any effect of wind in the interior forest but the overall level of wind was lower than on the road or forest edge. However, we measured wind speed at ground level which is not necessarily representative of wind speed at canopy height where birds may call from. Future studies should consider measuring wind using the Beaufort scale as this is related to canopy wind speed and is used during point counts to account for wind related noise. Our study design also minimizes effects of wind by deliberately sampling during periods of low wind velocity. Therefore, our study may not be informative regarding the effect of wind. Relative humidity had a negative relationship with detection probability but since we found strong correlation with temperature, further studies are needed to separate the importance of each of these variables.

Our conclusion about how to correct EDR between road-based and forest surveys assumes that playback experiments adequately represent how real bird sounds propagate through forests and along roads, and how observers detect them. Our choice of recordings, broadcast and recording equipment, as well as volume settings are not necessarily reflective of the conditions of a standard BBS point count although 90dB is within the range of what is considered natural amplitudes in many species (Brumm 2004, Patricelli et al. 2007). However, several of our EDR values are many times higher than published EDRs for real birds such as those from the Boreal Avian Modelling Project (BAM; www.borealbirds.ca) suggesting that our broadcasts could be much louder than the singing volume of some species. Height from which a signal is broadcast relative to height at which is received is known to influence sound attenuation. Increasing source or receiver height can decrease attenuation (Padgham 2004, Brumm and Naguib 2009). However, we always broadcasted sounds from the same height for roads (from the forest edge), forest edges, and within the interior forest. Improved roads with pavement or gravel are often elevated above the surrounding landscape which means the observer may be elevated as well for roadside surveys, possibly increasing detection distance even further. We strongly emphasize the importance of using our EDR measurements as a relative comparison between treatments. The value in these results lies not with the raw EDR measures, which may be unrealistically high (i.e. we estimate Ovenbird EDR to be 204m compared to published data suggesting an EDR of 84m; Cumming et al. 2011). However, the correction factors that are calculated from our approach represent percentages that will remain the same regardless of the actual EDR. We presented correction factors based on two different shapes, a simple ellipse and a shape which factors the angle of detection to the road and the proportion of the signal that travels through the road compared to the forest. We believe the ellipse to be at the upper bound of the effective area surveyed while the other shape to be at the lower end. Realistically, detection area and correction values are likely somewhere between these two values as the road corridor may act to propagate sound (i.e. less attenuation than expected at close distances) suggesting that while sound travelling directly through the forest may attenuate at a given rate, we can’t discount a proximity effect of the road. Instead, we believe some sort of gradient effect is more realistic as sound travels spherically from the source and could still be carried by the road corridor. Sound attenuation through the road/forest interface is complicated and not fully understood and our models are our best approximation of the processes that are occurring.

The narrow gravel or dirt roads we studied may also have differed from some of the wider roads on which many BBS routes are located. Narrow roads likely have less influence on sound attenuation than wider roads because the total volume of the hemisphere around the sound source is lower. In addition, more improved roads tend to have wider ditch width that is often maintained by haying or mowing activities. The low-use forestry roads we studied generally had sharp shoulders and narrow ditches which terminated sharply at the forest edge. Furthermore, our classification of deciduous and conifer forests along roadways may not be as accurate within interior forests as some form of early stage vegetation was usually present on forest edges and generally favoured fast-growing aspen that were quite dense. Finally, our comparison of EDR between roads and the interior forest may represent a more extreme outcome than what is realistic. During roadside point counts, most bird detections are from within the forest itself and the distribution of vocalizing individuals within the area of detection may not be homogenous. Thus, while some birds will call from at or near the forest edge and be detected at greater distances, most birds will vocalize from within the forest interior.

Nevertheless, our results demonstrate that differential transmission along open road corridors may significantly alter observer bird counts, a situation particularly relevant when comparing roadside data such as the BBS to off-road surveys. Detection radius of birds in a homogenous forested habitat is assumed to be circular. With roadside surveys, this detection radius becomes elliptical in shape. Our results suggest that, for some species, area surveyed can more than double when surveying from a road rather than within the interior forest. This yields avian estimates that can be twice as large if we assume area surveyed is constant between those two environments. Having this type of information is fundamental for interpreting results from any type of avian point count, as different species can be detected at different maximum distances in different environments (Schieck 1997). When making relative comparisons of bird counts between environmental factors (i.e. on versus off-road, different forest types, etc.), we suggest using statistical methods, such as distance sampling, to correct for inequalities in detectability (Marques et al. 2010). However, roads present a directionally dependent effect on sound attenuation which cannot be solved using conventional distance sampling. Our results allow us to quantify this pattern to estimate effect on survey area and help address this challenge as first approximations. As we strive to understand how avian populations are changing across landscapes, it is important to ensure that we do not make incorrect assessments because we have failed to meet the underlying assumptions of our survey methods.

Figure 2.1. Sampling design schematic for playback experiments. Wildlife Acoustics SM2 recorders were placed on the forest edge (1) and on the road (2) and playbacks were conducted to both recorders simultaneously along a transect following the forest edge. For forested playbacks, recorders were placed within the interior forest (3) and playbacks transects ran perpendicular to the road.

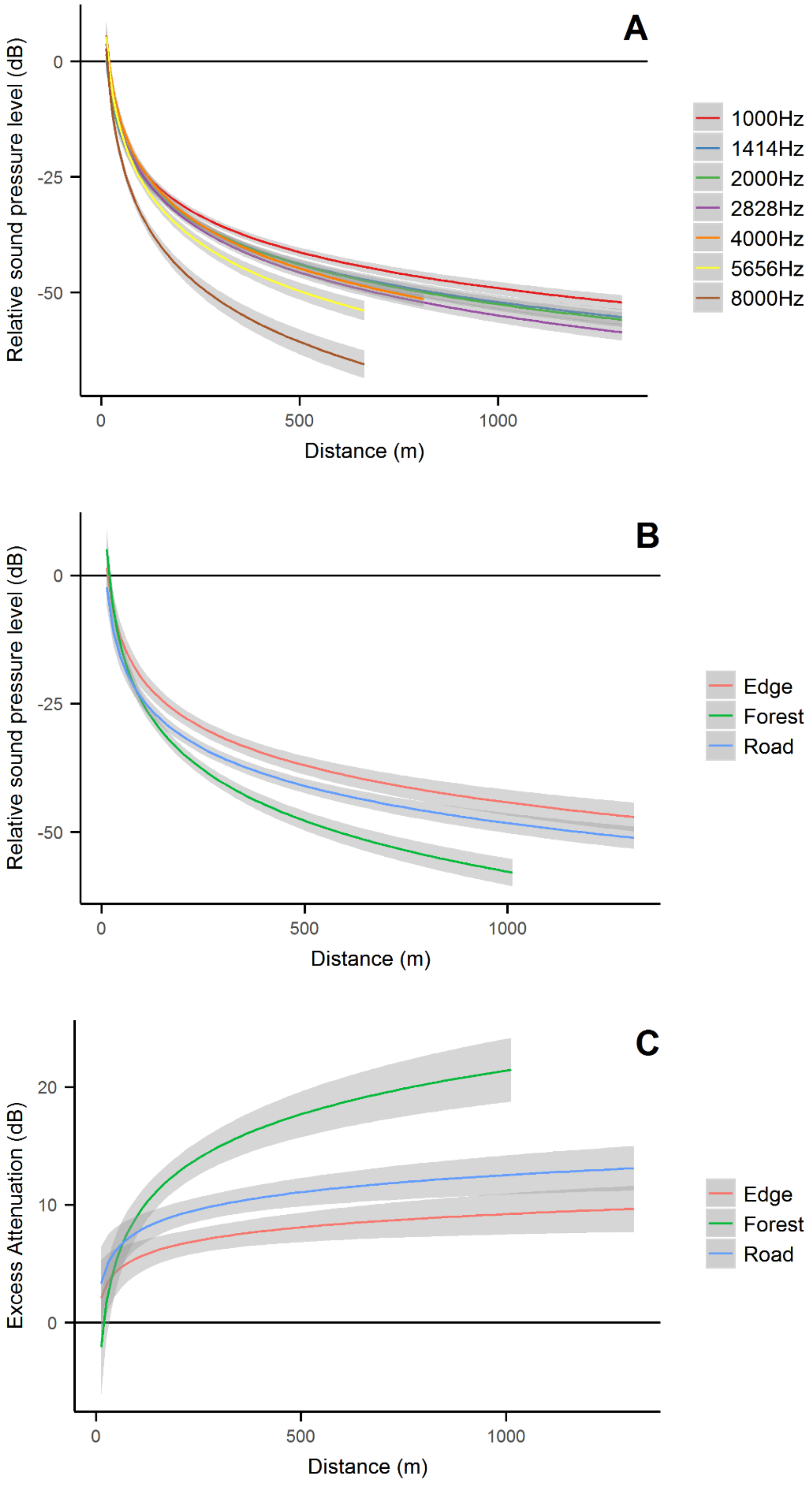
A
Relative sound pressure level (dB)
0
-25
-50
0
500
1000
Distance (m)
1000Hz
1414Hz
2000Hz
2828Hz
4000Hz
5656Hz
8000Hz
B
Relative sound pressure level (dB)
0
-25
-50
0
500
1000
Distance (m)
Edge
Forest
Road
C
Excess Attenuation (dB)
20
10
0
0
500
1000
Distance (m)
Edge
Forest
Road

Figure 2.2. Predicted values for the effect of frequency on attenuation of relative SPL (**A**), attenuation of relative SPL along different transects for a 1000Hz pure sine wav (**B**) and excess attenuation from what is expected from the inverse distance law (**C**) for a 1000Hz pure sine wave with distance. The reference value for relative SPL measurements was defined as the measured voltage for each transect at a distance of 12.5 metres and theoretical slope backward fit to zero in the absence of data. Predictions are calculated from measurements of relative SPL and plotted with 95% confidence intervals.

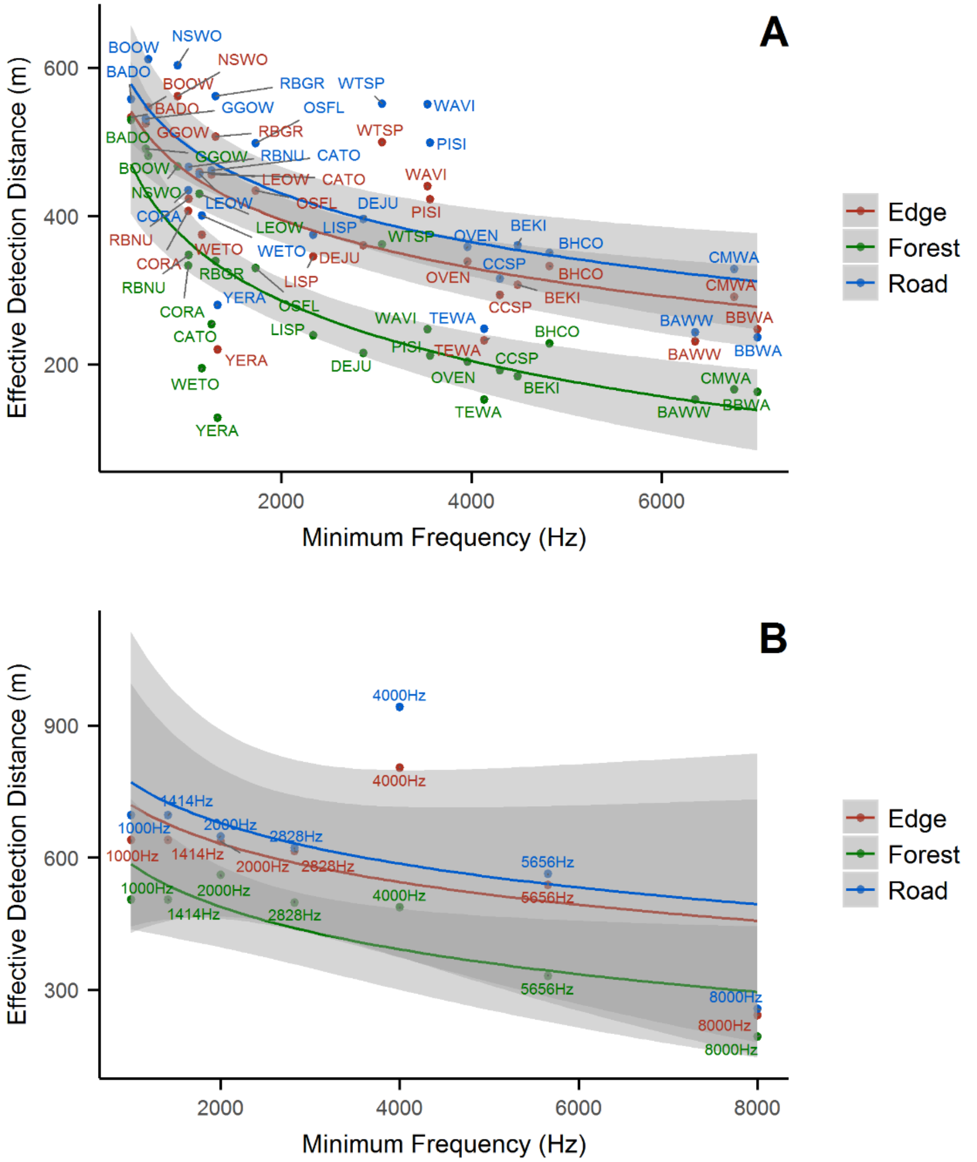

Figure 2.3. Influence of minimum frequency on effective detection distance (EDR) for each species (**A**) and tone (**B**) along different transects with 95% confidence intervals.

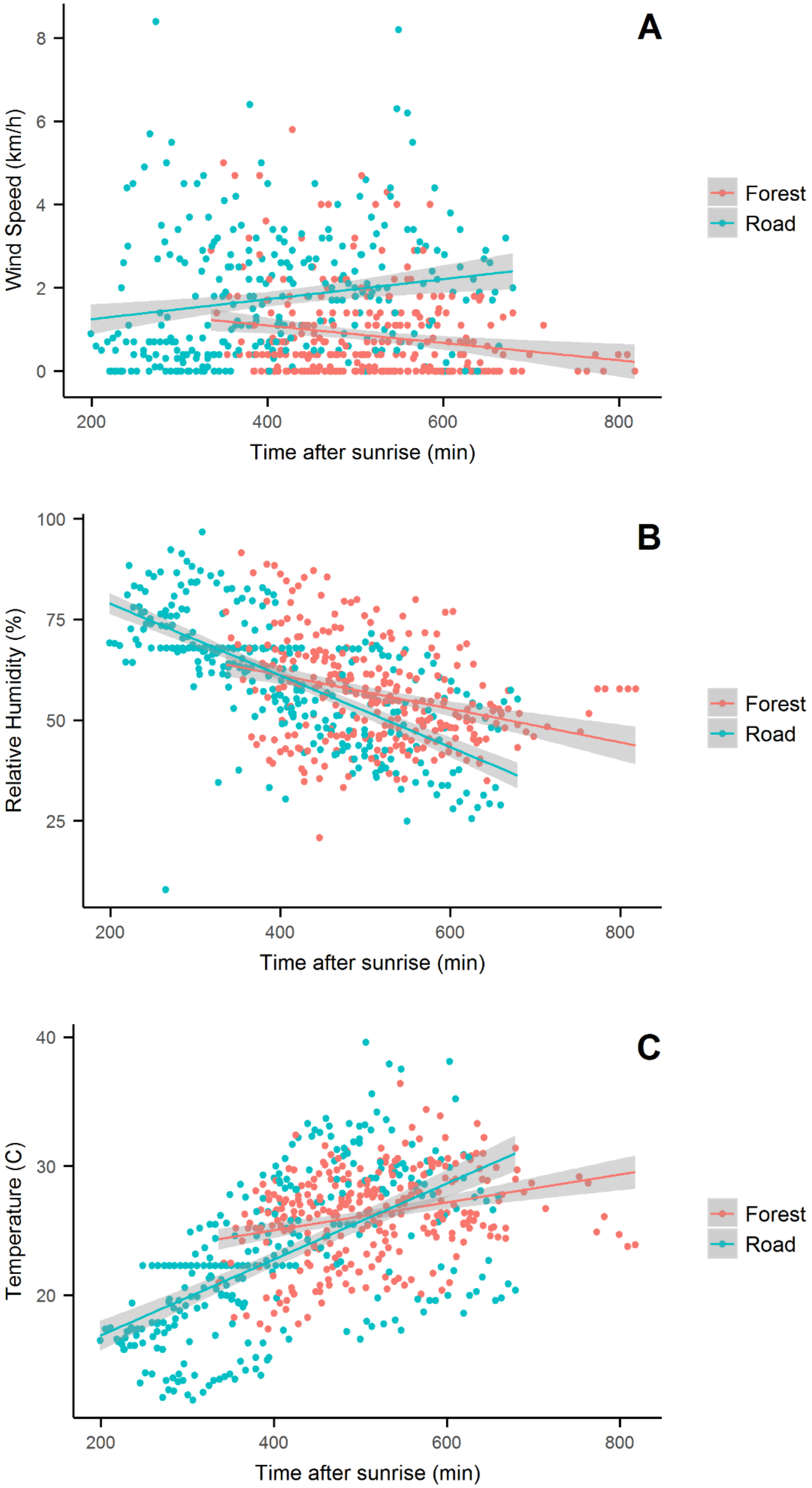
A
Wind Speed (km/h)
8
6
4
2
0
200
400
600
800
Time after sunrise (min)
Forest
Road
B
Relative Humidity (%)
100
75
50
25
200
400
600
800
Time after sunrise (min)
Forest
Road
C
Temperature (C)
40
30
20
200
400
600
800
Time after sunrise (min)
Forest
Road

Figure 2.4. Regression lines for wind speed (**A**), relative humidity (**B**), and temperature (**C**) over time for road and forest transects with 95% confidence intervals. Time indicates elapsed time in minutes since average sunrise for sample period.

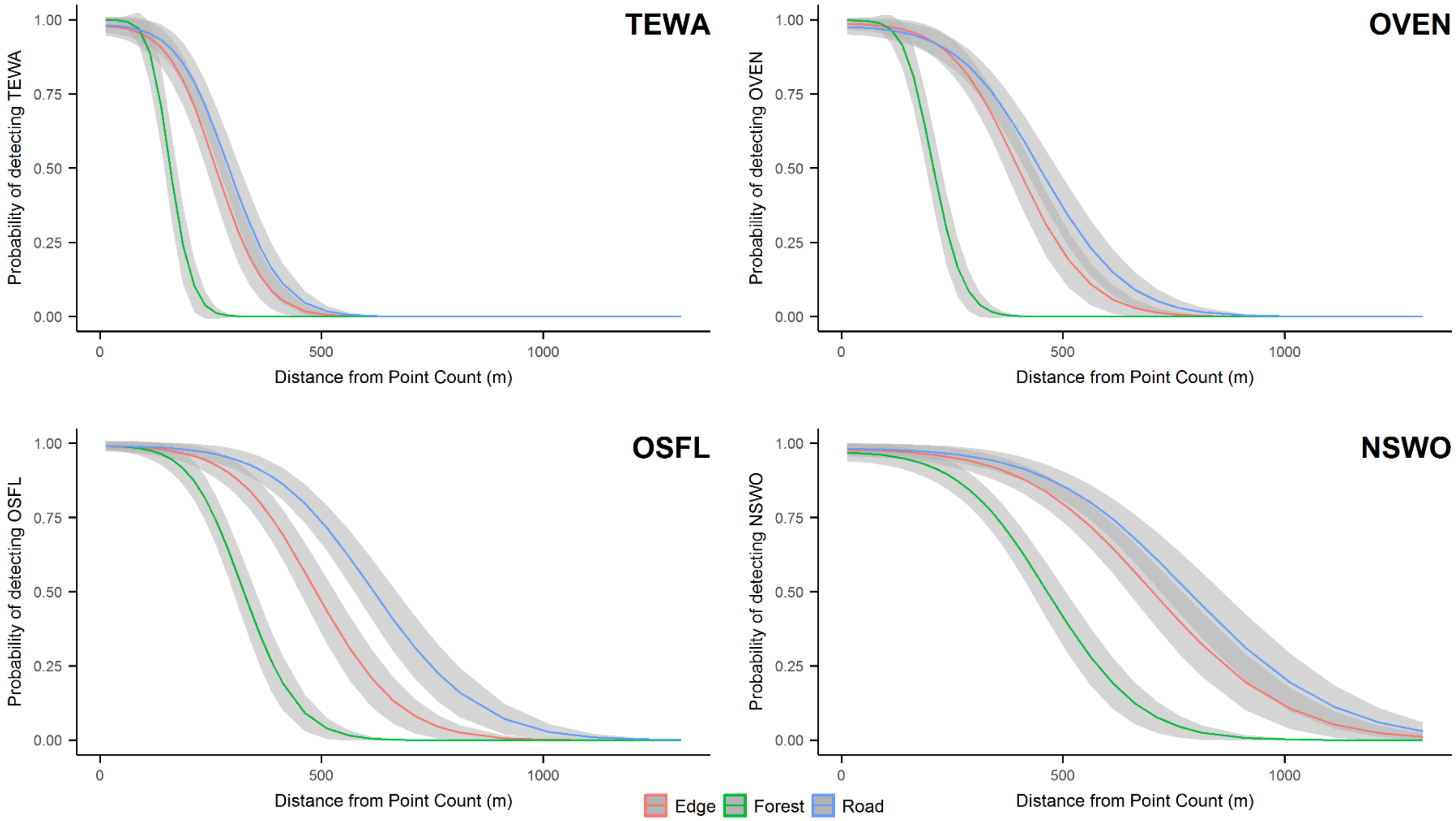

Figure 2.5. Probability of detecting Tennessee Warbler (**TEWA**), Ovenbird (**OVEN**), Olive-sided Flycatcher (**OSFL**), and Northern Saw-whet Owl (**NSWO**) with distance and transect type. Predictions are calculated from binomial detection data and plotted with 95% confidence intervals.

Chapter 3. Experimentally derived detection distances from audio recordings and human observers enable integrated analysis of point count data

INTRODUCTION

There is growing interest in combining data from multiple point count studies to draw inferences about environmental processes influencing birds at larger spatial and temporal scales than the original studies intended (Cumming et al. 2010). Traditionally, human observers have collected point count data (hereafter HPC) by identifying species using acoustic and visual cues while following standardized protocols (Ralph et al. 1995). However, many differences exist between HPC studies in the point count methods used (i.e. duration of count, fixed or unlimited distance counts; Matsuoka et al. 2014). As well, concerns about human observers not detecting species that are present during a single visit have led to calls for replicating effort at the same locations (Royle and Nichols 2003, Kéry et al. 2005). The use of repeated point counts at the same location within a season to account for varying detection probability among visits has increased interest in the use of autonomous recording units (ARUs; Hobson et al. 2002, Haselmayer and Quinn 2000).

A major benefit of ARUs is that humans only visit each location twice and spend time only deploying and picking the ARU. The ARU itself can record over an extended period and create an almost unlimited number of repeated surveys of virtually any duration (Hobson et al. 2002, Haselmayer and Quinn 2000). Human observers are more likely to detect some species visually which can increase the odds of detection, although visual detection area is likely much smaller than aural detection area in heavily vegetated environments (Haselmayer and Quinn

2000, Hutto and Stutzman 2009). Human observers can also estimate distances to individual birds to enable the use of a bounded point count radius and/or distance-based density estimation (Buckland et al. 1993). The relative importance of being able to cost-effectively conduct repeated visits via ARUs versus estimate distance via HPC is unclear in terms of accuracy and precision when assessing trend and status of birds. Regardless, to make the best use of point count data, ornithologists need to evaluate ways to standardize HPC and ARU data to use both data types in the same analyses.

To accurately use data from different point count datasets, ornithologists have converted counts to a common standard, which is typically density (Sólymos et al. 2013). Estimating density of birds using point counts requires: 1) accounting for individuals that are available to be detected but do not vocalize or are not seen (Farnsworth et al. 2002, Dawson and Efford 2009); and 2) accounting for declining detection of more distant individuals (Buckland et al. 1993). Removal sampling can address the problem of animal availability based on multiple time intervals that can exist for both HPC and ARU data. However, the second problem of correcting for the area sampled and the distance over which birds are counted is more fundamental. Sound travels different distances depending on the vegetation and atmospheric conditions occurring between the signaler and the receiver (Padgham 2004; Pacifici et al. 2008, Tarrero et al. 2008; Holland 2001, Simons et al. 2007). Detectability can also vary between observers depending on factors such as age, sex, and experience (Pearson et al. 1995; Helzner et al. 2005). To compare the observed number of bird detections between point counts in two separate studies or in two separate vegetation types within the same study, ornithologists should account for the distance travelled by bird song and effective area sampled (Yip et al. 2017*a*). Otherwise, biases in our understanding of habitat selection, population status, and temporal trend may occur if environmental conditions influencing sound transmission significantly differ between sites and times.

There are three main approaches for calculating the area over which bird sounds are detected and thus converted to density: 1) fixed-distance point counts, hereafter FIXED (Hutto et al. 1986, Petit et al. 1995); 2) Maximum Detected Distance (MDD) at which a given species can be detected (Emlen and DeJong 1981, Rosenberg and Blancher 2005); or 3) Effective Detection Radius (EDR) based on distance-sampling methods (Buckland et al. 1993). The FIXED approach does not seem to be possible for ARU-based point counts because signal strength from a species, and hence accuracy of distance estimation will differ due to sound absorption and reflectance varying among environmental conditions (Petit et al. 1995, Padgham 2004; Pacifici et al. 2008). In addition, such approaches discard a lot of useful data on birds that are detected past the fixed distance. In contrast, ornithologists can calculate MDD and EDR for a species from ARU-based data if: 1) there are known distances to recordings of birds, and 2) if there is some simultaneously collected distance data from HPC for which MDD or EDR and ARUs can be compared and calibrated. Partners in Flight has used MDD to estimate population sizes (Rosenberg and Blancher 2005), but the Partners in Flight approach to estimating MDD is coarse and does not consider vegetation or atmospheric effects that influence MDD, leading to concerns about this approach when calculating density (Thogmartin et al. 2006). EDR accounts for the decline in detectability as the distance from an observer increases, but like the FIXED approach, EDR varies among species and environmental conditions, and reliable EDR estimates depend on well-trained field observers, accurate distance estimation, and point count methods meeting assumptions of distance sampling (Buckland et al. 1993).

Understanding how microphone and recording settings influence the area sampled for birds is crucial to ensuring that long-term monitoring and comparisons made between studies are valid using ARU techniques. Research programs and monitoring agencies have different preferences, goals, and budgets, which influences the type of ARU they decide to use and these must be calibrated to account for differences in area sampled if results are to be compared. Availability of different ARUs also changes over time as ARUs are continuously improved.

Our approach to comparing ARU models and how far they detect birds relative to human observers relies on using song broadcasts of known amplitude and distance. Distance based broadcasts where a sound is played at varying distances from the observer or recorder are labour-intensive. A potential alternative could involve using a relatively limited number of distances when conducting broadcast trials but varying the volume (amplitude) of the broadcast speaker between ambient background levels and the upper range that birds are known to sing. Quantifying the relationship between amplitude and distance of different species for different ARUs could be a cost-effective way of ensuring that all ARUs are calibrated to a known and documented standard. While the true relationship between amplitude and distance is unknown, this approach effectively identifies relative differences among ARUs.

We had three objectives. First, we developed and tested two field broadcast and modelling methods to evaluate how detection of birds is influenced by distance, ARU type, amplitude, and environmental variables relative to HPC. We did this by broadcasting sounds with varying frequencies and under different vegetation conditions over a range of distances. We then tested which sounds were detected by HPC in the field and when listening to ARU recordings in the lab. Second, we used known principles of sound physics to estimate EDR and MDD for various species. Third, we provided an approach for standardizing HPC and ARU data in the same analysis by creating generalized correction factors and a simple approach to calibration that that can be used to standardize raw counts to density regardless of the method of sampling.

METHODS

Using known distance data to estimate effects of recorder technology, vegetation, weather, and species on detection radius

Study area

We collected data near Calling Lake (55°11’ N, 113°12’ W) and Lac la Biche, Alberta (54°38’ N, 111°58’ W) in August, 2014. We conducted our surveys in August to reduce the chance of confusing broadcasted sounds (see below) with the songs of real birds. Broadcasts took place between 07:00 – 20:00 MST. We recorded broadcasted sounds that we used in our study at a total of 20 sites using ARUs (10 road sites, 5 coniferous forests, and 5 deciduous forests). Coniferous sites consisted primarily of white spruce (*Picea glauca*) while deciduous sites consisted primarily of trembling aspen (*Populus tremuloides*). Road sites occurred on flat, low-use forestry roads composed of gravel and clay. At a subset of the 20 sites (8 road, 4 coniferous, and 4 deciduous), observers stood adjacent to the ARUs and indicated which broadcasted sounds they were able to detect.

Data collection

At each site, we broadcasted known sounds from varying distances (see below) and evaluated whether or not a human observer could detect them. At the same time and location, we also recorded the broadcast sounds on four types of ARUs. All recordings made by the ARUs used 2-channel stereo recordings at 44 kHz and 16-bit .wav format. The four ARUs were: 1) Wildlife Acoustics' SongMeter SM2+ GPS-enabled recording units equipped with SMX-II weatherproof microphones (5 units); 2) Wildlife Acoustics' SM3 ARUs (5 units); 3) RiverForks CZM recorders (2 units); and 4) Zoom H1 handheld recorders (3 units). We broadcasted sounds with an Alpine ® SPR-60, 6-1/2" car speaker/tweeter and an Alpine ® UTE-42BT car stereo/audio player (Gentec Int'l, Markham, Ontario), both installed into an 11" (width) x 10" (depth) x 15" (height) plywood speaker box, along a transect from 12 to 1312m. We placed the speaker at 25m intervals for the first 400m, 50m intervals between 400-800m, and 100m intervals for broadcasts beyond 800m. The same sequence of calls was broadcast at each distance. On forested transects where the ARU was not visible from the transmitting unit, we used a GPS and compass to properly align the speaker towards the ARU.

The broadcasted sequence began with a series of 7 pure tones (at frequencies of 1000Hz, 1414Hz, 2000Hz, 2828Hz, 4000Hz, 5656Hz, and 8000Hz) generated using Adobe Audition CS6. The song sequence following the tones consisted of 23 boreal bird species and two amphibian species broadcast in the following order: Clay-colored Sparrow (*Spizella pallida*) (CCSP), Black-and-White Warbler (*Mniotilta varia*) (BAWW), Lincoln's Sparrow (*Melospiza lincolnii*) (LISP), Brown-headed Cowbird (*Molothrus ater*) (BHCO), Red-breasted Nuthatch (*Sitta canadensis*) (RBNU), Bay-breasted Warbler (*Setophaga castanea*) (CMWA), Dark-eyed Junco (*Junco hyemalis*) (DEJU), White-throated Sparrow (*Zonotrichia albicollis*) (WTSP), Cape May Warbler (*Setophaga tigrina*) (CMWA), Common Raven (*Corvus corax*) (CORA), Belted Kingfisher (*Megaceryle alcyon*) (BEKI), Olive-sided Flycatcher (*Contopus cooperi*) (OSFL), Pine Siskin (*Cardeulis pinus*) (PISI), Tennessee Warbler (*Oreothlypis peregrina*) (TEWA), Warbling Vireo (*Vireo gilvus*) (WAVI), Rose-breasted Grosbeak (*Pheucticus ludovicianus*)

(RBGR), Ovenbird (*Seiurus aurocapila*) (OVEN), Yellow Rail (*Coturnicops novaeboracensis*) (YERA), Western Toad (*Anaxyrus boreas*) (WETO), Canadian Toad (*Anaxyrus hemiophrys*) (CATO), Northern Saw-Whet Owl (*Aegolius acadicus*) (NSWO), Boreal Owl (*Aegolius funereus*) (BOOW), Long-eared Owl (*Asio otus*) (LEOW), Great Grey Owl (*Strix nebulosa*) (GGOW), and Barred Owl (*Strix varia*) (BADO). We selected these species for a variety of song characteristics that may affect probability of detection (pitch, song length). All sounds were normalized in Audition to bring peak amplitude to a standardized level. We broadcasted sounds at 90dB, which we measured 1m from the speaker system (based on fast-time A-weighting) using a handheld sound meter (Sper Scientific 840018).

At each transect, we attached each of the 4 ARU types to a tree or post at a height of 1.5m. This was the same height as the speaker broadcasting the recordings at the starting point of the transect and we chose transects with minimal elevational change. For each point along a transect, we recorded the time of the broadcast and distance of the broadcast speaker from the ARUs and human observer using a GPS (+/- 3m). We also measured temperature, humidity, and wind speed during each broadcast using a Kestrel 3000 pocket weather meter. Following the end of the broadcasted sequence, the first observer moved the speaker an additional 25m along the transect and the process was repeated.

We clipped recordings into individual files for each distance from each type of ARU. Observers in the lab listened to these files at 90dB and noted which species and tones they could identify and detect for each distance and each type of ARU recording. For this experiment, observers in the lab listened to tones and songs in the recordings in the original sequence that the tones and songs were broadcast to make things directly comparable to the HPC. For pure tones, observers only had to identify that a tone was present, not what frequency was broadcast. Using this method, we generated a large dataset of detections or non-detections from sounds that were known to have occurred (n = 96,502). During the HPC, the observer in the field recorded whether they could hear and correctly identify each sound as it was broadcast in sequence.

Modelling sources of variation influencing detection of sounds

We divided data randomly into 70% training data (n = 1,898 for each species or tone, without replacement) for model development and 30% test data (n = 813 for each species or tone) for model validation (**sample** function, R [R Core Team 2013]). We assessed the detection/non-detection of each species or tone using generalized linear models (**glm** function, R [R Core Team 2013]) with a binomial error family. All models included distance as a predictor of whether a tone or song was detected. We used a model where distance was the only predictor as a null model, where $p(d)$ declined with distance at the same rate in different habitats, in different weather conditions, and for human observers versus different ARU brands. We compared this null model to 11 candidate models (Table 3.1). For the weather models, we had considered temperature as well, but dropped that variable because it was positively correlated with humidity.

We used Akaike's Information Criterion to rank the relative fit of models (Burnham and Anderson 2002, Arnold 2010). To assess the absolute model fit or goodness-of-fit of the top AIC-ranked model, we used the area-under-the-curve (AUC) within receiver-operator curves for each species as a test statistic (**roc** function, *pROC* package, R [Robin et al. 2011]). AUC measures the proportion of actual detections and non-detections that were correctly predicted by the best model as opposed to false negatives or positives. We calculated AUC for the test data set excluded from model generation. We rated models with AUC > 0.70 as having sufficient ability to correctly predict if a song or tone was or was not detected (Vanagas 2004).

Estimating effective detection radius for different sounds

EDR gives the radius of the circle where the expected number of available individuals not detected within the distance equals the expected number of the detected individuals outside of that distance (Buckland et al. 1993). We estimated EDR for our Calling Lake dataset with a separate set of models rather than the set used for modelling detectability. The shape of the distance function describes how detection probability attenuates as a function of broadcast speaker distance (d) from the ARUs and human observer. The distance function is a strictly monotonic decreasing function with increasing distance. There are many different mathematical formulations to describe this shape, however we chose the half-normal distance function because of its simplicity, as well as the fact that its standard deviation parameter (τ) is directly interpretable as effective detection radius (EDR) for unlimited (i.e. not truncated) point counts in bird surveys (Sólymos et al. 2013). In the half-normal distance function, detection at a given distance can be modeled as $p(d) = \exp(-d^2/\tau^2)$ in which detection declines as object distance (d) from the observer increases, but declines at a slower rate as τ increases. We transformed distance in metres to $-d^2$ prior to modeling to linearize the relationship. We used the coefficients for different predictors in the best model to calculate EDR for each species or tone for different vegetation types, human observers, and ARU types. In all models, we set the intercept to zero so that $p(d) = 1$ at $d = 0$, and used a complementary log-log link function instead of the usual logit link function for GLMs with a binomial dependent variable, to simplify the estimation of EDR and approximate a log-linear model (Yip et al. 2017*a*). EDR was estimated as $\tau = (1/\beta)^{0.5}$, where β is the sum of coefficients for the main effect of distance (transformed as $-d^2$) and any interaction effects with $-d^2$ (for example: $\beta_{\text{ARU[relative to human observer]}} + \beta_{-d^2} + \beta_{\text{Habitat[relative to coniferous forest]}}$). After calculating EDR for the human observer and each ARU type, we then calculated a correction factor for the effective area sampled by each ARU type relative to human observers ($A'/A = EDR^2_{ARU}'/EDR^2_{human}$) in each vegetation type. This correction factor can be used to standardize the area parameter for animal density when comparing data from ARUs and human observers.

We performed Monte Carlo simulations to 1) estimate uncertainty in EDR point estimates for each sound, and 2) test for statistical differences between different vegetation types. We generated coefficients (n=1000) using maximum-likelihood estimates and variance-covariance matrices from the original models to calculate 90% confidence intervals from the predicted values (Appendix 2.3.1; Yip et al. 2017*a*). We omitted EDR estimates that 1) failed to solve due to lack of non-detections in the raw data, or 2) failed to generate confidence intervals due to high uncertainty when predicting from the original model.

We estimated MDD for the same data by selecting the largest distance with a correctly identified detection based on the 95% quantile of positive detections for each species. We estimated MDD separately for ARUs and human observers using the same data for our EDR calculations to compare results from both approaches. After estimating MDD, we calculated the maximum area sampled and correction factors for each ARU type relative to human observers ($A'/A = MDD^2_{ARU}'/MDD^2_{human}$) in each vegetation type, using the same method as for calculating correction factors for EDR.

Using known distance data to estimate effects of sound amplitude on detection

Study area

We used known distance data and broadcasts of the same species and tones to explore effects of sound amplitude on detection by ARUs. We conducted the amplitude study from

September - October 2014 in the Blackfoot-Cooking Lake Natural Area (53°25’ N, 112°49’ W) near Edmonton, Alberta from 09:00 – 16:00 MST. We placed ten transects in open vegetation (> 75% grass cover, < 5% shrub cover, 0% tree cover) and ten in denser vegetation (mature deciduous stands composed primarily of trembling aspen [*Populus tremuloides*] with small amounts of balsam poplar [*P. balsamifera*] and white spruce [*Picea glauca*]).

Data collection

At each transect we placed a SM2+ ARU in the same setup as the previous experiment and broadcasted songs and tones from a distance of 50, 100, and 150m away. We broadcast each song or tone at 11 sound pressure levels (a-weighted SPL, a measure of sound pressure relative to the threshold for human hearing) from 40 to 90 dB at 5 dB increments (=23 songs*11 amplitudes = 253 sounds played at each of the three distances). Each sequence of sounds at each amplitude lasted 1:43 and the full broadcast for all amplitudes was 18:53. For each distance within a transect, we noted temperature, humidity, and wind speed values averaged over the duration of the broadcast using a handheld Kestrel 3000 handheld weather metre (Nielsen-Kellerman Co., Boothwyn, Pennsylvania).

Following field data collection, we used the programs PRAAT © version 5.4 and Adobe Audition © version 5.0 to cut all recordings into separate clips for each call on the recording and labelled calls according to site type (open or closed), site number (1 – 10), species call/tone, and amplitude. We randomized the clipped files by shuffling them with generic empty clips (containing only ambient background noise). Without knowing the file contents, 4 volunteers trained in avian call detection and recognition listened to and labelled each sound clip by whether or not a call was heard, and if so, of what species.

Modelling sources of variation influencing detection of sounds

As in the HPC/ARU study, we used GLMs with intercept set to 0, distance transformed to $-d^2$, and a complimentary log-log link function to model whether or not a given song or tone was detected by observers listening to the ARU recordings. For each species or tone, we used a model where additive effects of distance and SPL were the only predictors of detection as a null model, where $p(d)$ declined with distance at the same rate in different habitats and weather conditions, and varied with broadcast amplitude. We compared this null model to five candidate models (Table 3.4). We followed the same procedure for assessing the relative fit of the above GLMs using AIC, and assessed the goodness-of-fit of the highest ranked or most parsimonious model for each species, using AUC statistics and receiver operating curves as in the HPC/ARU experiment (Table 3.5).

Estimating effective detection radius for different sounds

We used the coefficients for different predictors in the best model to calculate EDR for each species or tone for different vegetation types and SPLs as with the previous experiment. EDR was estimated as $\tau = (1/\beta)^{0.5}$, where β is the sum of coefficients for the main effect of distance (transformed as $-d^2$) and any interaction effects with $-d^2$ (for example: $\beta_{\text{SPL[45-90 dB in 5-dB increments]}} + \beta_{-d^2} + \beta_{\text{Open habitat[relative to closed habitat]}}$). We estimated uncertainty using the same Monte Carlo method to calculate 90% confidence intervals for our EDR estimates. We did not estimate MDD for our second experiment due to a lack of precision with our distance variables (only three were used).

RESULTS

Using known distance data to estimate effects of recorder technology, vegetation type, weather, species detection

Effective detection radii for humans and ARUs in different vegetation types with known-distance data

Detectability declined as distance to sound increased for all species and tones (mean ± SD across all models $\beta_x = 1.312\text{x}10^{-5} \pm 1.399\text{x}10^{-5}$; Table 3.3). Declines in detection rate were greater in both coniferous (mean $\beta_{\text{coniferous}} = -0.165 \pm 1.066$ relative to road) and deciduous (mean $\beta_{\text{deciduous}} = -1.482 \pm 1.456$ relative to road) vegetation types in comparison to open roadside transects (Fig. 3.1). 90% confidence intervals for our estimates of EDR from human detection data showed significant differences between roadside and forested detection distance for 18 of 32 sounds (5656Hz, 8000Hz, BAWW, BEKI, BHCO, BLWA, CCSP, DEJU, LISP, OSFL, OVEN, PISI, RBGR, RBNU, TEWA, WAVI, WTSP, YERA; Table 3.2). We were unable to assess roadside confidence intervals for five sounds (1414Hz, 2828Hz, CMWA, BOOW, NSWO) due to undefined EDR estimates. We found no significant difference in detection distance between coniferous or deciduous vegetation types. ARU type also influenced detectability although this varied depending on the species or tone present. However, detectability was generally higher for human observers relative to ARUs (mean relative to human: $\beta_{\text{SM2}} = -2.108 \pm 1.312$, $\beta_{\text{SM3}} = -0.963 \pm 1.086$, $\beta_{\text{RiverForks}} = -1.181 \pm 1.353$, $\beta_{\text{Zoom}} = -1.643 \pm 1.407$; Fig. 3.1). All top performing models included distance, transect type, and ARU type as important predictors (Table 3.2). The top performing model for 16 species and tones (1000Hz, 1414Hz, 2000Hz, BADO, CMWA, BOOW, CATO, CORA, GGOW, LEOW, NSWO, OSFL, RBGR, RBNU, WETO, WTSP) included humidity which positively influenced detectability for all sounds with the exception of

CMWA (mean $\beta_{humidity} = 0.020 \pm 0.013$). Three species (CATO, WETO, YERA) had wind in their top performing model which also had a positive influence (mean $\beta_{wind} = 0.191 \pm 0.046$). Interaction effects between ARU and transect type were part of the top performing model for seven sounds (BADO, BAWW, CMWA, BOOW, GGOW, LEOW, TEWA) indicating that detectability varied with both the type of ARU and the transect the sounds were broadcast through. For these sounds, detectability declines suddenly relative to ARUs as distance increases, particularly in coniferous vegetation types. Mean (± SD) wind speed averaged over the duration of the broadcast sequence at each distance along a transect was 1.1 ± 1.4km/h. Mean temperatures during each broadcast was 23.7 ± 6.5 ºC. Relative humidity was 59.0 ± 18.9%. Performance for all models was excellent (AUC: min = 0.9180, max = 0.9659, median = 0.9647; Table 3.2).

EDR and MDD values showed consistent differences between humans and different ARUs (Mean ± SD EDR for all sounds: Human = 494 ± 233m, SM2 = 421 ± 188m, SM3 = 461 ± 198m, RiverForks = 470 ± 222m, Zoom = 431 ± 183m; MDD: Human = 567 ± 266m, SM2 = 427 ± 235m, SM3 = 485 ± 231m, RiverForks = 516 ± 250m, Zoom = 442 ± 208m; Fig. 3.2; Appendix 2.1-2.2). Species and tones with lower detection probability (e.g. higher frequency tones, CMWA, BAWW, BLWA, YERA) had smaller EDR values than species with higher detection probability (e.g. lower-frequency tones, RBGR, toads, owls). EDR and MDD values were generally higher along roadsides than in forests (Mean EDR: Roadside = 612 ± 182m, Coniferous = 365 ± 114m, Deciduous = 378 ± 163m; Mean MDD: Roadside = 674 ± 227m, Coniferous = 364 ± 155m, Deciduous = 425 ± 221m). Human observers were consistently able to hear farther than the ARUs and had higher EDR and MDD values. SM2s had the lowest EDR and MDD values (mean ratios across all sounds: $EDR_{SM2}/EDR_{Human} = 0.789 \pm 0.624$;

$MDD_{SM2}/MDD_{Human} = 0.558 \pm 0.212$; Fig. 3.2). RiverForks ($EDR_{RiverForks}/EDR_{Human} = 0.940 \pm 0.680$; $MDD_{RiverForks}/MDD_{Human} = 0.861 \pm 0.354$) and SM3 ($EDR_{SM3}/EDR_{Human} = 0.897 \pm 0.137$; $MDD_{SM3}/MDD_{Human} = 0.770 \pm 0.259$) had the most similar detection distance relative to humans. These ratios increased at higher sound frequencies for the SM2 and RiverForks but decreased with Zoom recorders (Fig. 3.2; Appendix 2.1-2.2). Thus, SM2s require larger correction factors ($=[EDR_{SM2}/EDR_{Human}]^{-1}$) than other types of ARUs relative to humans.

Using known distance data to estimate effects of sound amplitude on detection

Effective detection radii for sounds at different amplitudes in different vegetation types

For all species and tones in the sound amplitude study, detection probability declined with increasing distance (mean ± SD across all models $\beta_x = 2.913 \times 10^{-4} \pm 1.476 \times 10^{-4}$; Table 3.6) and decreasing sound amplitude (mean $\beta_{SPL} = 0.183 \pm 0.037$). Probability of detection at a given distance was higher in open vegetation than in closed vegetation (mean $\beta_{OpenHabitat} = 1.983 \pm 0.899$, relative to closed habitat). The best model predicting detection of each species or tone generally included distance, vegetation type, and amplitude (Table 3.5). Four sounds (1414Hz, LEOW, YERA) included wind in their top performing model, two sounds (4000Hz, WETO) included humidity, and one sound (CMWA) included both wind and humidity. Wind negatively influenced detectability (mean $\beta_{Wind} = -0.168 \pm 0.076$) for all four sounds while humidity had a positive effect for CMWA ($\beta_{Humidity} = 0.023$) and WETO ($\beta_{Humidity} = 0.042$) but negative for 4000Hz ($\beta_{Humidity} = -0.036$). Mean wind speed averaged over the duration of the broadcast sequence at each distance along a transect was 4.0 ± 2.8km/h. Mean temperatures during each broadcast was 15.2 ± 6.4°C. Relative humidity was 50.5 ± 14.2%. Performance for all models was excellent (AUC: min = 0.8705, max = 0.9836, median = 0.9495; Table 3.5).

As in the human-ARU comparison study, species with relatively low detection probability (e.g. BAWW, CMWA) had smaller EDR values than species with relatively high detection probability (e.g. owls; Appendix 2.3). EDR values were generally higher in open vegetation than closed vegetation and increased as sound amplitude increased. When sounds were pooled into one general model, we found no significant interaction effects between SPL and the type of sound (i.e. species or tone) indicating a consistent positive relationship between EDR and SPL for all sounds broadcasted (Fig. 3.3). Many EDR values were undefined at higher broadcast SPL in open vegetation due to an inadequate number of non-detections. For EDR to be defined, non-detections must occur at the furthest distances which did not occur at higher sound amplitudes.

DISCUSSION

Detectability of avian vocalizations can be influenced by the surrounding environment (Darras et al. 2016, Yip et al. 2017*a*) and by the methods used to record and identify observations (Haselmayer and Quinn 2000). We compared detection distances of different ARUs as well as human observers in the field and found differences in detectability depending on which method was used. Using the ARU-human comparison calculated here, we conclude that ARU data can be integrated with HPC datasets into larger analyses to increase the scope of inferences made about birds (Cummings et al. 2010). For example, EDR has been estimated for over 100 species by the Boreal Avian Modelling Project (hereafter BAM; www.borealbirds.ca) using human-based distance estimation. Similarly, MDD for all North American species have been agreed upon by Partners in Flight (hereafter PIF; Rosenberg and Blancher 2005). For example, BAM estimates EDR for BAWW to be 50.1m and PIF uses a MDD value of 100m

(PIF Science Committee 2013). Thus, for surveys in deciduous forest using an SM2 wildlife recorder, the EDR correction factor calculated from our study would be 0.757 and the MDD correction factor 0.779 (Appendix 2.1-2.2). The corrected EDR would then be 37.9m and corrected MDD would be 77.9m for counts done using an SM2 in similar habitat. Ornithologists can directly compare density estimates from HPC and ARU data after standardizing both data types using this technique, enabling organizations like BAM or PIF to augment their existing HPC data with ARU data.

Human field observers had the highest detectability and detection distances in comparison to recordings from the SM2s, SM3s, RiverForks, and Zoom recorders. SM2s had the lowest detectability and detection distances followed by Zoom recorders, RiverForks, and SM3s. The use of ARUs to record animals introduces additional static, white noise, and electronic interference during the detection process of avian vocalizations, likely contributing to the patterns of decreasing detectability from recordings. However, we presented observers with a limited variety of species and sounds and in the first experiment, observers knew the order that the sounds would be occurring. When sounds are unpredictable and there is uncertainty about what species may be present, detections from recordings will likely increase relative to field surveys from humans due to the opportunity to double check observations in a lab-based environment.

Probability of detecting species declined more rapidly with increasing distance in closed vegetation than in open vegetation in both of our experiments (first experiment: roadside vs forest, second experiment: open grassland vs closed forest). These results are consistent with previously documented differences in detection between vegetation types (Schieck 1997, Pacifici et al. 2008). However, we observed differences in the effect of weather variables between experiments which may have been due to the distance over which the experiments occurred. Weather effects were influential for sounds with larger EDR values (17/32 sounds; Table 3.2) in our first experiment as in Holland (2001) and Simons et al. (2007), but were not as prevalent in our second experiment (6/32 sounds; Table 3.5). In our second experiment, broadcasts only occurred to a maximum of 150m, meaning weather variables may not have as much distance over which to act on broadcasted signals, suggesting there may be an interaction between weather conditions, distance, and sound transmission. Humidity had a consistently positive effect on detectability except for one species (CMWA) in our first experiment and one tone (4000Hz) in our second. However, the relationship between wind and detectability differed between the first (positive relationship) and second (negative relationship) experiment although wind was not included in many of our top performing models. We did not record the direction of the wind relative to the direction of our broadcasts, which may have contributed to this pattern. We also recorded higher but more consistent wind speeds in our second experiment relative to the first. A more limited range of wind speeds in the second experiment may be the reason wind was not included in those models as often. Knowing how factors like weather influences the area sampled is crucial to converting counts from ARUs and humans to accurate density estimates and is an area that we argue needs more work.

We found that EDR was consistently, positively correlated with broadcast SPL regardless of species (Fig. 3.3). This is important for two reasons. First, we broadcast sounds at 90dB which we believe to be the upper range of amplitudes that birds might vocalize at (Brumm 2004, Patricelli et al. 2007). We also had our speaker oriented directly at the receiver which may result in unrealistic and overestimated EDRs. However, the importance of this study lies in the relative difference in EDR between treatments, which should remain the same regardless of SPL. Given that EDR increased consistently with SPL for all species (Fig. 3.3), we believe singing volume could be estimated for real birds using predictions from our EDR models, corrections factors, and applying our model predictions to EDRs from BAM's human based estimates of EDR, albeit with varying degrees of uncertainty depending on model performance. This would also be under the assumption that EDRs estimated from BAM were calculated under similar conditions and that human observers estimate EDR accurately. It is not clear how accurate EDR measurements are by humans and our results show the importance of environmental variables such as the openness of the surrounding environment. Although our best performing models suggest that EDR increases consistently with SPL for most sounds, there were outlier sounds (BADO, LEOW) where EDR increased differently relative to the general trend (Fig. 3.3), possibly due to uncertainty in our EDR estimates.

The second reason that the consistent response of EDR to SPL is important is that it may provide a simpler way to calibrate ARUs to humans and each other. More recorder models are becoming available and the ones currently in use are routinely being updated with newer models, which have different gain settings, sensitivities, and residual electronic noise. All of these factors influence the area sampled for birds relative to humans and other ARUs (Rempel et al. 2005). Sound frequency acted differently on each recorder suggesting that microphone frequency response plays a role in detectability. Detectability decreased and differences in EDR and resulting correction factors increased with frequency for SM2s while the opposite was observed with SM3s and Zoom recorders (Fig. 3.2). The method we used to compare EDR between various recorders and human observers in our first experiment provided high resolution information on relative differences in detection distance, but was time consuming to carry out. We argue that, in the future, we could calibrate EDR at different amplitudes for multiple brands of ARUs using relatively few distances as in our second experiment, since EDR decreased consistently for most sounds as SPL declines and would be comparable to the relative difference in EDR at 90dB. This would allow researchers to calculate a correction factor more quickly based on the relative difference.

Our results provide further evidence supporting conclusions of previous researchers (Haselmayer and Quinn 2000, Hobson et al. 2002, Celis-Murillo et al. 2009) that the counts derived from both ARUs and human observers are relatively comparable. However, our study tested detectability under relatively controlled conditions through broadcasts and with a limited variety of species and sounds. The results found in this study may differ when field observers must identify overlapping vocalizations, unfamiliar species, or sounds in acoustically busy sampling periods which would likely have a larger influence on detectability than with ARUs. Although human observers appeared to generally detect more of the broadcasted sounds than different ARUs (particularly the SM2+), EDR and effective area sampled by some ARUs was comparable to that for human observers for some species. Furthermore, differences between recorders should be irrelevant if we can standardize data from different sources by offsetting varying detection distances and areas of ARUs. Influences of weather on EDR can be controlled to an extent by survey protocol (e.g. survey only when wind is <2 on the Beaufort scale, when there is no rain, etc.) and corrections for variables such as vegetation/habitat type can be calculated separately (Yip et al. 2017*a*) and applied in conjunction with corrections calculated in this study.

Although we demonstrate that simultaneous comparisons of HPC and ARU data potentially enable the calculation of EDR and densities of birds from ARU recordings, this approach still relies on accurate distance estimation during HPCs, an assumption that is frequently violated during avian surveys (Alldredge et al. 2007, Nadeau and Conway 2012). Errors in distance estimation can bias EDR and bird density calculations and will persist when using our correction approach for ARU data. There are also factors unrelated to distance estimation that should be also considered before collating these two types of point counts for the same analysis. First, some detections in HPC may be only visual, particularly of rare or of quiet species that are unavailable to ARUs, or rarely vocalizing species that are unlikely to be detected in short-duration recordings (Haselmayer and Quinn 2000, Hutto and Stutzman 2009). Second, as ARUs provide a permanent record for review, there may be a negative bias associated with species detection in HPC relative to ARU recordings as people listening to ARU data can re-listen to a sound (Tegeler et al. 2012). This bias could be modelled as observer effects. Calibration of ARUs should also be an important part of the permanent record. Microphone sensitivity can decrease with use (Turgeon et al. 2017) and influence the area surveyed. Microphone quality should be checked regularly to ensure minimal variation in detection distance within recorder models. Variation in detectability between observers can be large and influence results in both HPC and from ARU recordings in part due to differences in hearing ability and experience identifying species (Sauer et al. 1994). Observer variation within ARU point counts is likely lower than HPC as a permanent record allows multiple observers to process recordings and double check unknown species. Our study should minimize inter-observer variability because observers were presented with a limited number of sounds which they could review prior to the experiment. Observers were also comprised of males and females between the ages of 18-28 who are more likely to have similar hearing levels (Emlen and DeJong 1992).

Our objectives were to investigate relative differences between ARUs and HPC. We provide methods for standardizing and correcting detection distances to derive avian densities from

ARUs by accounting for differences in the area surveyed through each method. We used the ecosystems presented in this study as a case study to demonstrate application of this method, however these methods can be applied to other habitat types to broaden their use. This approach to density estimation would be more logistically feasible and affordable than studies using microphone arrays to obtain density (Efford and Dawson 2009). Integration of data from ARUs and HPCs could allow for larger meta-analyses to make environmental inferences about interactions between birds and the environment at larger spatial scales (Cumming et al. 2010).

Table 3.1. Candidate models to be compared against a null distance model for the ARU experiment.

Model	Parameters
D*V+A*V+H	Distance * Vegetation + ARU Type * Vegetation + Humidity
D*V+A*V+W+H	Distance * Vegetation + ARU Type * Vegetation + Wind + Humidity
D*V+A*V+W	Distance * Vegetation + ARU Type * Vegetation + Wind
D*V+A*V	Distance * Vegetation + ARU Type * Vegetation
D*V+A+H	Distance * Vegetation + ARU Type + Humidity
D*V+A+W+H	Distance * Vegetation + ARU Type + Wind + Humidity
D*V+A+W	Distance * Vegetation + ARU Type + Wind
D+V*A	Distance + Vegetation * ARU Type
D*V+A	Distance * Vegetation + ARU Type
D+V+A	Distance + Vegetation + ARU Type
null	Distance

Table 3.2. Model selection for factors influencing detection probability of different sounds for the ARU experiment and AUC statistics on test data for the top AIC-ranked model testing differences in detection distance between multiple models of ARU. All sounds used the same models for selection. We selected top models using lowest AICc value and ΔAICc. For multiple models with ΔAICc < 2, we selected the simplest model with fewest parameters (Arnold et al. 2010). "df" is the degrees of freedom and "logLik" is the log likelihood value for that particular model. "*" indicates variable interactions.

Sound	Model	df	logLik	AICc	ΔAIC	AICw	AUC
1000Hz	D*V+A+H	11	-678.06	1378.21	0	0.51881	0.9441
	null	2	-916.19	1836.39	458.183	0	
1414Hz	D*V+A+H	11	-689.35	1400.8	0	0.49834	0.9360
	null	2	-936.46	1876.91	476.112	0	
2000Hz	D*V+A+H	11	-623.6	1269.31	0	0.6919	0.9672
	null	2	-942.84	1889.69	620.382	0	
2828Hz	D*V+A	10	-659.49	1339.06	1.21257	0.21324	0.9636
	null	2	-1036.5	2077.1	739.249	0	
4000Hz	D*V+A	10	-618.16	1256.4	0.44416	0.28574	0.9648
	null	2	-1047.1	2098.23	842.276	0	
5656Hz	D*V+A	10	-534.65	1089.37	0.49016	0.29669	0.9752
	null	2	-914.53	1833.06	744.179	0	
8000Hz	D*V+A	10	-391.46	802.998	1.89928	0.13075	0.9856
	null	2	-647.63	1299.26	498.162	0	
BADO	D*V+A*V+H	19	-965.55	1969.38	0	0.70662	0.9203
	null	2	-1215	2434.02	464.639	0	
BAWW	D*V+A*V	18	-379.28	794.816	1.30815	0.18797	0.9862
	null	2	-646.36	1296.73	503.219	0	
BEKI	D*V+A	10	-556.69	1133.46	0.08014	0.24845	0.9758
	null	2	-924.58	1853.17	719.793	0	
BHCO	D*V+A	10	-622.73	1265.54	1.04612	0.14687	0.9662
	null	2	-1006.3	2016.59	752.104	0	
BLWA	D*V+A	10	-444.07	908.223	0.75359	0.29277	0.9858
	null	2	-763.45	1530.91	623.443	0	
BOOW	D*V+A*V+H	19	-827.59	1693.47	0	0.54341	0.9436
	null	2	-1074.3	2152.68	459.214	0	
CATO	D*V+A+W+H	12	-733.55	1491.24	0.23228	0.46589	0.9416
	null	2	-1007.2	2018.32	527.319	0	
CCSP	D*V+A	10	-468.75	957.582	0	0.35225	0.9859
	null	2	-897.44	1798.89	841.306	0	
CMWA	D*V+A*V+H	19	-368.18	774.646	0	0.65587	0.9865
	null	2	-641	1286.01	511.363	0	
CORA	D*V+A+H	11	-735.12	1492.33	0.92028	0.28789	0.9490
	null	2	-1172.7	2349.34	857.927	0	
DEJU	D*V+A	10	-590.54	1201.15	1.62045	0.11057	0.9765
	null	2	-1026.7	2057.33	857.799	0	
GGOW	D*V+A*V+H	19	-855.99	1750.26	0	0.73321	0.9483

	null	2	-1142	2288.09	537.832	0	
LEOW	D*V+A*V+H	19	-892.55	1823.39	0.08974	0.48878	0.9180
	null	2	-1258.4	2520.75	697.458	0	
LISP	D*V+A	10	-628.42	1276.92	0	0.29553	0.9655
	null	2	-1062.2	2128.4	851.48	0	
NSWO	D*V+A+H	11	-852.58	1727.25	0	0.47978	0.9359
	null	2	-1115.4	2234.75	507.495	0	
OSFL	D*V+A+H	11	-688.72	1399.54	0	0.58399	0.9564
	null	2	-1097.5	2198.97	799.422	0	
OVEN	D*V+A	10	-575.18	1170.44	0	0.27342	0.9789
	null	2	-1010.3	2024.55	854.107	0	
PISI	D*V+A	10	-508.41	1036.89	0	0.37464	0.9829
	null	2	-900.73	1805.46	768.572	0	
RBGR	D*V+A+H	11	-737.08	1496.26	0	0.64593	0.9634
	null	2	-1171.1	2346.27	850.011	0	
RBNU	D*V+A+H	11	-671.8	1365.71	0	0.42648	0.9602
	null	2	-1107.2	2218.38	852.67	0	
TEWA	D*V+A*V	18	-508.71	1053.67	1.96814	0.17829	0.9786
	null	2	-910.98	1825.97	774.272	0	
WAVI	D*V+A	10	-588.4	1196.88	0	0.38132	0.9740
	null	2	-1014.6	2033.14	836.257	0	
WETO	D*V+A+W+H	12	-825.33	1674.79	0	0.63449	0.9302
	null	2	-1085.2	2174.5	499.706	0	
WTSP	D*V+A+H	11	-661.53	1345.16	0	0.61309	0.9711
	null	2	-1065.4	2134.85	789.682	0	
YERA	D*V+A+W	11	-447.41	916.932	0	0.54501	0.9776
	null	2	-699.65	1403.31	486.381	0	

Table 3.3. Model coefficients (recorder type, habitat type, distance, interactions between habitat type and distance, wind, humidity) for the top AIC-ranked model predicting probability of detecting each species and tone with RiverForks (RF), SM2, SM3, and Zoom (Zm) recorders, in listening trials conducted at 20 transects near Calling Lake and Lac La Biche, Alberta, Canada in 2014. x is equal to -(Distance)^2. The reference level for coniferous (Co) and deciduous (Dec) habitat is roadside habitat. "NA" means that variable was not included in the top model for that sound. "*" indicates variable interactions.

Sound	Int.	x	Co	Dec	RF	SM2	SM3	Zm	Wind	Humidity	x*Co	x*Dec	Co*RF	Co*SM2	Co*SM3	Co*Zm	Dec*RF	Dec*SM2	Dec*SM3	Dec*Zm
1000 Hz	3.54 ± 0.46	2.84E-06 ± 2.54E-07	-1.48 ± 0.36	-1.58 ± 0.35	-0.58 ± 0.31	-1.28 ± 0.30	-1.18 ± 0.30	-1.23 ± 0.30	NA	3.07E-02 ± 5.94E-03	3.11E-06 ± 6.22E-07	1.52E-06 ± 5.11E-07	NA	NA	NA	NA	NA	NA	NA	NA
1414 Hz	3.72 ± 0.47	3.08E-06 ± 2.53E-07	-1.67 ± 0.35	-1.68 ± 0.34	-0.73 ± 0.32	-1.43 ± 0.31	-1.16 ± 0.31	-1.65 ± 0.31	NA	3.17E-02 ± 5.79E-03	2.95E-06 ± 6.46E-07	1.47E-06 ± 5.26E-07	NA	NA	NA	NA	NA	NA	NA	NA
2000 Hz	4.04 ± 0.44	3.70E-06 ± 2.83E-07	-1.20 ± 0.42	-1.99 ± 0.36	-0.61 ± 0.30	-1.07 ± 0.30	-0.39 ± 0.30	-1.09 ± 0.30	NA	2.30E-02 ± 5.94E-03	6.64E-06 ± 1.01E-06	1.44E-06 ± 5.93E-07	NA	NA	NA	NA	NA	NA	NA	NA
2828 Hz	5.02 ± 0.35	4.07E-06 ± 2.87E-07	-0.81 ± 0.42	-2.13 ± 0.34	-0.11 ± 0.30	-1.24 ± 0.29	-0.20 ± 0.30	-0.82 ± 0.29	NA	NA	1.05E-05 ± 1.46E-06	2.15E-06 ± 7.06E-07	NA	NA	NA	NA	NA	NA	NA	NA
4000 Hz	5.21 ± 0.37	6.66E-06 ± 4.84E-07	-0.25 ± 0.54	-2.68 ± 0.37	-0.31 ± 0.30	-1.02 ± 0.30	0.22 ± 0.31	-0.85 ± 0.30	NA	NA	2.27E-05 ± 3.26E-06	5.42E-06 ± 1.36E-06	NA	NA	NA	NA	NA	NA	NA	NA
5656 Hz	5.78 ± 0.44	1.49E-05 ± 1.05E-06	-1.22 ± 0.53	-2.40 ± 0.47	-0.66 ± 0.33	-1.55 ± 0.33	-0.06 ± 0.34	-0.68 ± 0.33	NA	NA	2.34E-05 ± 4.38E-06	2.72E-05 ± 4.95E-06	NA	NA	NA	NA	NA	NA	NA	NA
8000 Hz	6.66 ± 0.52	5.17E-05 ± 3.99E-06	-1.03 ± 0.46	-0.48 ± 0.57	-1.62 ± 0.41	-4.34 ± 0.46	-2.31 ± 0.42	-3.28 ± 0.44	NA	NA	4.19E-05 ± 1.13E-05	1.11E-04 ± 2.11E-05	NA	NA	NA	NA	NA	NA	NA	NA
BADO	3.91 ± 0.57	4.37E-06 ± 3.22E-07	-1.18 ± 0.76	-2.69 ± 0.62	-2.48 ± 0.49	-2.96 ± 0.50	-2.18 ± 0.50	-3.54 ± 0.50	NA	2.73E-02 ± 4.63E-03	4.66E-06 ± 1.02E-06	9.00E-07 ± 6.64E-07	-0.36 ± 0.74	-0.05 ± 0.76	0.34 ± 0.75	0.78 ± 0.76	2.18 ± 0.66	2.29 ± 0.66	1.04 ± 0.64	1.59 ± 0.64
BAWW	8.57 ± 0.82	4.55E-05 ± 3.84E-06	-1.20 ± 1.40	-4.78 ± 1.11	-4.53 ± 0.67	-4.74 ± 0.68	-2.72 ± 0.64	-4.84 ± 0.69	NA	NA	5.43E-05 ± 1.39E-05	5.91E-05 ± 1.54E-05	0.16 ± 1.20	0.12 ± 1.22	0.09 ± 1.11	1.44 ± 1.15	4.66 ± 1.05	5.04 ± 1.07	2.47 ± 1	3.40 ± 1.05
BBWA	9.37 ± 1.01	5.61E-05 ± 4.80E-06	-1.13 ± 1.49	3.58 ± 2.62	-4.54 ± 0.71	-6.10 ± 0.77	-4.00 ± 0.72	-5.30 ± 0.74	NA	-0.0196 ± 0.00732	1.01E-04 ± 2.47E-05	2.15E-04 ± 5.33E-05	1.29 ± 1.26	0.85 ± 1.40	1.38 ± 1.25	2.22 ± 1.28	-0.14 ± 1.74	-1.52 ± 2.19	-4.24 ± 2.20	-3.92 ± 2.31
BEKI	4.48 ± 0.35	1.49E-05 ± 1.02E-06	9.08E-04 ± 0.43	-0.40 ± 0.44	-0.94 ± 0.33	-2.26 ± 0.32	-0.24 ± 0.33	-0.91 ± 0.32	NA	NA	3.96E-05 ± 5.89E-06	5.47E-06 ± 8.35E-06	NA	NA	NA	NA	NA	NA	NA	NA
BHCO	4.58 ± 0.32	1.05E-05 ± 6.94E-07	-0.28 ± 0.41	-1.60 ± 0.35	-0.82 ± 0.29	-2.06 ± 0.29	-0.32 ± 0.30	-0.61 ± 0.30	NA	NA	2.86E-05 ± 4.04E-06	2.17E-05 ± 3.79E-06	NA	NA	NA	NA	NA	NA	NA	NA
BLWA	4.79 ± 0.39	2.76E-05 ± 2.21E-06	-0.21 ± 0.53	-1.18 ± 0.45	-0.97 ± 0.34	-1.82 ± 0.34	-0.52 ± 0.35	-1.03 ± 0.35	NA	NA	6.02E-05 ± 1.12E-05	5.11E-05 ± 1.02E-05	NA	NA	NA	NA	NA	NA	NA	NA
BOOW	3.82 ± 0.53	4.12E-06 ± 2.94E-07	-0.72 ± 0.73	-2.23 ± 0.60	-0.86 ± 0.47	-1.08 ± 0.48	-1.36 ± 0.46	-2.51 ± 0.45	NA	2.00E-02 ± 4.97E-03	3.68E-06 ± 8.09E-07	2.15E-06 ± 7.26E-07	-0.97 ± 0.74	-1.42 ± 0.75	-0.34 ± 0.72	0.32 ± 0.72	0.54 ± 0.66	1.45 ± 0.68	1.12 ± 0.65	1.22 ± 0.63
CATO	1.09 ± 0.40	4.64E-06 ± 3.52E-07	0.52 ± 0.40	-0.40 ± 0.28	-0.43 ± 0.27	-1.70 ± 0.26	-0.64 ± 0.28	-0.96 ± 0.27	0.24 ± 0.08	3.66E-02 ± 5.10E-03	1.72E-05 ± 2.61E-06	3.34E-06 ± 1.01E-06	NA	NA	NA	NA	NA	NA	NA	NA
CCSP	5.81 ± 0.43	1.66E-05 ± 1.17E-06	-0.93 ± 0.46	-0.85 ± 0.51	-1.72 ± 0.36	-2.22 ± 0.36	-0.93 ± 0.36	-1.89 ± 0.37	NA	NA	2.79E-05 ± 4.78E-06	6.33E-05 ± 9.80E-06	NA	NA	NA	NA	NA	NA	NA	NA

CORA	3.15 ± 0.42	5.41E-06 ± 3.74E-07	1.68 ± 0.61	-1.83 ± 0.28	-0.21 ± 0.29	-1.35 ± 0.28	-0.70 ± 0.29	-1.17 ± 0.28	NA	1.84E-02 ± 5.09E-03	4.25E-05 ± 5.51E-06	5.44E-06 ± 1.4E-06	NA	NA	NA	NA	NA	NA	NA	NA
DEJU	5.02 ± 0.36	1.12E-05 ± 7.42E-07	-0.33 ± 0.43	-1.08 ± 0.40	-1.34 ± 0.33	-2.10 ± 0.33	-0.78 ± 0.33	-1.26 ± 0.32	NA	NA	3.10E-05 ± 4.51E-06	3.70E-05 ± 5.60E-06	NA	NA	NA	NA	NA	NA	NA	NA
GGOW	3.17 ± 0.48	4.13E-06 ± 3.00E-07	-0.94 ± 0.66	-1.35 ± 0.60	-2.08 ± 0.41	-2.05 ± 0.42	-1.55 ± 0.42	-2.74 ± 0.41	NA	2.54E-02 ± 4.74E-03	1.15E-05 ± 1.61E-06	3.71E-06 ± 8.79E-07	1.32 ± 0.69	0.28 ± 0.71	1.38 ± 0.71	1.90 ± 0.69	1.08 ± 0.63	1.60 ± 0.66	0.64 ± 0.64	0.87 ± 0.62
LEOW	6.12 ± 0.77	5.11E-06 ± 3.79E-07	0.04 ± 1.27	-4.58 ± 0.82	-5.19 ± 0.67	-5.26 ± 0.67	-4.22 ± 0.66	-5.58 ± 0.69	NA	2.51E-02 ± 4.73E-03	1.40E-05 ±2.26E-06	3.83E-07 ± 7.43E-07	-0.49 ± 1.18	-1.05 ± 1.19	1.90 ± 1.12	0.32 ± 1.15	4.16 ± 0.81	4.45 ± 0.82	2.26 ± 0.79	3.42 ± 0.82
LISP	4.80 ± 0.34	1.02E-05 ± 6.82E-07	0.46 ± 0.55	-1.78 ± 0.35	-0.93 ± 0.30	-1.75 ± 0.30	-0.69 ± 0.30	-0.82 ± 0.30	NA	NA	3.84E-05 ± 5.77E-06	1.94E-05 ± 3.43E-06	NA	NA	NA	NA	NA	NA	NA	NA
NSWO	3.32 ± 0.39	4.28E-06 ± 2.96E-07	-1.49 ± 0.30	-1.86 ± 0.28	0.65 ± 0.27	-0.44 ± 0.25	-0.18 ± 0.24	-0.94 ± 0.24	NA	1.32E-02 ± 4.70E-03	5.95E-06 ± 1.07E-06	2.94E-07 ± 5.70E-07	NA	NA	NA	NA	NA	NA	NA	NA
OSFL	3.18 ± 0.43	7.36E-06 ± 5.11E-07	1.55 ± 0.68	-2.06 ± 0.31	-0.15 ± 0.28	-1.13 ± 0.28	0.01 ± 0.28	-0.48 ± 0.28	NA	1.82E-02 ± 5.46E-03	3.91E-05 ± 5.60E-06	5.52E-06 ± 1.65E-06	NA	NA	NA	NA	NA	NA	NA	NA
OVEN	5.38 ± 0.38	1.21E-05 ± 8.18E-07	-0.38 ± 0.44	-1.51 ± 0.39	-1.49 ± 0.33	-2.39 ± 0.34	-1.22 ± 0.33	-1.40 ± 0.33	NA	NA	3.16E-05 ± 4.70E-06	3.16E-05 ± 5.04E-06	NA	NA	NA	NA	NA	NA	NA	NA
PISI	5.16 ± 0.38	1.49E-05 ± 1.03E-06	-0.36 ± 0.47	-1.09 ± 0.45	-1.27 ± 0.33	-1.91 ± 0.34	-0.72 ± 0.32	-0.91 ± 0.33	NA	NA	3.36E-05 ± 5.29E-06	4.50E-05 ± 7.08E-06	NA	NA	NA	NA	NA	NA	NA	NA
RBGR	2.97 ± 0.39	4.67E-06 ± 3.24E-07	1.19 ± 0.55	-1.68 ± 0.27	0.26 ± 0.27	-0.99 ± 0.25	0.06 ± 0.27	-0.34 ± 0.26	NA	0.01193 ± 0.004757	3.59E-05 ± 4.65E-06	4.54E-06 ± 1.12E-06	NA	NA	NA	NA	NA	NA	NA	NA
RBNU	3.23 ± 0.43	4.61E-06 ± 3.14E-07	1.53 ± 0.63	-1.54 ± 0.29	-0.27 ± 0.29	-1.42 ± 0.28	-0.24 ± 0.29	-0.72 ± 0.29	NA	1.82E-02 ± 5.33E-03	3.21E-05 ± 4.49E-06	5.27E-06 ± 1.07E-06	NA	NA	NA	NA	NA	NA	NA	NA
TEWA	4.96 ± 0.49	1.83E-05 ± 1.37E-06	2.50 ± 1.32	-0.07 ± 1.00	-1.87 ± 0.47	-2.91 ± 0.48	-1.05 ± 0.50	-1.22 ± 0.48	NA	NA	6.83E-05 ± 1.20E-05	7.19E-05 ± 1.28E-05	-1.79 ± 1.13	-2.62 ± 1.24	-2.61 ± 1.13	-3.17 ± 1.19	-0.47 ± 0.96	0.51 ± 0.99	-0.82 ± 0.92	-1.34 ± 0.96
WAVI	4.62 ± 0.34	1.13E-05 ± 7.54E-07	-0.05 ± 0.49	-2 ± 0.36	-0.52 ± 0.30	-1.52 ± 0.30	-0.17 ± 0.30	-0.71 ± 0.30	NA	NA	3.48E-05 ± 5.18E-06	2.16E-05 ± 3.98E-06	NA	NA	NA	NA	NA	NA	NA	NA
WETO	0.82 ± 0.37	3.72E-06 ± 2.92E-07	0.62 ± 0.33	0.23 ± 0.27	-0.41 ± 0.25	-1.67 ± 0.24	-0.84 ± 0.25	-1.44 ± 0.24	0.15 ± 0.06	3.21E-02 ± 4.65E-03	1.21E-05 ± 1.91E-06	6.41E-06 ± 1.20E-06	NA	NA	NA	NA	NA	NA	NA	NA
WTSP	3.67 ± 0.42	5.97E-06 ± 4.18E-07	0.62 ± 0.55	-2.18 ± 0.30	-0.06 ± 0.29	-1.03 ± 0.27	0.09 ± 0.29	-0.44 ± 0.28	NA	1.15E-02 ± 4.95E-03	2.56E-05 ± 3.78E-06	3.95E-06 ± 1.23E-06	NA	NA	NA	NA	NA	NA	NA	NA
YEAR	3.78 ± 0.37	2.55E-05 ± 2.10E-06	0.86 ± 0.53	0.48 ± 0.52	-0.96 ± 0.35	-2.65 ± 0.35	-0.60 ± 0.36	-1.23 ± 0.35	0.18 ± 0.07	NA	7.10E-05 ± 1.28E-05	8.27E-05 ± 1.51E-05	NA	NA	NA	NA	NA	NA	NA	NA

Table 3.4. Candidate models to be compared against a null distance model for the SPL experiment.

Model	Parameters
D*V+S+W+H	Distance * Vegetation + SPL + Wind + Humidity
D*V+S+H	Distance * Vegetation + SPL + Humidity
D*V+S+W	Distance * Vegetation + SPL + Wind
D*V+S	Distance * Vegetation + SPL
D+S+V	Distance + SPL + Vegetation
null	Distance

Table 3.5. Model selection for factors influencing detection probability of different sounds for the SPL experiment and AUC statistics on test data for the top AIC-ranked model testing differences in detection with varying SPL. All sounds used the same models for selection. We selected top models using lowest AICc value and ΔAICc. For multiple models with ΔAICc < 2, we selected the simplest model with fewest parameters (Arnold et al. 2010). “df” is the degrees of freedom and “logLik” is the log likelihood value for that particular model. “*” indicates variable interactions.

Sound	Model	df	logLik	AICc	ΔAIC	AICw	AUC
1000Hz	D+S+V	4	-174.77	357.624	1.02958	0.23285	0.8989
	null	3	-204.68	415.407	58.8134	0	
1414Hz	D*V+S+W	6	-157	326.164	0	0.70592	0.9337
	null	3	-212.93	431.9	105.736	0	
2000Hz	D*V+S	5	-130.41	270.956	0	0.47529	0.9376
	null	3	-196.99	400.037	129.08	0	
2828Hz	D+S+V	4	-128.21	264.511	1.05645	0.18359	0.9530
	null	3	-183.54	373.134	109.679	0	
4000Hz	D*V+S+H	6	-137.36	286.892	0	0.65231	0.9286
	null	3	-200.76	407.57	120.678	0	
5656Hz	D*V+S	5	-134.05	278.227	0	0.47408	0.9468
	null	3	-219.32	444.684	166.457	0	
8000Hz	D+S+V	4	-145.2	298.489	0	0.4728	0.8732
	null	3	-154.28	314.617	16.1271	0.00015	
BADO	D*V+S	5	-174.47	359.069	0.04153	0.29076	0.9026
	null	3	-184.18	374.401	15.3734	0.00014	
BAWW	D*V+S	5	-121.15	252.422	0.17268	0.34988	0.9484
	null	3	-188.9	383.846	131.597	0	
BEKI	D*V+S	5	-94.142	198.408	0	0.43996	0.9669
	null	3	-179.37	364.798	166.39	0	
BHCO	D*V+S	5	-138.66	287.446	0	0.51571	0.9150
	null	3	-231.26	468.563	181.116	0	
BLWA	D*V+S	5	-122.69	255.513	0	0.41554	0.9556
	null	3	-185.04	376.137	120.623	0	
BOOW	D*V+S	5	-141.16	292.459	0	0.44656	0.9473
	null	3	-168.2	342.459	50.0003	0	
CATO	D+S+V	4	-125.29	258.672	0.65638	0.26736	0.9612
	null	3	-173.07	352.203	94.1878	0	
CCSP	D*V+S	5	-110.37	230.876	0	0.34889	0.9627
	null	3	-212.21	430.469	199.593	0	
CMWA	D*V+S+W+H	7	-115.55	245.34	0	0.57437	0.8705
	null	3	-140.1	286.247	40.907	0	
CORA	D*V+S	5	-131.11	272.361	1.91579	0.20263	0.9286
	null	3	-190.52	387.094	116.648	0	
DEJU	D*V+S	5	-121.69	253.499	0	0.50504	0.9476
	null	3	-221.87	449.795	196.296	0	
GGOW	D+S+V	4	-154.01	316.097	1.41848	0.19217	0.9205

	null	3	-177.89	361.824	47.1454	0	
LEOW	D*V+S+W	6	-167.41	347.01	0	0.58855	0.9505
	null	3	-173.06	352.173	5.16266	0.04454	
LISP	D*V+S	5	-107.61	225.361	0	0.53271	0.9808
	null	3	-197.36	400.777	175.416	0	
NSWO	D*V+S	5	-152.5	315.116	0	0.4052	0.9113
	null	3	-209.02	424.082	108.967	0	
OSFL	D*V+S	5	-126.27	262.68	0	0.44356	0.9836
	null	3	-193.46	392.968	130.289	0	
OVEN	D*V+S	5	-99.705	209.536	0	0.53143	0.9649
	null	3	-213.27	432.587	223.051	0	
PISI	D*V+S	5	-103.87	217.868	0.38708	0.32376	0.9721
	null	3	-216.71	439.46	221.979	0	
RBGR	D*V+S	5	-149.31	308.756	0.53372	0.2544	0.9569
	null	3	-208.46	422.974	114.752	0	
RBNU	D*V+S	5	-95.736	201.6	0	0.40291	0.9823
	null	3	-187.34	380.727	179.127	0	
TEWA	D*V+S	5	-94.862	199.85	0	0.51786	0.9828
	null	3	-155.97	317.992	118.142	0	
WAVI	D*V+S	5	-110.61	231.344	0	0.32514	0.9561
	null	3	-187.42	380.898	149.554	0	
WETO	D*V+S+H	6	-134.66	281.524	0	0.68689	0.9363
	null	3	-180.56	367.18	85.656	0	
WTSP	D*V+S	5	-97.034	204.205	0	0.40879	0.9708
	null	3	-190.93	387.906	183.701	0	
YERA	D*V+S+W	6	-96.075	204.342	0	0.43954	0.9650
	null	3	-134.19	274.437	70.0948	0	

Table 3.6. Model coefficients (amplitude, distance, habitat type, interactions between habitat type and distance, wind, humidity) for the top AIC-ranked model predicting probability of detecting each species and tone, in listening trials conducted along 20 transects in the Blackfoot-Cooking Lake Natural Area near Edmonton, Alberta, Canada in 2014. x is equal to -(Distance)^2. SPL = amplitude (dB). The reference level for open habitat is closed habitat. "NA" means that variable was not included in the top model for that sound.

Sound	Intercept	x	HabitatOPEN	SPL	Wind	Humidity	x*HabitatOPEN
1000Hz	-5.522 ± 0.8325	1.05E-04 ± 2.09E-05	2.151 ± 0.3579	0.1075 ± 0.01356	NA	NA	NA
1414Hz	-9.444 ± 1.16	1.74E-04 ± 3.29E-05	2.505 ± 0.6005	0.181 ± 0.02048	-0.1651 ± 0.06309	NA	-4.16E-05 ± 4.16E-05
2000Hz	-8.87 ± 1.232	2.05E-04 ± 3.60E-05	1.999 ± 0.6706	0.1708 ± 0.02141	NA	NA	-1.39E-04 ± 4.89E-05
2828Hz	-9.332 ± 1.204	1.55E-04 ± 2.55E-05	3.335 ± 0.4805	0.1725 ± 0.0205	NA	NA	NA
4000Hz	-8.304 ± 1.295	2.06E-04 ± 3.96E-05	3.444 ± 0.7512	0.1861 ± 0.02251	NA	-0.0356 ± 0.01425	6.09E-05 ± 4.81E-05
5656Hz	-8.75 ± 1.184	2.91E-04 ± 4.59E-05	2.197 ± 0.6653	0.1569 ± 0.01883	NA	NA	-1.68E-04 ± 5.14E-05
8000Hz	-8.673 ± 1.214	1.52E-04 ± 2.90E-05	1.334 ± 0.3882	0.1071 ± 0.01543	NA	NA	NA
BADO	-8.549 ± 1.046	1.73E-04 ± 3.29E-05	0.5262 ± 0.544	0.1614 ± 0.01756	NA	NA	-6.68E-05 ± 4.02E-05
BAWW	-11.46 ± 1.605	4.53E-04 ± 9.51E-05	2.023 ± 0.778	0.1832 ± 0.02288	NA	NA	-2.77E-04 ± 9.32E-05
BEKI	-15.62 ± 2.215	5.49E-04 ± 1.21E-04	2.134 ± 0.8948	0.2316 ± 0.03046	NA	NA	-4.11E-04 ± 1.19E-04
BHCO	-11.11 ± 1.447	3.37E-04 ± 5.96E-05	2.265 ± 0.6906	0.1859 ± 0.02231	NA	NA	-2.31E-04 ± 6.24E-05
BLWA	-10.33 ± 1.472	4.09E-04 ± 9.06E-05	1.271 ± 0.7414	0.1591 ± 0.01998	NA	NA	-2.95E-04 ± 9.21E-05
BOOW	-7.506 ± 1.05	1.85E-04 ± 3.42E-05	0.9213 ± 0.6025	0.1457 ± 0.01773	NA	NA	-8.26E-05 ± 4.37E-05
CATO	-12.3 ± 1.453	1.38E-04 ± 2.60E-05	2.844 ± 0.4705	0.1898 ± 0.02177	NA	NA	NA
CCSP	-13.21 ± 1.783	5.16E-04 ± 9.73E-05	2.498 ± 0.794	0.221 ± 0.02743	NA	NA	-3.60E-04 ± 9.33E-05
CMWA	-12.48 ± 2.066	2.82E-04 ± 9.71E-05	1.866 ± 0.7697	0.1466 ± 0.0229	-0.05099 ± 0.1022	0.02312 ± 0.016	-8.02E-05 ± 1.01E-04
CORA	-12.54 ± 1.567	2.33E-04 ± 4.63E-05	1.486 ± 0.6848	0.2076 ± 0.02417	NA	NA	-1.50E-04 ± 5.13E-05
DEJU	-11.94 ± 1.577	3.22E-04 ± 5.93E-05	2.774 ± 0.7522	0.1919 ± 0.02333	NA	NA	-1.96E-04 ± 6.31E-05
GGOW	-9.475 ± 1.07	1.31E-04 ± 2.39E-05	2.06 ± 0.3742	0.1564 ± 0.0168	NA	NA	NA
LEOW	-7.861 ± 0.9351	1.02E-04 ± 2.97E-05	0.5742 ± 0.527	0.1354 ± 0.01439	-0.09756 ± 0.05937	NA	6.13E-06 ± 3.86E-05
LISP	-11.07 ± 1.461	3.68E-04 ± 7.15E-05	1.741 ± 0.6862	0.1805 ± 0.02161	NA	NA	-2.49E-04 ± 7.50E-05
NSWO	-10.13 ± 1.253	2.57E-04 ± 3.77E-05	0.8892 ± 0.6186	0.184 ± 0.02056	NA	NA	-1.91E-04 ± 4.64E-05
OSFL	-8.271 ± 1.1	2.19E-04 ± 3.94E-05	2.247 ± 0.6157	0.145 ± 0.01765	NA	NA	-9.70E-05 ± 4.50E-05
OVEN	-14.44 ± 2.058	4.93E-04 ± 1.03E-04	3.408 ± 0.959	0.2366 ± 0.03041	NA	NA	-2.80E-04 ± 9.77E-05
PISI	-13.97 ± 1.972	5.63E-04 ± 1.13E-04	2.798 ± 0.9211	0.2329 ± 0.0294	NA	NA	-4.07E-04 ± 1.09E-04
RBGR	-9.132 ± 1.157	2.59E-04 ± 4.40E-05	0.6957 ± 0.598	0.1522 ± 0.01721	NA	NA	-1.92E-04 ± 4.89E-05
RBNU	-12.5 ± 1.646	3.32E-04 ± 5.34E-05	2.046 ± 0.777	0.2222 ± 0.02729	NA	NA	-2.24E-04 ± 5.73E-05
TEWA	-15.43 ± 2.033	4.40E-04 ± 1.11E-04	2.095 ± 0.8189	0.2191 ± 0.02727	NA	NA	-2.87E-04 ± 1.11E-04
WAVI	-12.28 ± 1.496	4.03E-04 ± 7.74E-05	1.22 ± 0.71	0.2048 ± 0.02313	NA	NA	-2.99E-04 ± 8.00E-05

WETO	-13.72 ± 1.78	2.04E-04 ± 3.84E-05	1.527 ± 0.649	0.19 ± 0.02214	NA	0.04153 ± 0.01314	-1.18E-04 ± 4.55E-05
WTSP	-11.42 ± 1.575	2.44E-04 ± 4.56E-05	3.909 ± 0.858	0.2021 ± 0.02622	NA	NA	-1.01E-04 ± 5.44E-05
YERA	-14.08 ± 2.14	3.79E-04 ± 1.21E-04	1.593 ± 0.8316	0.1949 ± 0.02761	-0.1427 ± 0.09392	NA	-2.44E-04 ± 1.22E-04

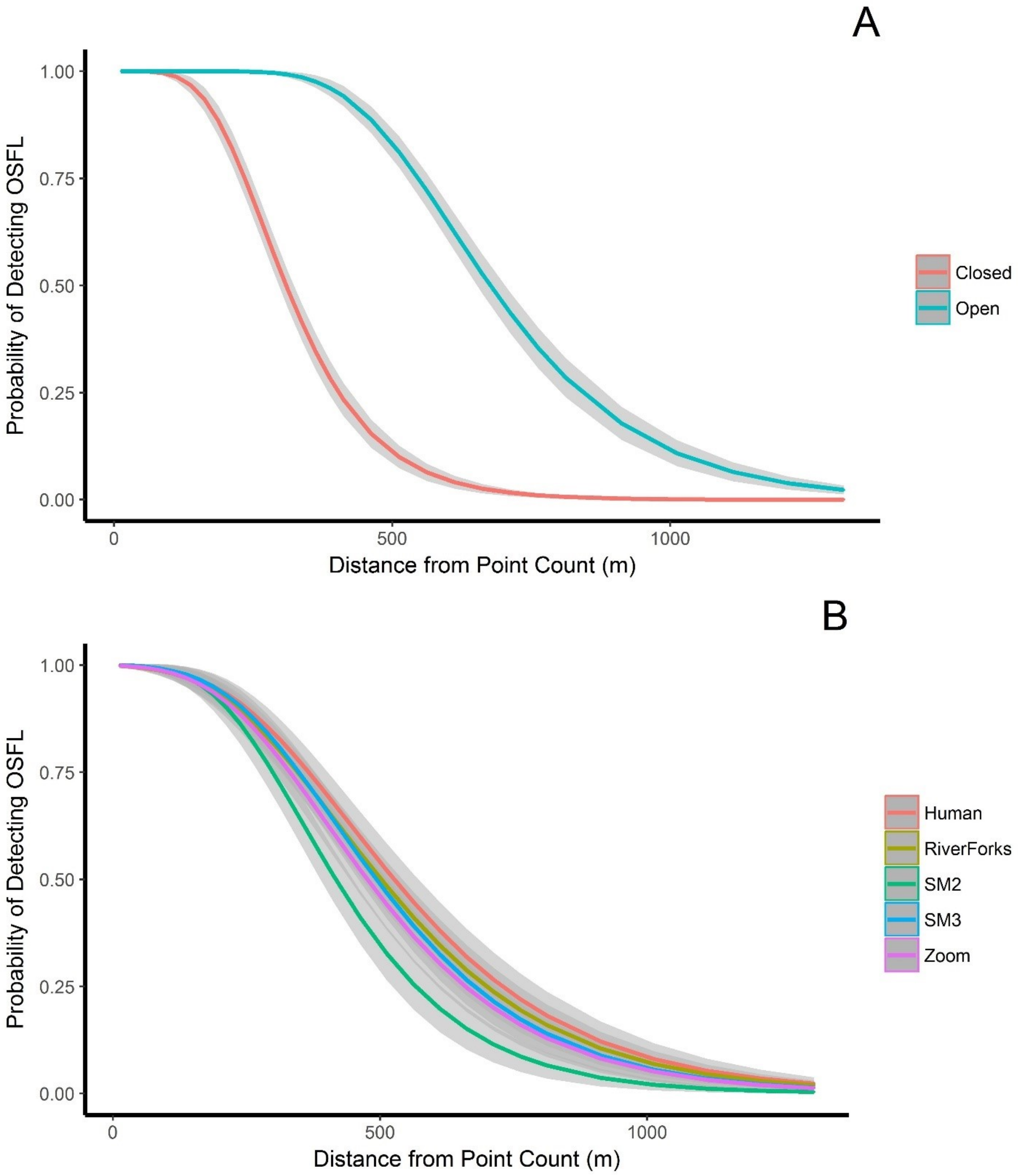

Figure 3.1. Probability of detecting OSFL with distance from ARU in (**A**) open (roadside) and closed (forested) habitat, and (**B**) with human observers, RiverForks, SM2, SM3, and Zoom recorders. Predictions are calculated from binomial detection data and plotted with 95% confidence intervals.

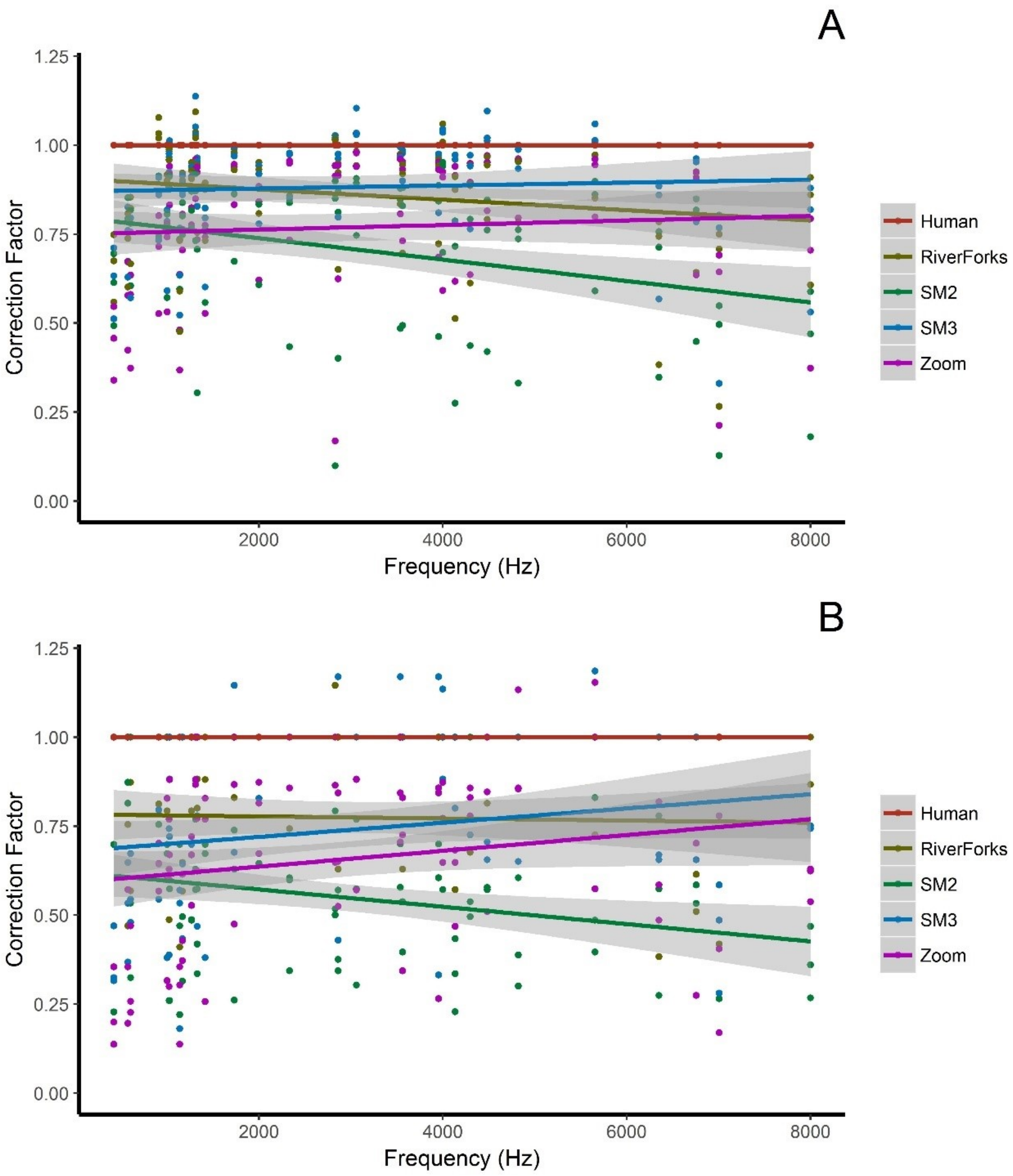

Figure 3.2. Correction factors for (**A**) EDR and (**B**) MDD of various ARU types at different frequencies. ARUs are in comparison to human detection as a reference. Correction factors are calculated using a ratio of detection area of ARU to detection area of a field observer (Appendix 2.1-2.2). Correction factors less than 1 mean smaller detection distances than human observers in the field and can be applied to ARU data to standardize it with data from HPC.

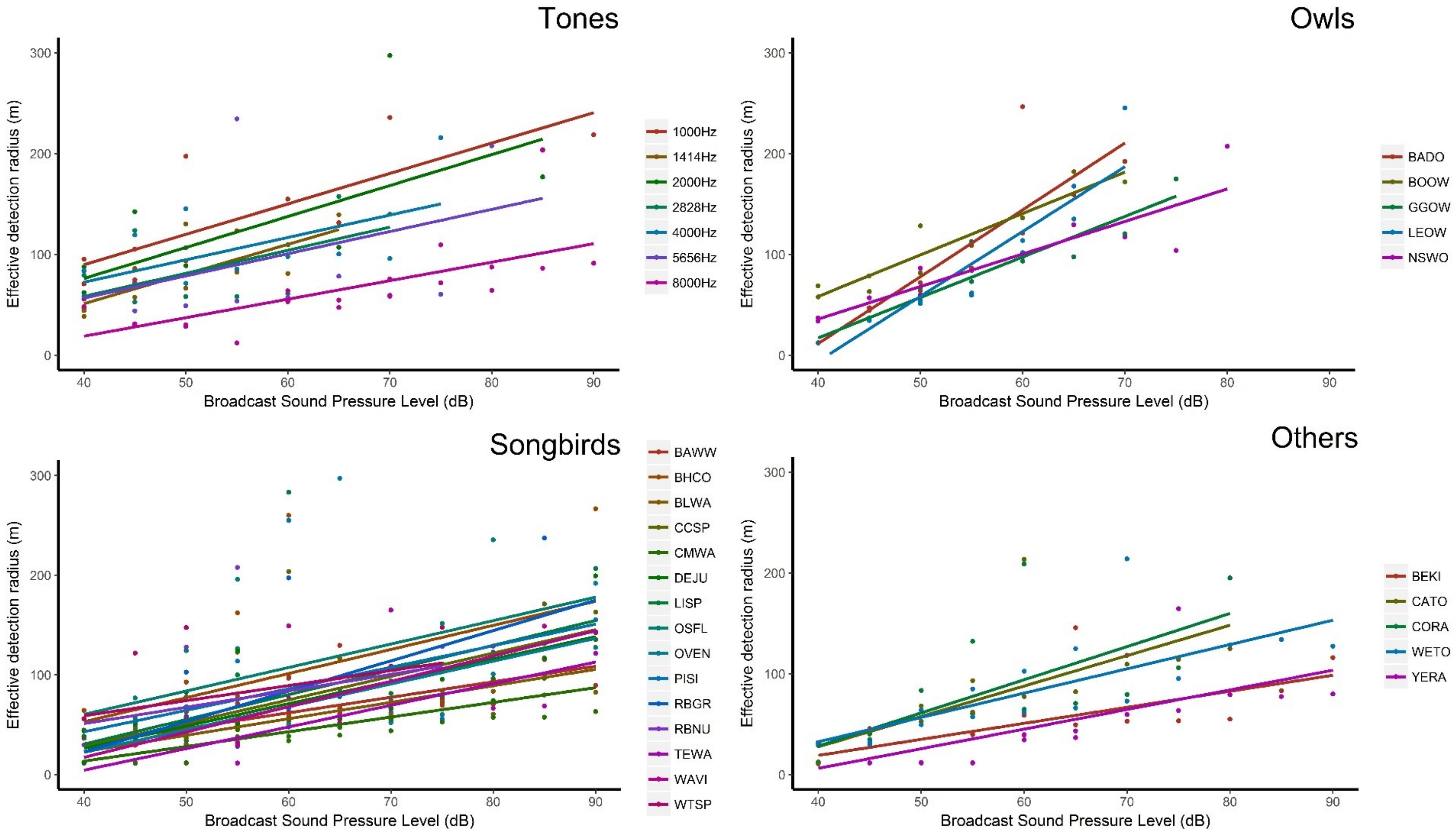

Figure 3.3. Influence of the sound pressure level (dB) of our song broadcasts on EDR for tones, owls, songbirds, and all other species, plotted separately. We found no statistically significant interaction between different species/tones although EDR for two species of owl (GGOW and LEOW) appear to increase at a greater rate with distance than other sounds.

Chapter 4. Correcting for environmental variation in avian detectability using playback experiments

INTRODUCTION

The use of passive monitoring technology is increasing in ecological research as a less invasive alternative to traditional surveys and sampling methods such as point and transect surveys and mark-recapture approaches. In particular, passive acoustic monitoring has been used by wildlife researchers to successfully study a variety of taxa, including birds (Wilson and Bayne 2018, Shonfield et al. 2018), amphibians (Corn et al. 2011), bats (Parkins and Clark 2015), cetaceans (Stimpert et al. 2015), and fish (Luczkovich et al. 2008). Developments in acoustic monitoring technology have resulted in higher quality recordings and lower cost devices. Autonomous recording units (ARUs) allow the user to program the duration, timing, and number of recordings that occur at a location. Computer recognition software further increases the efficiency of ARUs by automating the detection process for target species (Knight et al. 2017). Application and future use of this technology, as well as current constraints and limitations have been well documented and reviewed as passive acoustic monitoring becomes more widespread (Shonfield and Bayne 2017, Gibb et al. 2018).

One major concern with acoustic monitoring, whether by ARUs or traditional methods, is controlling for variation in detectability for species of interest. In a free field environment, acoustic signals attenuate at a predictable rate due to spherical spreading (Wiley and Richards 1982). However, excess attenuation and degradation of acoustic signals beyond what is predicted from free field calculations are directly related to the environment they pass through. Densely vegetated environments may increase scattering, refraction, and reverberation of sound waves (Richards and Wiley 1980, Yang et al. 2013) and atmospheric properties such as temperature and humidity can interacts with sound waves (Morton 1975). Vocalization structure also strongly influences signal propagation and varies among species. For example, higher frequency vocalizations are absorbed by the surrounding environment at a higher rate (Forrest 1994) and pure tone or whistle-like vocalizations can be enhanced in forested environments (Morton 1975, Brumm and Naguib 2009). Furthermore, species inhabiting open habitats are more likely than forest species to use trills to maximize signal propagation (Wiley 1991, Brumm and Naguib 2009). In biodiversity surveys that rely heavily on acoustic detections, failure to take into account differences in detectability and sound attenuation across various environments could lead to inaccurate assessments of animal relative abundance, density, diversity, and occupancy (Denes et al. 2015). Several approaches have been suggested to correct for variable detectability from environmental sources, particularly from vegetation variation. Royle (2018) proposed using a non-Euclidean cost-weighted distance approach to model sound attenuation in heterogeneous vegetation. Solymos et al. (2013) and Yip et al. (2017) suggested the use of statistical offsets to correct for changes in survey radius due to variable detectability. Other studies have further quantified detectability and detection distance for different environments (Darras et al. 2016; MacLaren et al. 2018).

While accounting for variation in detectability is recommended, there are numerous factors that need to be considered when conducting surveys. These include the distance of the animal from observer or sensor, ability or skill when interpreting animal presence, behaviour of the signaller, and the acoustic environment which influences attenuation of sound signals between the source and receiver (Johnson 2008). Addressing some or all of these variables may be logistically or financially difficult, particularly with large monitoring or survey programs. Previous studies have investigated sound transmission and detectability with respect to vegetation type (Richards 1981, Darras et al. 2016, MacLaren et al. 2018) and weather (Anderson and Ohmart 1977), and all advocated for taking these factors into account when correcting for detectability. However, the relative contribution of each of these factors to the total amount of bias in population estimates is not well understood.

We investigate the effect of environmental and species-specific variables on the detectability of avian and anuran vocalizations by human observers through sound playback experiments at known distances. Our objectives were to 1) evaluate the effect and relative importance of local atmospheric conditions, vegetation types, and song structure on the ability of signals to be detected, 2) compare possible biases in population size estimation resulting from these factors, and 3) present a method for standardizing variable detection probability using generalized song characteristics and discuss recommendations for implementing these corrections in acoustic monitoring. We aim to help researchers prioritize the most important factors when accounting for bias in population estimates due to variable detection probability and provide a method to decrease bias and increase accuracy when assessing species abundance, distribution, and diversity.

METHODS

Data Collection

We collected data in various locations throughout north-east Alberta between 26 July and 16 October 2014. We conducted field broadcasts across 57 different site transects, in seven different environments including grassland (n = 7), graminoid fen (n = 4), black-spruce bog (n = 10), conifer-dominated upland (n = 4), deciduous-dominated upland (n = 4), road corridors (n = 10), and forest edge (n = 10). We selected sites using the Alberta Vegetation Inventory (AVI) in locations with at least 1.5km of homogenous vegetation and visually confirmed by field observers. These environments represent the wide range of forest and feature types found in the parkland and boreal forest regions of Northern Alberta. We broadcast 31 different sounds and species at 30 different standardized distances at regular intervals from 12 to 1312m for each transect for a total of 1710 unique locations. The broadcast sequence consisted of six 1-second pure tones escalating in half-octave intervals (1000Hz, 1414Hz, 2000Hz, 2828Hz, 4000Hz, 5656Hz) followed by recordings of 25 avian and amphibian species obtained from Thayer's Birding Software (version 3.0) selected to represent a variety of frequencies and song complexities in the following order: Clay-coloured Sparrow (*Spizella pallida*, CCSP), Black-and-white Warbler (*Mniotilta varia*, BAWW), Lincoln's Sparrow (*Melospiza lincolnii*, LISP), Brown-headed Cowbird (*Molothrus ater*, BHCO), Red-breasted Nuthatch (*Sitta canadensis*, RBNU), Bay-breasted Warbler (*Setophaga castanea*, BBWA), Dark-eyed Junco (*Junco hyemalis*, DEJU), White-throated Sparrow (*Zonotrichia albicollis*, WTSP), Cape May Warbler (*Setophaga tigrina*, CMWA), Common Raven (*Corvus corax*, CORA), Belted Kingfisher (*Megaceryle alcyon*, BEKI), Olive-sided Flycatcher (*Contopus cooperi*, OSFL), Pine Siskin (*Spinus pinus*, PISI), Tennessee Warbler (*Oreothlypis peregrina*, TEWA), Warbling Vireo (*Vireo gilvus*, WAVI), Rose-breasted Grosbeak (*Pheucticus ludovicianus*, RBGR), Ovenbird (*Seiurus aurocapilla*, OVEN), Yellow Rail (*Coturnicops noveboracensis*, YERA), Western Toad (*Anaxyrus boreas*, WETO), Canadian Toad (*Bufo hemiophrys*, CATO), Northern Saw-whet Owl (*Aegolius acadicus*, NSWO), Boreal Owl (*Aegolius funereus*, BOOW), Great Gray Owl (*Strix* *nebulosa*, GGOW), Long-eared Owl (*Asio otus*, LEOW), and Barred Owl (*Strix varia*, BADO). All sounds were separated by a two second interval to avoid overlap of signals. We normalized all sounds using peak amplitude and broadcast at a sound pressure level (SPL) of 90dB (re 20 μPA) which was calibrated using a handheld sound meter (Sper Scientific 840018) and measuring the 1000Hz tone at one metre from the speaker (fast-time A-weighting).

Sounds were broadcast from an Alpine digital receiver (CDE-122) paired with an Alpine 6.5 inch speaker/tweeter combination (SPR-60) mounted on a tripod 1.5m above the ground and recorded at standardized distances between 12 and 1312 m using a Wildlife Acoustics Song Meter SM2+ automated audio recorder in WAV format at a sampling rate of 44.1kHz, 16 bit depth, and default gain. Broadcasts were conducted at 25 m intervals from 12 to 412 m, 50m intervals from 412 to 612m, and 100m intervals from 612 to 1312 m. Following each broadcast, the speaker apparatus was moved to the next distance at that transect. Distance was measured with a handheld GPS (GARMIN GPSmap 78, accuracy ± 3m). The direction of the speaker was oriented towards the audio recorder during each broadcast by taking the bearing of the audio recorder using GPS. Average wind speed, temperature, and relative humidity was measured during each broadcast using a handheld weather monitor (Kestrel 4000).

Sound Processing

We clipped individual sounds from continuous recordings using an automated script in Praat 5.4.06 (Boersma and Weenink 2015). Sounds were randomized and presented to 12 observers who identified sounds and species by 1) visual scanning of spectrograms in Adobe Audition (window type: Blackman-Harris; window length: 2048), and 2) using standardized volumes and headphones. We inserted blank clips consisting of ambient background noise and low levels of wind and vegetation noise to control for false positive identification. We generated a dataset of binomial data with positive identifications and known missed detections (including false negative and incorrect identifications) from these observations.

We measured acoustic parameters for each sound and species using the original playback file used for broadcasts. We calculated minimum frequency as the lowest peak frequency at any point in the spectrogram, bandwidth as the difference between the maximum frequency and minimum frequency, and syllable rate as the number of syllables (repeated elements) divided by the duration of the sound in seconds for sounds with repeated elements. All measurements were done using visual inspection of spectrograms.

Modelling Effects of Song Structure, Vegetation, and Environmental Conditions

First, we fit generalized linear mixed models (GLMMs) with a binomial distribution and logit link with the probability of detecting a sound or species as the response and known distance of playback as a predictor term. We built a set of candidate models that included environmental predictors (vegetation type, wind, temperature, and humidity) and song structure predictors (syllable rate, bandwidth, and minimum frequency). We also included two-way interactions between distance and vegetation type, wind and vegetation type, and vegetation type and each song structure predictor in our model selection process because sound attenuation rate is known to vary based on sound structure variables and in different environments. Continuous predictor terms were centred and standardized prior to modelling and variance inflation factors (VIF) were calculated to test for collinearity (Naimi et al. 2014). We used small sample size corrected Akaike's Information Criterion (AIC_c) to rank and select the model with the lowest AIC_c or the simplest model when multiple candidate models had ΔAIC_c less than 2 (Arnold 2010). We calculated intraclass correlation coefficients (ICC) to determine if site or observer were important random effects (defined as ICC > 0.30) and did not include them in model selection (ICC < 0.08 for both terms). However, we included sound type as a random effect to account for pseudo-replication of song structure predictors because each sound had identical structural values. Finally, we used commonality analysis (Nimon and Oswald 2013) to investigate relative explained variation by each predictor in the final model and whether explained variation between environmental and sound structure parameters were related.

Next, we fit generalized linear models (GLMs) with the same data distribution and link function for each species or sound individually to investigate patterns between species. We used the same model selection process to build a list of candidate models for each species that included distance, vegetation type, wind, temperature, and humidity as predictor terms for probability of detection. We included two-way interactions between distance and vegetation type, and wind and vegetation type in the selection process as well. We did not include any random effects in these models after calculating site and observer ICC coefficients for each species (all site ICC < 0.15; all observer ICC < 0.05).

Pairwise Comparison of Detectability Across Vegetation Types

We estimated effective detection radius (EDR) for each sound and species, in each vegetation type. EDR is defined as the distance at which the number of detections greater than this distance is equal to the number of detections missed within this distance (Buckland et al. 2001). We used a half-normal detection function estimated from our binomial detection data and fit with GLMs with a binomial distribution, fixed zero intercept, and complementary log-log ("cloglog") link (see Yip et al. 2017). We used a Monte Carlo simulation to test for significant differences in detectability between vegetation types. We used the above-mentioned GLMs to generate coefficients ($n = 1000$) using maximum-likelihood estimates and variance co-variance matrices to calculate 90% confidence intervals for EDR for each species in each vegetation type. We excluded species and vegetation type combinations when GLMs had convergence issues (i.e. < 95% successful convergence) which inflated confidence intervals due to an insufficient number of missed detections. We compared overlap between confidence intervals to test for statistical differences for each species. Vegetation types with confidence intervals that did not overlap were considered significantly different.

Estimating Corrections to Survey Area

We estimated EDR for each species with different classifications for vegetation to calculate correction factors which can be applied to survey data to offset variation in detectability caused by the surrounding vegetation type. We estimated EDR for 1) each species, with surrounding vegetation classified as “open” (road, forest edge, graminoid fen, and grassland) or “closed” (conifer forest, deciduous forest, treed bog) canopy, and 2) each species, with surrounding vegetation categorized by vegetation type. We then calculated the area over which each species could be detected (i.e. $A = pi(EDR)^2$). We calculated correction factors for “open” relative to “closed” canopy, and different vegetation types relative to forest edge by taking the ratio of area surveyed for each species in each vegetation type over the area surveyed for each species in the reference vegetation type.

We modelled correction factors and song characteristics using each species and sound as a replicate, to predict the correction factors that should be used for a given vegetation type and species combination and to evaluate accuracy of predictions. We also used linear regression with correction factor as the response variable and vegetation type and song characteristics as predictors, and leave-one-out (LOO) cross validation to predict correction factors that could be used for species in these vegetation types that were not included in our playback surveys. We calculated error in predicted correction factors by calculating the difference in predicted values from cross-validation and the true value. We also calculated relative error by dividing the true value by the predicted value so that prediction accuracy across different vegetation types or species were comparable.

RESULTS

Effects of Song Structure, Vegetation, and Environmental Conditions

The top performing model when pooling all sounds and species included distance, vegetation type, minimum frequency, bandwidth, wind, temperature, and humidity as predictor variables. Two-way interactions between distance and vegetation type, wind and vegetation type, minimum frequency and vegetation type, and bandwidth and vegetation type were also significant. Detectability decreased as distance of broadcast increased, however this effect differed among vegetation types (Appendix 3.1). Detectability was also negatively related to minimum frequency and bandwidth and declined faster in closed vegetation (coniferous forest, deciduous forest, and treed bog) compared to open vegetation (road, forest edge, graminoid fen, and grassland). Temperature and wind had a negative effect on detectability and humidity had a positive effect.

When each species or sound was modelled individually, each top performing model included a negative effect of distance, vegetation type, and a two-way interaction between distance and vegetation type (Appendix 3.2). All but six species included a two-way interaction between vegetation type and wind. Of these six species, BBWA and LISP did not include any weather variables, YERA and CATO included negative effect of temperature, and OVEN and PISI included a positive effect of humidity (Appendix 3.3). PISI also included a positive effect of temperature while CATO included a negative effect. All other sounds included a two-way interaction between wind and vegetation type indicating differential effects on detectability. 10 species (4000Hz, BEKI, BHCO, CCSP, CMWA, DEJU, OSFL, RBGR, TEWA, WAVI) did not have any other weather covariates included in the top model. Six species (1000Hz, 2828Hz, BADO, GGOW, NSWO, WETO) included temperature as a generally negative additional significant predictor, four species (1414Hz, 2000Hz, CORA, RBNU) included a positive effect of humidity, and five species (5656Hz, BAWW, BOOW, LEOW, WTSP) included both humidity and temperature.

Distance was the primary predictor explaining probability of detection. In the pooled model, distance was associated with 65.37% of explained unique variation (Appendix 3.4). Vegetation type (8.32%), minimum sound frequency (6.56%), and sound bandwidth (10.15%) were also importance sources of explained unique variation. While included in the top performing model, environmental covariates including wind (0.12%), humidity (0.21%), and temperature (0.04%) provided limited explained unique variation relative to other predictors. The proportions of unique variation explained by each predictor was similar when each species was modelled individually. Distance was the most important predictor, explaining 79.82 ± 6.60% (mean ± SD). Vegetation type explained 10.72 ± 2.73%, wind was 0.36 ± 0.45%, humidity was 0.82 ± 0.56%, and temperature was 1.42 ± 1.53%. Minimum frequency was positively related to the proportion of unique variation explained by distance (P = 0.005, Fig. 1a) and negatively related to the proportion explained by vegetation (P = 0.008, Fig. 1b).

Differences Across Vegetation Type

We omitted 65 different species/vegetation type combinations from pairwise comparison due to insufficient convergence leaving 152 unique species/vegetation type combinations. Nine species (CATO, BOOW, BADO, GGOW, NSWO, LEOW, WETO, 1000Hz, and 2828Hz) were omitted completely. Single vegetation types were omitted for two other species (YERA and RBGR). When comparing detectability between vegetation types for each species, we found statistical differences in detectability generally depended on the "openness" of vegetation (Fig. 2). Within most species, detectability was similar for closed vegetation types including black-spruce bog, coniferous forest, and deciduous forest. Open vegetation types, including road, forest edge, grassland, and graminoid fen, were not significantly different from each other. However, for most species, open vegetation types had significantly higher detectability than closed vegetation types. Three species (BAWW, WTSP, and 5656Hz) did not have any significant differences in detectability for any of the vegetation types tested.

Application of Correction Factors to Survey Data

We calculated correction factors (Table 1) for "open" relative to "closed" canopy cover and found open canopy environments resulted in an average of 363.4% (± 98.7% SD) greater area surveyed than closed canopy environments. We then compared area surveyed and calculated correction factors (Table 2) for each specific vegetation type relative to forest edge for each species and found smaller average survey area for bog (408.2 ± 140.2%), coniferous forest (331.2 ± 158.5%), deciduous forest (202.0 ± 59.1%), and graminoid fen (19.4 ± 103.1%). We found average survey area increased for road (32.2 ± 21.2%) and grassland (11.1 ± 63.4%) relative to forest edge as well.

Mean prediction error for correction factors by species was 0.696 ± 0.416 and relative error was 34.0 ± 27.0% (Fig. 3). Owl species (NSWO, BOOW, GGOW, LEOW, BADO), and higher frequency songbirds (BBWA, BAWW) had higher relative error than other species. Mean prediction error for correction factors by vegetation type was 0.686 ± 0.357 and relative error was 34.1% ± 13.4% (Fig. 3). Mean relative error was higher for open vegetation types (44.9%) than closed vegetation types (23.4%).

DISCUSSION

We demonstrate that detectability is strongly influenced by the surrounding environment. Differences in microclimate, vegetation type, and vocalization structure causes variation in sound attenuation due to scattering, absorption, and refraction (Richards and Wiley 1980, Morton 1975, Wiley 1991, Brumm and Naguib 2009, Yang et al. 2013). We evaluated the effect of atmospheric covariates (temperature, humidity, and wind), vegetation, and frequency/bandwidth of sound and found that all variables were important in predicting changes in detectability of signals in human observers. Distance was selected in all models predicting detection probability as expected due to the spherical spreading (Wiley and Richards 1982). Interactions between distance and vegetation type were also important as detectability declined with distance at different rates depending on the surrounding vegetation. Wind was important for most species, and interactions between wind and vegetation were present, indicating that wind influenced detectability differently based on the vegetation present. This is likely due to changes in ambient noise associated with vegetation movement, although the mechanism remains unclear. Finally, temperature and humidity were included in the pooled model, but only some of the species-specific models showed an influence on detectability, suggesting these predictors may not be as important as other variables in the model. Evaluating the relative contributions of each predictor to the final models indicates distance contributes the majority of variation to detection probability (~80%). The next most important predictors were vegetation (~10% across species-specific models), frequency (~6% in pooled model), and bandwidth (~10% in pooled model). Atmospheric covariates had the least influence on detection probability with the most important being temperature (~1.5%) and wind and humidity both being < 1%.

We found sound bandwidth and frequency to be of similar importance to vegetation when modelling detection probability. Patterns in this study for both of these traits follow common themes from the literature where propagation of acoustic signals is maximized for the environment that species typically inhabits (Morton 1975, Brumm and Naguib 2009). Higher frequency sounds are subject to increased scattering, reverberation, and absorption by forested environments resulting in shorter distances over which such species can be observed. We found that the detectability of higher frequency vocalizations were lower in the forested vegetation types (black-spruce bog, upland deciduous, and upland coniferous) and the significant interaction between vegetation and frequency indicated that detectability declined at a faster rate in these vegetation types as well. Additionally, the variation explained by environmental factors depends on sound frequency. Higher frequency sounds attenuate faster and are less likely to be influenced by the surrounding environment. We found the distance of a sound to explain more variation as frequency increased, due to spherical spreading being the most important factor influencing sound attenuation. Inversely, vegetation explained less variation with increasing frequency due to a decreasing distance over which the surrounding environment could influence the propagation of a signal. Pure sine waves have lower rates of excess attenuation due to scattering, reverberation, and absorption effects from vegetation (Richards and Wiley 1980). We found that lower bandwidth sounds (which have more sound energy focused into a narrow frequency range) had a similar pattern. Detectability of sounds decreased with increasing bandwidth, and detection probability declined even faster in forested habitats as bandwidth increased.

Vegetation type was an important predictor for detection probability in all models, however we were interested in how vegetation type would influence estimation of abundance, density, or occupancy if not accounted for. In general, we found the specific type of vegetation was less important than if the environment was 'open' or 'closed'. Closed habitats increase the amount of scattering, refraction, and absorption due to an increased number of physical obstacles that influence sound waves. Furthermore, closed vegetation had less of an influence on lower frequency sounds and these sounds were less likely to have a significantly lower detection distance in closed than in open vegetation types. These findings are well supported in the literature, however, what is not discussed in detail is the bias differences in detection distance and detectability may have on estimates of animal numbers. Based on our results, assuming consistent detectability in open and closed vegetation types can result in up to 360% bias in estimates of animal numbers. When assuming consistent detectability in specific vegetation types, this bias can increase to 10-400%. We found variables which decrease detectability to have a greater influence on bias due to the geometry of a circle, where a decrease in detection radius results in a non-linear decrease to survey area.

While quantifying bias demonstrates the implications of ignoring detectability across variable vegetation, our main objective was to provide a potential solution that is applicable outside of the narrow range of species tested in this study. We present a method to correct for detectability across different vegetation types using broadcasts of different species with a predictive error of approximately 40%. This is a significant improvement from biases we calculated as high as 400%. We present correction factors to standardize open versus closed environments and forest edge relative to other vegetation types as we believe these are applicable to many situations where monitoring occurs across heterogenous landscapes. However, correction factors and predictive error will vary depending on the vegetation or environments being standardized. Furthermore, we found predictive error to be higher at the low end of the frequency spectrum. We believe a low number of species in these frequency bands decreases predictive performance of our model. Increasing the number of species and different species vocalization traits included in this study would greatly increase predictive performance and estimation of correction factors. Similar studies have examined the relationship between detectability and species characteristics or phylogeny (Solymos et al. 2018). However, our method utilizes sound playback to estimate correction factors which can be useful when existing data on detectability for a species or vegetation type is limited.

We modelled correction factors using sound structure as predictive variables rather than species, to show that generalized song characteristics can be used to estimate correction factors for species. The success of this approach broadens the applicability of our methods, as it suggests that a correction factor can be estimated even when playbacks have not been conducted for that species. However, accurate prediction requires an adequate number of species be included in the playback calibration dataset, especially in the frequency and bandwidth range of the species to be predicted. In general, accuracy will increase when more species playbacks are included in predictive models. The correction factors described in this study can be used to standardize estimates of relative abundance between different vegetation types by offsetting for differences in detectability, detection distances, and survey area. In cases where survey area is unknown, correction factors can be applied to count data to adjust the number of individuals counted based on changes in detection distance and area surveyed. Correction factors can also be used when estimating animal density, if an existing value for density or survey area is already known (i.e. the boreal avian modelling project; www.boreabirds.ca). In this case, density or survey area can be adjusted using correction factors depending on the species and habitat type of the original value and the vegetation type to be predicted.

Our results contribute to a growing amount of evidence that avian detectability can be strongly influenced by the surrounding environment. More importantly, we provide a method using sound playbacks to estimate correction factors necessary to standardize detectability, which is useful when existing detection data is not readily available. Admittedly, the sample size of avian species included in this study is small and may not be representative of other systems. However, we strongly believe that the accuracy of this approach will improve with the inclusion of more species and the effort required to standardize detectability using this method is low enough to be easily accessible by most wildlife managers and researchers. As we continue to improve and refine methods for estimating wildlife populations, we hope to contribute another tool to the toolkit of wildlife biologists and ecologists.

Table 4.1. Correction factors to standardize area surveyed for closed canopy vegetation relative to open canopy. Area surveyed in open canopy vegetation can result in more area surveyed and more individuals detected, and correction factors can be used to offset the difference in detection due to sampling radius for closed canopy vegetation.

Species	Correction Factor
Barred owl	3.98
Black-and-white warbler	3.53
Bay-breasted warbler	3.00
Belted Kingfisher	3.92
Brown-headed cowbird	4.58
Boreal owl	6.35
Canadian toad	4.64
Clay-coloured sparrow	4.73
Cape-may warbler	3.47
Common raven	5.27
Dark-eyed junco	5.34
Great gray owl	4.24
Long-eared owl	3.61
Lincoln’s sparrow	4.86
Northern saw-whet owl	5.10
Olive-sided flycatcher	4.51
Ovenbird	5.57
Pine siskin	4.99
Rose-breasted grosbeak	6.04
Red-breasted nuthatch	6.13
Tennessee warbler	2.71
Warbling vireo	4.73
Western toad	6.13
White-throated sparrow	4.61
Yellow rail	3.80

Table 4.2. Correction factors to standardize area surveyed for forest edge relative to other vegetation types. Area surveyed along forest edges can result in variation in area surveyed and individuals detected, and correction factors can be used to offset the difference in detection due to sampling radius for different vegetation types.

Species	Bog	Conifer	Deciduous	Graminoid Fen	Grassland	Road
Barred owl	5.72	3.63	1.84	2.15	-	0.37
Black-and-white warbler	3.04	3.23	2.98	0.58	1.09	0.82
Bay-breasted warbler	4.53	2.49	3.45	0.68	2.49	1.09
Belted Kingfisher	3.29	2.77	2.96	0.54	0.71	0.72
Brown-headed cowbird	5.95	3.34	3.33	0.82	0.76	0.80
Boreal owl	4.59	3.74	2.34	0.14	-	0.13
Canadian toad	4.36	5.48	3.15	1.49	0.53	0.88
Clay-coloured sparrow	5.15	3.86	3.45	0.76	0.95	0.72
Cape-may warbler	3.04	3.45	2.87	0.81	0.97	0.79
Common raven	7.05	4.72	2.93	1.48	0.71	0.61
Dark-eyed junco	5.57	5.78	3.50	1.12	0.88	0.71
Great gray owl	8.10	6.09	2.85	3.09	0.53	0.78
Long-eared owl	7.64	8.89	3.60	5.27	3.00	1.14
Lincoln’s sparrow	6.18	3.55	3.25	0.77	0.84	0.70
Northern saw-whet owl	5.22	4.49	2.55	0.79	0.12	0.59
Olive-sided flycatcher	5.14	2.69	2.49	0.74	0.58	0.53
Ovenbird	6.55	4.68	4.12	0.86	0.93	0.77
Pine siskin	4.91	4.64	3.63	0.90	0.86	0.73
Rose-breasted grosbeak	6.23	4.44	3.66	1.27	0.51	0.57
Red-breasted nuthatch	5.16	4.29	3.11	1.19	0.39	0.39
Tennessee warbler	3.58	3.46	1.38	0.77	0.70	0.79
Warbling vireo	4.85	3.42	3.05	0.75	0.73	0.64
Western toad	4.29	8.10	2.81	1.34	0.47	0.50
White-throated sparrow	4.03	4.13	3.32	0.76	1.08	0.57
Yellow rail	2.88	2.43	2.87	0.78	0.59	0.62

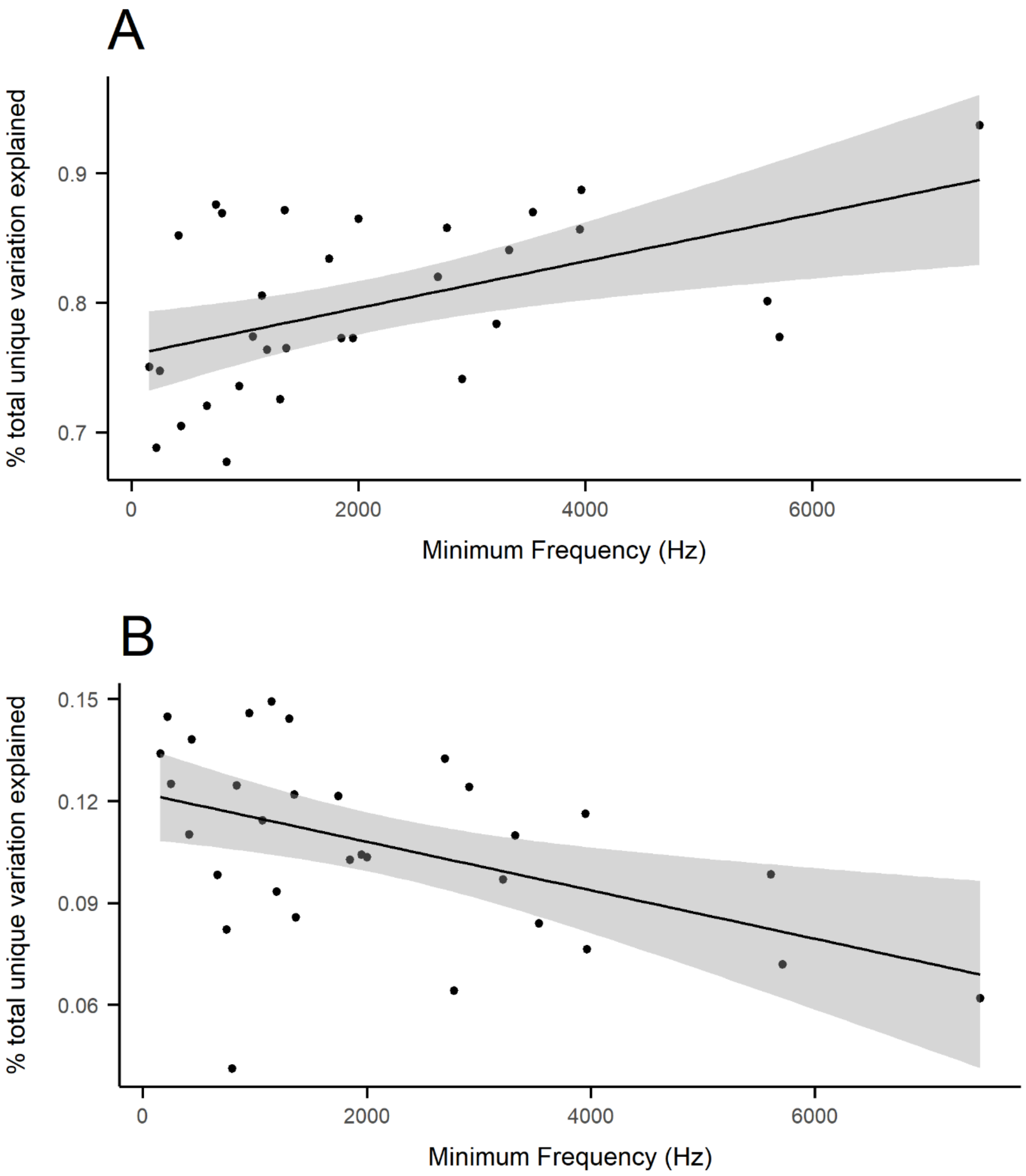

Figure 4.1. Effect of minimum frequency on the percent of total unique variation explained by distance (A) and vegetation (B). Predictions are plotted with 95% confidence intervals.

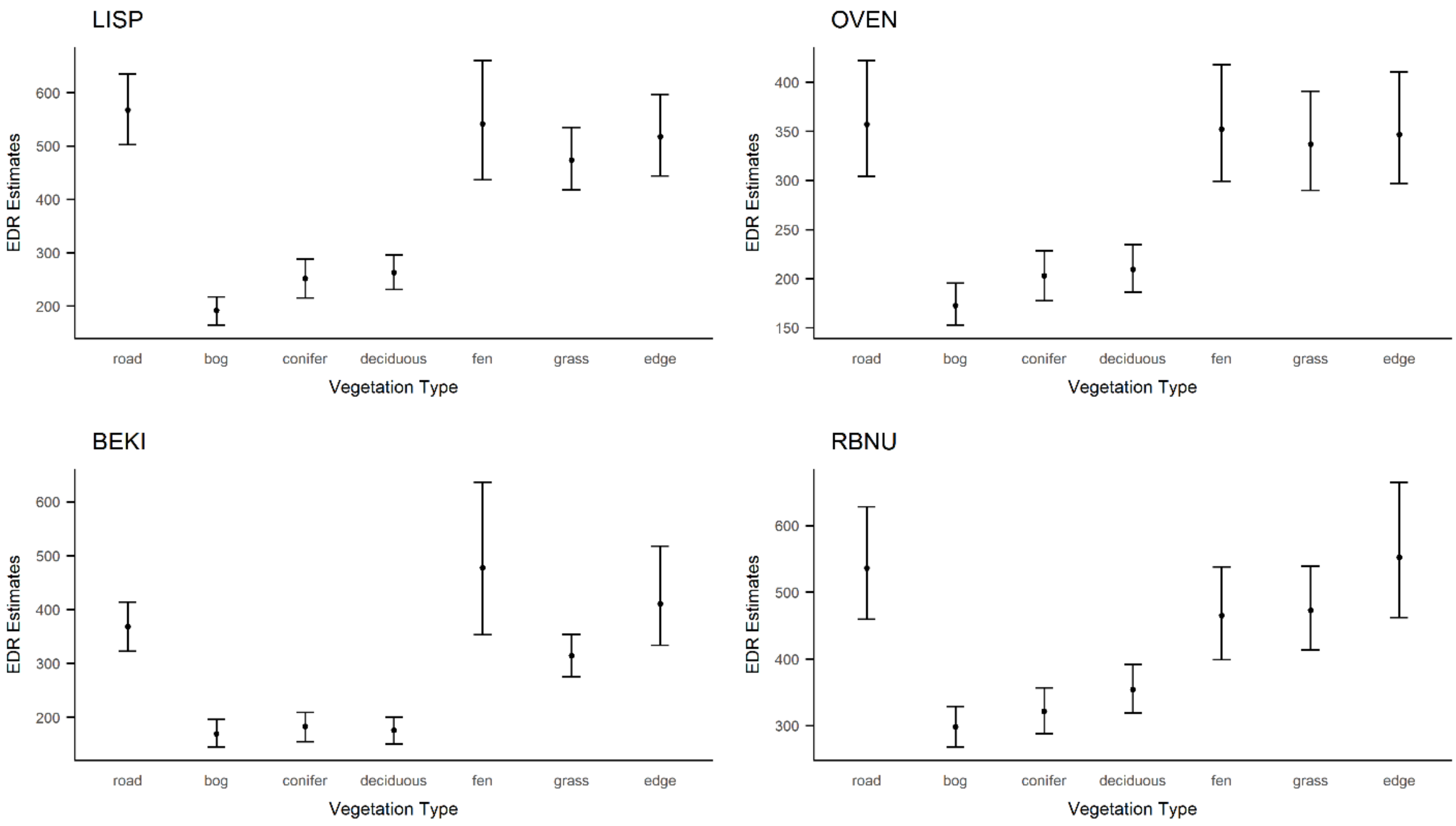

Figure 4.2. Differences in effective detection radius (EDR) for Lincoln Sparrow, Ovenbird, Belted Kingfisher, and Red-breasted Nuthatch in different vegetation types. 90% confidence intervals for EDR were estimated using Monte Carlo simulation.

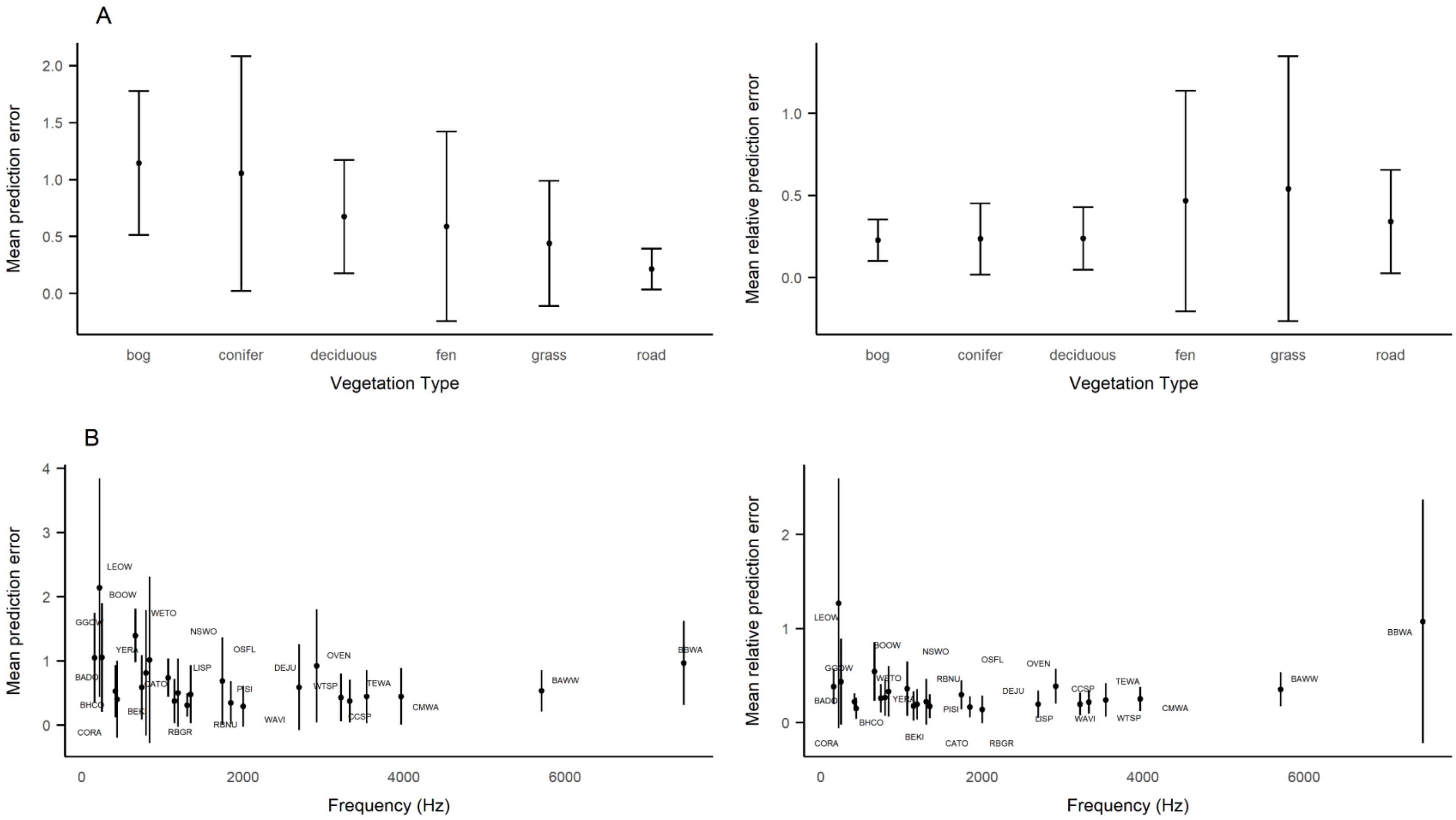

Figure 4.3. Mean error (left) and relative mean error (right) for predicting correction factors for vegetation type (A) and species (B). Prediction error for species (B) are plotted against vocalization frequency. Error bars represent standard deviation

Chapter 5. Sound level measurements from audio recordings provide objective distance estimates for distance sampling wildlife populations

INTRODUCTION

Estimating density is a fundamental objective of wildlife management. Distance sampling corrects for the decline in detection probability that occurs as distance from an animal to the observer increases (Buckland et al. 2001) and is among the most widely used approaches for estimating animal density. Distance sampling has five key assumptions: 1) distance to individuals is measured independent of animal movement, 2) individuals are perfectly detected at zero distance, 3) distance is measured without error, 4) individuals are detected at their initial location, and 5) individuals are not double counted (Table 5.1). Distance sampling is commonly applied to acoustic surveys (Buckland et al. 2001), where a human surveyor estimates the distance of a sound signal. However, the assumptions of distance sampling are often violated when distances are estimated by human surveyors (Table 5.1; Scott et al. 1981, Alldredge et al. 2007, Nadeau and Conway 2012).

We focus on the assumption that distance is measured without error (hereafter "distance estimation assumption"; Table 5.1). Field evaluations of point count surveys by human surveyors have found distance estimates are generally inaccurate and often biased, and as a result, often binned into distance intervals (e.g. 0-50, 50-100, > 100 m). Estimates of distance by humans can range from 0.25 to almost 30 times the true distance (Scott et al. 1981, Nadeau and Conway 2012), and error often increases with distance (Nadeau and Conway 2012). After comparing human distance estimates to true distances, Alldredge et al. (2007) concluded that humans cannot accurately estimate distances over 65 m. A human's ability to determine distance from aural cues can be hindered by environmental effects on sound attenuation and degradation (Wiley and Richards 1982, Pacifici et al. 2008, Yip et al. 2017*b*), as well as interference from background noise (Simons et al. 2007). Estimates by people can also be biased and are often clumped because training and experience create bias and variation in distance estimates (Scott and Ramsay 1981, Alldredge et al. 2007, Simons et al. 2007).

Audio recordings present an opportunity to remove the subjectivity from distance estimation and potentially reduce estimation error. The relative sound level (RSL) of an acoustic signal in audio recordings has a predictable logarithmic relationship with distance and has the potential to be used as a proxy for estimating density in a distance sampling framework (Yip et al. 2017*a*). RSL is a relative measure of the energy of a sound signal at the point when sound waves reach a microphone and can be measured using acoustic software programs. RSL is generally measured in decibels (dB) that are relative to the maximum output of the microphone. In the absence of environmental factors that affect sound propagation, every doubling of distance results in a decrease in RSL of 6 dB due to spherical spreading (Wiley and Richards 1982). The potential for RSL to predict distance is not well understood and may be influenced by environmental factors, such as vegetation density, that affect spherical spreading via changes in attenuation (Darras et al. 2016). Distance prediction with RSL may also vary between species depending on the degree of directionality of each species' vocalizations (Catchpole and Slater 2008).

RSL distance prediction could be applied to audio recordings from autonomous recording units (ARUs), which are increasingly used to conduct ecological surveys (Shonfield and Bayne 2017) and have several advantages over human surveys that are consistent with the assumptions of distance sampling (Table 5.1). Previously, distance sampling with ARUs has been hindered by an assumed inability to estimate distance to a signal in a recording (Dawson and Efford 2009), and so has only been applied to ARU array datasets with localized individuals (Cato 1998, McDonald and Fox 1999), which are laborious to collect (Mellinger et al. 2007). More recently, distance sampling has been applied to point count ARU datasets via human estimation of distance on recordings (Darras et al. 2018*b*) and via distance prediction from RSL (Sebastián-González et al. 2018). We propose that distance can be automatically estimated from sound recordings with a four-step process: 1) Build a calibration dataset of a focal species recorded at known distance; 2) train a recognizer with signal recognition technology (Knight et al. 2017, Priyardarshani et al. 2018) to detect the focal species and measure RSL of each detection; 3) determine the source level (i.e., intercept) and attenuation rate (i.e., slope) of RSL relative to distance with a regression model; and 4) use the recognizer to automatically extract RSL of species detections from recordings of unknown distance and predict distance with the estimated regression equation.

We present a rigorous test of whether RSL distance prediction removes subjectivity and reduces error compared to human estimated distances. First, we tested whether RSL can be used to estimate distance by manually and automatically measuring RSL from calibration recordings of wild, free-ranging birds, predicting distance with the RSL measurements, and comparing to known distances of those recordings. We then compared the error in RSL predicted distances to human estimated error extracted from a literature case study to demonstrate that RSL distance prediction can reduce distance estimation bias and error. We also determined the sample size for calibration recordings that were required to reach an *a priori* threshold of variation in distance estimation error to help users determine the best approach for calibration recording collection. To examine whether RSL distance prediction violated the distance sampling assumption that distances are measured without error, we simulated ARU point count surveys and compared the true simulated estimate to density estimates from known distance, to those from RSL predicted distance, and to those contaminated with the human estimated error extracted from the literature.

METHODS

Calibration data collection

We collected acoustic recordings of live birds recorded at known horizontal distance (hereafter "known distance") for two bird species with contrasting acoustic characteristics, the Common Nighthawk (*Chordeiles minor*, CONI) and Ovenbird (*Seiurus aurocapilla*, OVEN). The two species differ in acoustic signal complexity that could affect the error rate of RSL distance prediction. OVEN has a complex multi-phrased song that is 2.5-4.0 s in length (Porneluzi et al. 2011; Fig. 5.1), whereas CONI produces a simple single-note vocalization that is ~ 0.3 s in length (Fig. 5.1). The two species also differ in acoustic behavior that could lead to differences in sound transmission, affecting RSL distance prediction. OVEN sing from an above-ground perch at a mean height of 8.8 m (Lein 1981), while CONI call from the wing above the forest canopy (Brigham et al. 2011).

We determined OVEN singing locations using an acoustic location system (ALS) placed at seven mixedwood sites in Alberta, Canada during June 2016 (see Wilson and Bayne 2018 for detailed methods). The ALS used 30 GPS-enabled SM3 ARUs equipped with external SMM-A1 microphones (Wildlife Acoustics, Concord, MA, USA) placed an average of 33.9 m (± 0.52 m SE) apart in a 5 x 5 grid, with a transect of five microphones extended from the centre of each grid (Fig. 5.2). OVEN vocalizations (n = 160) were localized with the microphone grids using time to arrival methods. Accuracy of localization determined through playback experiments was 2.03 m (± 0.55 m SE). We determined the horizontal distance of each vocalization to each of the ten microphones in the centre of the array to create a dataset of 1600 known distance clips (Fig. 5.2). We then clipped each vocalization using the *tuneR* R package (Ligges et al. 2016, R Core Team 2017), adding a buffer of 2 seconds to the beginning and end of the vocalization for further RSL measurement.

We collected acoustic recordings of CONI with known locations by attracting males to a transect of SM4 ARUs (Wildlife Acoustics, Concord, MA, USA) using conspecific broadcast calls (Appendix 4.1; Fig. 5.2). The transect approach is an efficient method of collecting calibration recordings because it simultaneously records the calls of the same individual at multiple distances. We used an 800 m long transect that consisted of 15 ARUs placed at standardized distances along a linear feature. An observer stood at the beginning of the transect and recorded the time in milliseconds, height, horizontal distance, and bearing of every CONI vocalization. We minimized distance estimation error by using the same observer for all observations, by the observer calibrating their horizontal and vertical distance estimates with a laser range finder prior to every observation period, and by limiting observations to those within 20 m horizontal distance of the observer, because human surveyor distance estimation error is minimized at short distances (Nadeau and Conway 2012). We note that there is likely 5-10 m of error in our known distance estimates due to this method. We collected recordings an hour before sunset at eight transects in July 2016. We measured temperature, wind speed, and humidity during each survey using a Kestrel 3000 (Kestrel Meters, Minneapolis, MN, USA). We played an airhorn from the beginning of the transect at the start of the recording period and subsequently clipped the recordings at the airhorn to synchronize the target vocalizations therein. We used the seewave package (Sueur et al. 2008) in R to clip each of 147 unmasked detections from each of the 15 recordings along the transect as 0.7 s clips for a total of 2205 clips (Fig. 5.1).

Human estimated error

We extracted human observer error from the literature to compare to our RSL estimated distances. Of the four known field tests of human observer distance estimation error, Nadeau and Conway (2012) was the only paper from which it was feasible to extract raw data. We emphasize, however, that human observation distance estimation can vary based on a variety of factors (Simons et al. 2007, Nadeau and Conway 2012), and that this comparison may not be representative of all human observer distance estimation. We used WebPlotDigitizer (Rohatgi 2017) to extract raw data from Figure 1b, which depicted distance estimation error against measured distance. We tested for heteroscedasticity of the extracted data using a Breusch-Pagan test (Breusch and Pagan 1979) and found error to be homoscedastic ($BP = 0.013$, $P = 0.91$). Since distance estimation error from human surveyors did not significantly change with distance from observer, we used the mean and standard deviation of the extracted data to add error values randomly sampled from a normal distribution to every known distance value from the OVEN and CONI manual measurement datasets. We constrained the resultant distances (hereafter "human estimated distances") to positive values.

RSL measurement

We measured RSL with two different methods: manual measurement and recognizer measurement. Ultimately, we were interested in using recognizer measurement to automate RSL distance prediction, but wanted to confirm the RSL measurements were sufficiently precise via comparison with manually extracted measurements because the RSL measurement will ultimately depend on the accuracy of the temporal and frequency boundaries within which the measurement is taken.

Manual measurement - We measured RSL manually from the clips of known distance of both species in Raven Pro 1.5 (Charif et al. 2010) using a 512-point Hamming window spectrogram for visualization. We used the max power function to measure RSL for each vocalization by selecting the smallest possible area around the vocalization (Bioacoustics Research Program 2014). We measured RSL from all clips where the target individual was detected and the vocalization was not masked by vocalizations of non-target individuals. We only used data points at distances where the RSL exceeded the level of ambient background noise (≤ 200 m for OVEN, ≤ 500 m for CONI).

Recognizer measurement - We also used automated signal recognition to automate the RSL extraction process using convolutional neural network (CNN) recognizers (Knight et al. 2017). We trained one recognizer for each species as moving window recognizers in the TensorFlow (Abadi et al. 2015) framework with the Python API for model training and definition (Appendix 4.2). We then processed the clips of known distance with the corresponding species recognizer to measure RSL of each clip, excluding clips of known distance beyond the same distance thresholds used for manual measurement. The recognizers output a time series of scores and RSL estimates generated from spectrogram inputs. We visually and aurally reviewed every hit for each species to confirm detections of the target individual and removed any hits where there was masking by non-target individuals. Analysis was conducted in Python (van Rossum 1995) version 3.5, using librosa (McFee et al. 2017) for audio loading and spectrogram generation, and scipy (Jones et al. 2001) for signal filtering.

Statistical analysis

Distance estimation - We fit generalized linear mixed models with a Gaussian distribution and log link function with known distance as the response and RSL as a second-order polynomial term for all four species-method datasets (hereafter referred to as: “OVEN manual", “OVEN recognizer”, “CONI manual”, “CONI recognizer”). We selected a second-order polynomial term after preliminary comparison to linear and log models using small sample size corrected Akaike’s Information Criterion (AIC_c). We built global models that included time of day, score (recognizer only), vertical height (CONI only), and any relevant interactions (Appendix 4.3). We modelled horizontal distance with vertical height as a covariate for CONI instead of calculating and modelling Euclidean distance because most applications of distance estimates, including distance sampling, require estimates of horizontal distance. In addition, we were interested in determining the relative importance of vertical distance in RSL distance prediction because in most applications of RSL distance prediction, vertical height will be unknown. All predictors, including RSL, were centered and standardized prior to modelling. We tested for collinearity between predictors by calculating the variance inflation factor (VIF) in a stepwise procedure for each predictor (Naimi et al. 2014). We retained all predictors for model selection (max VIF = 2.81). We excluded weather covariates to make this approach more generalizable because preliminary analyses indicated they were relatively small contributors to overall explained variance (Appendix 4.4). To further emphasize generalizability, we also calculated intraclass correlation coefficients (ICC) to determine importance of site, location within the ALS grid, and individual as random effects and removed any random effects with an ICC greater than 0.30 (*A. Zuur and E. Ieno personal communication*), leaving station as a random effect for both OVEN datasets (Appendix 4.5). We then used AIC_c to rank models and selected the model with the lowest AIC_c or the most parsimonious model when multiple candidate models had $\Delta AIC_c < 2$ (Arnold 2010; Appendix 4.3). We partitioned relative importance of each variable included in the best model for each dataset using commonality analysis, which provides the unique variance explained by a predictor and common variance shared by two or more predictors (Nimon and Oswald 2013).

We used 10-fold cross-validation to build a dataset of RSL distances for each of the four species-method combinations by fitting the trained regression model to the withheld data from each fold (Mosteller and Tukey 1968). We excluded random effects from distance prediction to test the generalizability of our method beyond the calibration dataset. We calculated the magnitude of error (hereafter "distance estimation error") as the absolute value of the difference between RSL predicted distance and known distance, and direction of mean error (hereafter "error bias") as the RSL predicted distance minus known distance. We tested whether error bias differed from zero using a one-sample t-test for each dataset, and for differences in error bias between manual and recognizer approaches with independent two-sample t-tests for each species. Validation accuracy is reported as the mean adjusted R^2 between observed and fitted values from cross validation.

We then used bootstrapping to determine the sampling effort required to create a suitable calibration dataset. We used a uniform distribution to randomly select a sample size for each species-method combination. We calculated absolute error using the same 10-fold cross-validation technique described above and calculated the coefficient of variation for different sample sizes at intervals of 20 samples. We estimated the sample size required to reach a coefficient of variation value of five, where variation in absolute error stabilized with increasing sample size.

Distance sampling - We used stochastic simulation to generate individual animal locations with a known population density to test whether RSL predicted distances produced accurate density estimates. We simulated OVEN and CONI locations within a 400-ha square survey plot with a random uniform distribution (Fig. 5.3). We imposed a minimum inter-individual distance of 40 m for OVEN and 100 m for CONI to represent territoriality. We determined the number of animal locations (i.e., population density) using random Poisson deviates with an average of 160 CONI (0.4 CONI / ha; *Knight unpublished data*) and 240 OVEN (0.6 OVEN / ha; Lankau et al. 2013). We repeated this simulation 50 times to represent a typical avian point count survey program.

Next, we simulated single-ARU point count locations at the centre of the square survey plot. We calculated the known distance and probability of detection for each individual in each simulation. We calculated the probability of detection using a half-normal detection function generated from binomial recognizer results of OVEN and CONI vocalizations at known distances that were detected or missed (see Yip et al. 2017*a* for details). We used the distribution of errors from our distance estimation models to simulate RSL for each known distance using mean error bias and standard deviation as a function of distance. We then used those simulated RSL measurements in our previously fitted models for distance prediction to generate RSL predicted distances for each individual in each simulation. We also used the distribution of errors from the human estimated distances extracted from Nadeau and Conway (2012) to generate human estimated distances for each individual in each simulation.

Finally, we used distance sampling to estimate the density with point count surveys in each simulation using the known distances, RSL predicted distances, and human estimated distances. For each set of distances, we used AIC_c to rank, compare, and select conventional distance sampling models with combinations of uniform, half normal, and hazard rate key functions and cosine and polynomial adjustment terms (MRDS package; Thomas et al. 2010; Appendix 4.6). We used 83% confidence intervals to determine if there were statistical differences in density estimates produced from known distances, RSL predicted distances, and human estimated distances (Krzywinski and Altman 2013).

RESULTS

We hand measured the RSL in 691 of the 1600 OVEN clips and 716 of the 2205 CONI clips. The maximum known distance that an individual was detected at with manual measurement was 187 m for OVEN and 500 m for CONI. After validation, the recognizer detected and measured RSL of 673 OVEN clips and 1223 CONI clips. The maximum known distance that an individual was detected at by the recognizer was 149 m for OVEN and 500 m for CONI.

We extracted 168 of 206 data points from Figure 1b in Nadeau and Conway (2012). We were unable to extract the remaining 38 data points due to overlap. The mean estimation error of the data we extracted was 42.5 m (± 84.8 m SD), which was similar to that reported in Nadeau and Conway (2012; 39 ± 79 m SD).

Distance estimation

RSL decreased with increasing distance and explained at least 93.4% of the total partitioned R^2 in all models except the OVEN recognizer model, where RSL and score combined explained 95.2% of total partitioned R^2 (Fig. 5.4; Appendix 4.4; Appendix 4.7). The selected models for OVEN distance estimation included a negative effect of time of day. The selected models for CONI included estimated vertical height of CONI as a positive predictor and time after sunset. Both models for recognizer measurement also included score. Adjusted R^2 between fitted and observed data in cross validation was between 0.61 and 0.73 for all models.

Distance estimation error was significantly greater than zero for all datasets but was lower for OVEN than CONI (Fig. 5.5; Appendix 4.8). Distance estimation error from manual measurements was higher than error from recognizer measurements for CONI ($P < 0.001$), but not for OVEN ($P = 0.187$; Appendix 4.8). Absolute distance estimation error was 14.69 m (± 12.24 m SD) for OVEN manual measurement, 13.85 m (± 10.75 m SD) for OVEN recognizer measurement, 47.64 m (± 40.83 m SD) for CONI manual measurement, and 37.62 m (± 38.19 m SD) for CONI recognizer measurement.

Mean error bias was significantly greater than zero for OVEN but not for CONI ($P < 0.001$, $P > 0.05$; Fig. 5.5; Appendix 4.8). There was no significant difference in error bias between manual measurement and recognizer measurement for either species (all $P > 0.05$; Appendix 4.8). Mean error bias was 5.66 m (± 18.27 m SD) for OVEN manual measurement, 4.15 m (± 17.04 m SD) for OVEN recognizer measurement, -0.31 m (± 62.76 m SD) for CONI manual measurement, and 0.39 m (± 53.61 m SD) for CONI recognizer measurement.

Variation in estimates of absolute error decreased with sample size (Fig. 5.6). A sample size of approximately 300 measurements was sufficient to reach the *a priori* threshold coefficient of variation (CV = 5) for all datasets (OVEN manual: 350; OVEN recognizer: 290; CONI manual: 250, CONI recognizer: 340).

Distance sampling

There was no significant difference between the density estimates produced with known distance and RSL predicted distance; however, the density estimate from manually measured RSL distance estimates was lower than true simulation density for OVEN (Fig. 5.7). Density estimates produced from human estimated distances were lower than density estimates from known distance and true simulation density for both species.

DISCUSSION

We show that relative sound level (RSL) can be used to estimate distance from autonomous recording units (ARUs) and is an improvement over human distance estimation. Distance estimation by observers in the field can be inaccurate with systematic or clumped error due to differences in skill, perception, and time since training (Alldredge et al. 2007, Camp 2007, Nadeau and Conway 2012). We found RSL distances were not clumped, and while models slightly overestimated smaller distances and underestimated greater distances, there was no significant error bias in CONI datasets and low error bias in OVEN datasets relative to reported error bias from human estimates of distance. Previous studies have reported mean error bias for human surveyors of -10.1% to 9.0% for distances up to 70 m (Scott et al. 1981), 7.6 m (± 21.4 m SD) for distances up to 98 m (Alldredge et al. 2007), -9 m (± 47 m SD) for distances up to 239 m (Nadeau and Conway 2012), and 53.3 m (± 58.6 m SD) for distances up to 500 m (Murray et al. 2011). Significant error bias in our RSL distances was 5.66 m (± 18.27 m SD) for OVEN manual measurement and 4.15 m (± 17.04 m SD) for OVEN recognizer measurement. Additionally, RSL provides individual distances instead of distance bins commonly used in bird counts. Our method of estimating error bias through cross-validation may provide optimistic results compared to distances predicted from a separate dataset but suggests less error than human surveyors. We note, however, that the human error that we extracted and compared to our RSL distance estimates is a case study and may not be representative because human observation distance estimation can vary based on a variety of factors (Simons et al. 2007, Nadeau and Conway 2012). In fact, the error bias reported in Nadeau and Conway (2012) is lower than the other case studies summarized above.

RSL distance prediction removes human subjectivity from distance estimation, and we suggest that automating extracting RSL estimates with recognizers further removes human subjectivity. We found that both distance estimation error and error bias were lower when we measured RSL with a recognizer. In contrast, the distance estimation error from manually measured RSL was large enough to significantly reduce the density estimate for OVEN. We suggest that automated RSL measurement with a recognizer is more accurate than manual measurement because it removes human subjectivity, variation, and error. Automated RSL measurement also improves the efficiency of the distance estimation process.

The improvement in distance estimation accuracy resulted in more accurate density estimates from distance sampling. We used simulation to show that the density estimates derived from RSL estimated distances did not differ from density estimates derived from known distances, despite the presence of some error and bias. Our results suggest that RSL distance prediction does not violate the assumption of distance sampling that distances are measured without error (Table 5.1). Density estimates should be relatively unaffected if distance estimation is unbiased on average, unless error in distance estimation is large (Buckland et al. 2001). In comparison, density estimates from human estimated distances were significantly lower than density estimates from known distance, likely due to human overestimation of distance in the dataset extracted from Nadeau and Conway (2012). We suggest that application of RSL distance prediction to real field recordings would improve compliance with the distance estimation assumption of distance sampling (Table 5.1), which is normally violated when using distances estimated by human surveyors (Buckland et al. 2001). RSL distance prediction also removes the subjectivity of human estimation, which can exacerbate bias in distance estimates (Sebastián-González et al. 2018). Future work should test whether distance sampling models that statistically incorporate quantified error in RSL estimated distance can further improve the accuracy of density estimates (Borchers et al. 2010).

Despite the improvement in distance estimates and density estimates from RSL distance prediction, some error remained in the RSL predicted distances. We investigated the residuals of the fitted models and found no correlation with any of our measured covariates, which suggests the remaining bias is due to an unmeasured covariate. The distance estimation error in our RSL distances is likely due to variation in individual acoustic behavior, such as vocalization directionality, height, and intensity. Animal vocalizations are not omnidirectional and the amount of spherical spreading can vary with signal type (Patricelli et al. 2007, Catchpole and Slater 2008). Sebastián-González et al. (2018) argue that directionality will not lead to biased density estimation if cues are oriented randomly relative to the ARU because they will average out. Height can also affect RSL because sounds emitted at greater heights suffer less attenuation than sounds emitted near the ground (Marten and Marler 1977), and we found that including vertical height as a covariate improved the parsimony of RSL distances. Alldredge et al. (2007) found that directionality of broadcast calls affected human surveyor estimation error, but height did not; however, they only tested to 12 m height, compared with up to 100 m height for our CONI. We also found that distance predictions were affected by time of day, which may be due to behavioral variation in the amplitude of bird song, with stronger levels earlier in the day (Porneluzi et al. 2011). This time-varying effect is also related to the assumption of perfect observability at zero distance, as availability and behavioral components are known to affect overall detectability (Sólymos et al. 2013). Finally, vegetation structure could also contribute to variation in RSL (Johnson 2008). We controlled for vegetative structure within each dataset by selecting study sites with similar vegetation, but there may have been differences between sites that introduced some variation in RSL distances.

Distance sampling from single point count ARUs has been infrequently attempted because the sampling radius of ARUs is typically unknown and may vary depending on recorder technology, vegetation, weather, and species (Yip et al. 2017*b,* Darras et al. 2018*a*). We found RSL was the main predictor of distance (93.4 - 99.7% total partitioned R^2), and several recent studies suggest that a reliable relationship between RSL and distance can be established for various taxa. Darras et al. (2018*b*) found that human listeners can estimate distance from recordings with 0.76-0.96 correlation with true distance for five species. Sebastián-González et al. (2018) found that sound power explained 37.45% of deviance in known distance of Hawai´i ´Amakihi (*Chlorodrepanis virens*). Both studies, however, did not quantify distance estimation error and only included known distances up to 80 m and 40 m, respectively. We suggest that distance sampling with RSL predicted distances from ARU recordings may be an easier method of density estimation than the spatially explicit capture-recapture (SECR) method because RSL distance prediction requires only one microphone (Dawson and Efford 2009). RSL distance prediction may also improve efficiency of distance estimation, as ARU deployment generally requires less time than field observations conducted by trained observers (Holmes et al. 2014).

RSL distance prediction does, however, require calibration recordings to establish the relationship between RSL and distance for the focal species. Calibration recordings can also be used for other applications, such as estimating distance by ear (Darras et al. 2018*b*) or setting recognizer classification thresholds (Knight and Bayne 2018). We showed that although RSL prediction error was smallest when we fit our model with our entire dataset (673 - 1223 clips), the reduction in error was minimal for datasets greater than 300 calibration recordings. We therefore suggest that the time required to collect calibration recordings for RSL distance should not be prohibitive for most species. We emphasize that calibration datasets for RSL distance prediction should be representative of the field recordings that the predictive model will be applied to. Distance estimation models should not be used across habitat types because attenuation varies with vegetation unless effective detection radius is tested for generalizability across vegetation types or corrected for with standardized variation (Yip et al. 2017*a*, *b*) or incorporating an attenuation coefficient (Royle 2018). Further, microphones for collecting calibration data and field recordings should be calibrated to the same standards to avoid bias in RSL measurements.

There are three known methods for developing calibration datasets. The first and most precise method, which we used here for OVEN, uses triangulation from an acoustic location system (ALS); however, this method is laborious to set up and post-process to obtain individual locations. We do not suggest this “ALS method” for anyone who does not already use an ALS for their focal species. The second method, introduced here for CONI, uses broadcast calls to attract an individual to a transect of recorders and a human surveyor to estimate bird location relative to that transect. This “transect method” requires only two to three hours of time each day for several days, produces an even distribution of known distances, and can also be used to control the known distances measured. The disadvantage of this method is that the precision of known distances is lower than triangulation, but precision could be improved if the focal species is one that sings from a perch and thus can be located with a laser rangefinder and compass. The third method, presented by Sebastián-González et al. (2018), involves walking the study area and manually recording vocalizing individuals that are visually detected while simultaneously measuring distance with a laser range-finder. A similar variant, presented by Darras et al. (2018*b*), involves conducting a point count survey with a human observer and an ARU, and measuring distance to any visual detections of vocalizing individuals. This "opportunistic method" requires a similar amount of field time as the broadcast-transect method, and likely has similar precision of known distances. The disadvantage of the haphazard method is that there is little control over the range of known distances recorded, and it may be difficult to obtain recordings at close range and far range, resulting in a RSL distance prediction model that does not perform well across all distances. We therefore recommend using the broadcast-transect method unless the acoustic behaviour of the focal species is altered by broadcast calls. Similar transect designs have been used in other acoustic studies to understand the effects of sound attenuation (Meyer et al. 2013, Yip et al. 2017*a*).

We thus conclude that RSL distance prediction is an accessible method that can be used to remove subjectivity, improve accuracy, and reduce bias of distance estimates and density estimates for most species. RSL distance prediction can also be used to improve the efficiency of density estimation because it can be applied to ARU recordings in an automated fashion. RSL predicted distances can be used in distance sampling to produce unbiased density estimates and thus not violate the assumption that distances are measured without error. Minimizing error in distance estimation is important for reducing error in density predictions from distance sampling (Buckland et al. 2001) and may prevent erroneous conclusions about wildlife populations.

Table 5.1. Violations of distance sampling assumptions and solutions to violations for point surveys conducted by human surveyors and ARUs. Multiple violations to the same assumption and corresponding solutions are lettered.

Distance sampling assumption	Violation by human surveyor surveys	Solution for human surveyor surveys	Violation by ARU surveys	Solution for ARU surveys	Advantage of ARU surveys
1. Distance to individuals is measured independent of animal movement	Only if sampling design is not randomly selected (Buckland et al. 2015).	Correct for bias by separating availability and detection functions (Marques et al. 2010).	Only if sampling design is not randomly selected (Buckland et al. 2015).	Correct for bias by separating availability and detection functions (Marques et al. 2010).	None
2. Individuals are perfectly detected at zero distance	a. Availability bias: if individuals at zero distance are not available for detection (e.g., does not vocalize). b. Perception bias: if observer fails to detect an individual.	a. Availability bias: Estimate proportion of available animals if availability is static, including any relevant covariates (Diefenbach et al. 2007, Thomson et al. 2012); incorporate intermittent availability pattern with hidden Markov models (Borchers et al. 2013, Langrock et al. 2013). b. Perception bias: Mark-recapture methods, double observer survey.	a. Availability bias: if individuals at zero distance are not available for detection (e.g., does not vocalize).	a. Availability bias: assume 100% availability by increasing sampling period to match vocalization availability (Barlow et al. 2013); other statistical methods used for human surveyors.	Permanent record from ARU recordings can be used to eliminate perception bias.

3. Distance is measured without error.	Significant error and bias in distance estimation by human surveyors.	Use a laser rangefinder to obtain estimates; integrate measurement error in distance sampling models (Borchers et al. 2010).	Often unknown for point count surveys (but see Darras et al. 2018b). Current methods rely on costly array designs and localization.	RSL distance prediction (this paper); integrate measurement error in distance sampling models (Borchers et al. 2010).	Error from RSL distance predictions small enough to not violate the assumption.
4. Individuals are detected at their initial location.	a. Individuals move around during survey. b. Individuals avoid the human surveyor.	a. Snapshot method (Buckland 2006). b. Allow individuals to “settle” before starting survey; revise methods if double observer data indicates avoidance (Buckland et al. 2015).	a. Individuals move around during survey.	a. Initial location assumed to be first vocalization event	Individuals less likely to be influenced by presence of ARU than human surveyor.
5. Individuals are not double-counted.	a. Movement of individuals during count can result in an individual being counted twice.	a. Cue counting (Hiby 1985, Buckland et al. 2015).	a. Movement of individuals during count can result in an individual being counted twice. b. Individuals can be difficult to separate without directional cues (unavailable for mono recordings).	a. Cue counting (Hiby 1985, Buckland et al. 2015). b. Separation of individuals using multichannel recordings (Dawson and Efford 2009).	Permanent record from ARU recordings can provide a more accurate cue count.

*Availability bias and perception bias can be hard to separate.

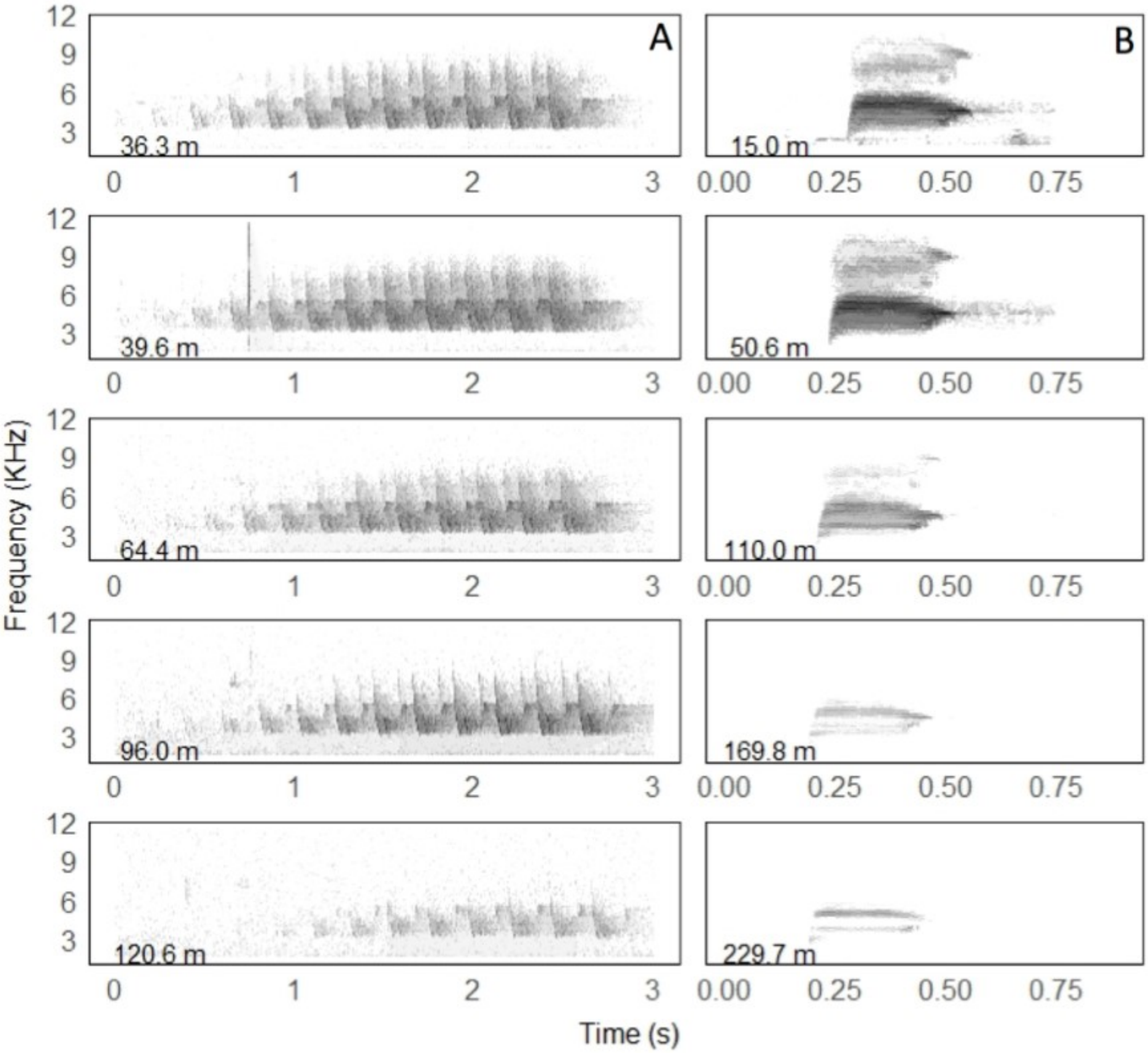

Figure 5.1. A) Spectrograms of a single call of an individual Ovenbird (*Seiurus aurocapilla*; OVEN) recorded at five microphones at varying distances, as determined by acoustic localization from an array of autonomous recording units (ARUs). B) Spectrograms of a single call of an individual Common Nighthawk (*Chordeiles minor*; CONI) recorded at ten microphones at varying distances, as determined by attraction of the bird with conspecific broadcast calls to the beginning of a transect of ARUs.

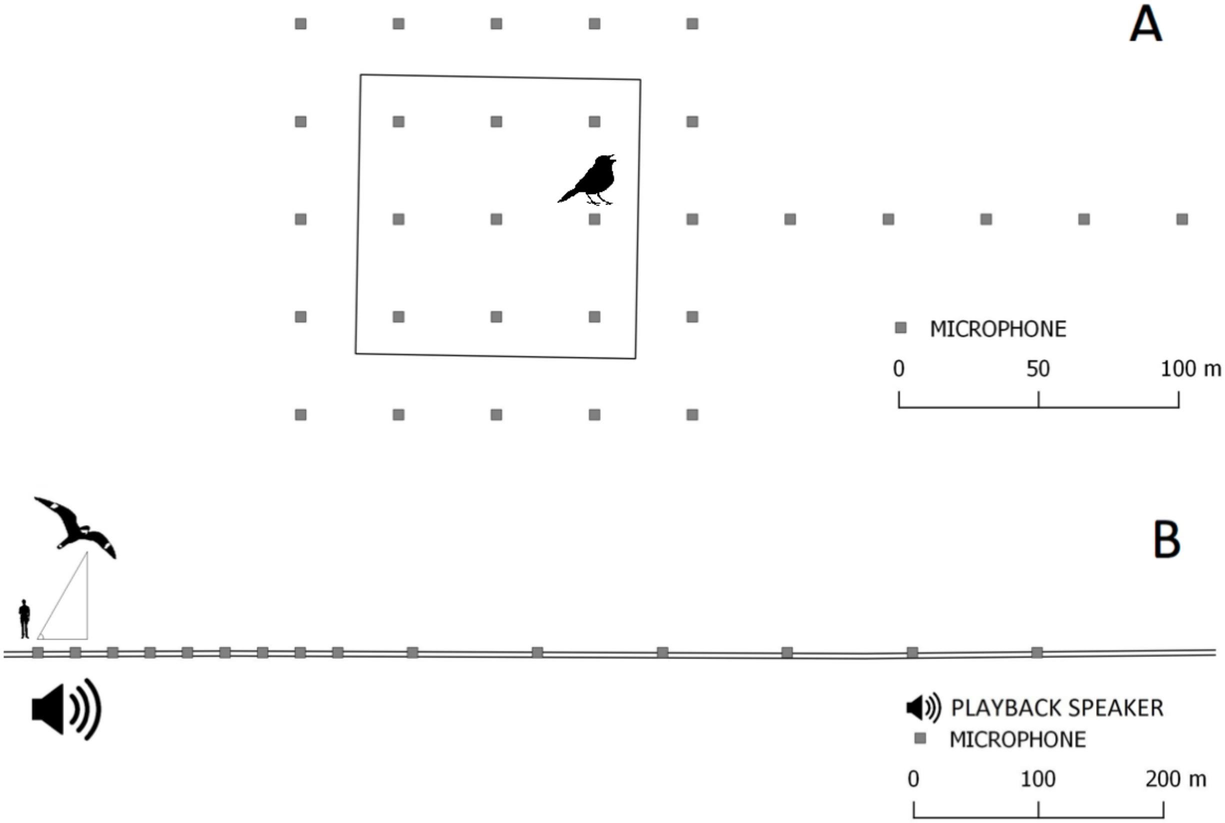

Figure 5.2. A) Autonomous recording unit (ARU) microphone array set-up at a wellsite (black square) for the localization of individual Ovenbird (*Seiurus aurocapilla*; OVEN) vocalizations.

B) Autonomous recording unit (ARU) microphone transect set-up along a linear feature (parallel lines) for the localization of individual Common Nighthawk (*Chordeiles minor*; CONI) vocalizations. An individual CONI was attracted with conspecific broadcast calls to the beginning of each transect, where an observer estimated the vertical and horizontal distance and bearing to the bird from the beginning of the transect for each vocalization.

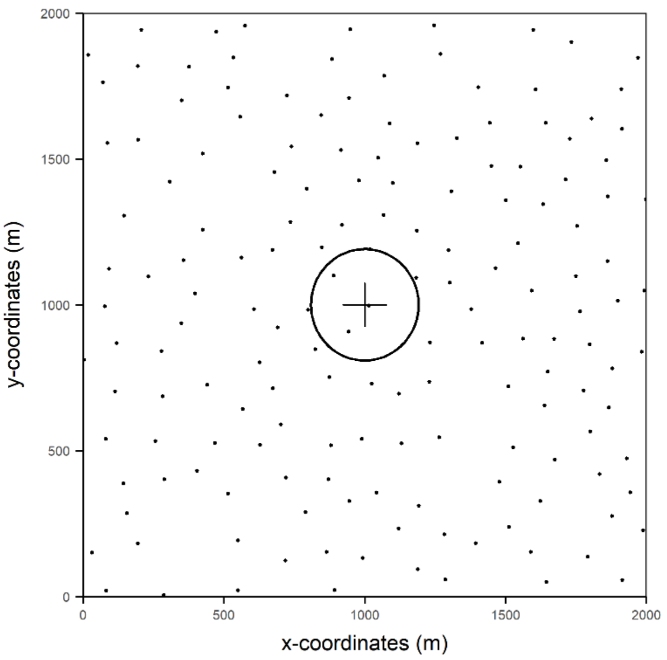

Figure 5.3. Example of CONI survey data generated through simulation. Each point represents the location of a vocalizing individual. The circle represents the effective detection radius for CONI at a survey location which is used to generate a set of detections and distances to individuals.

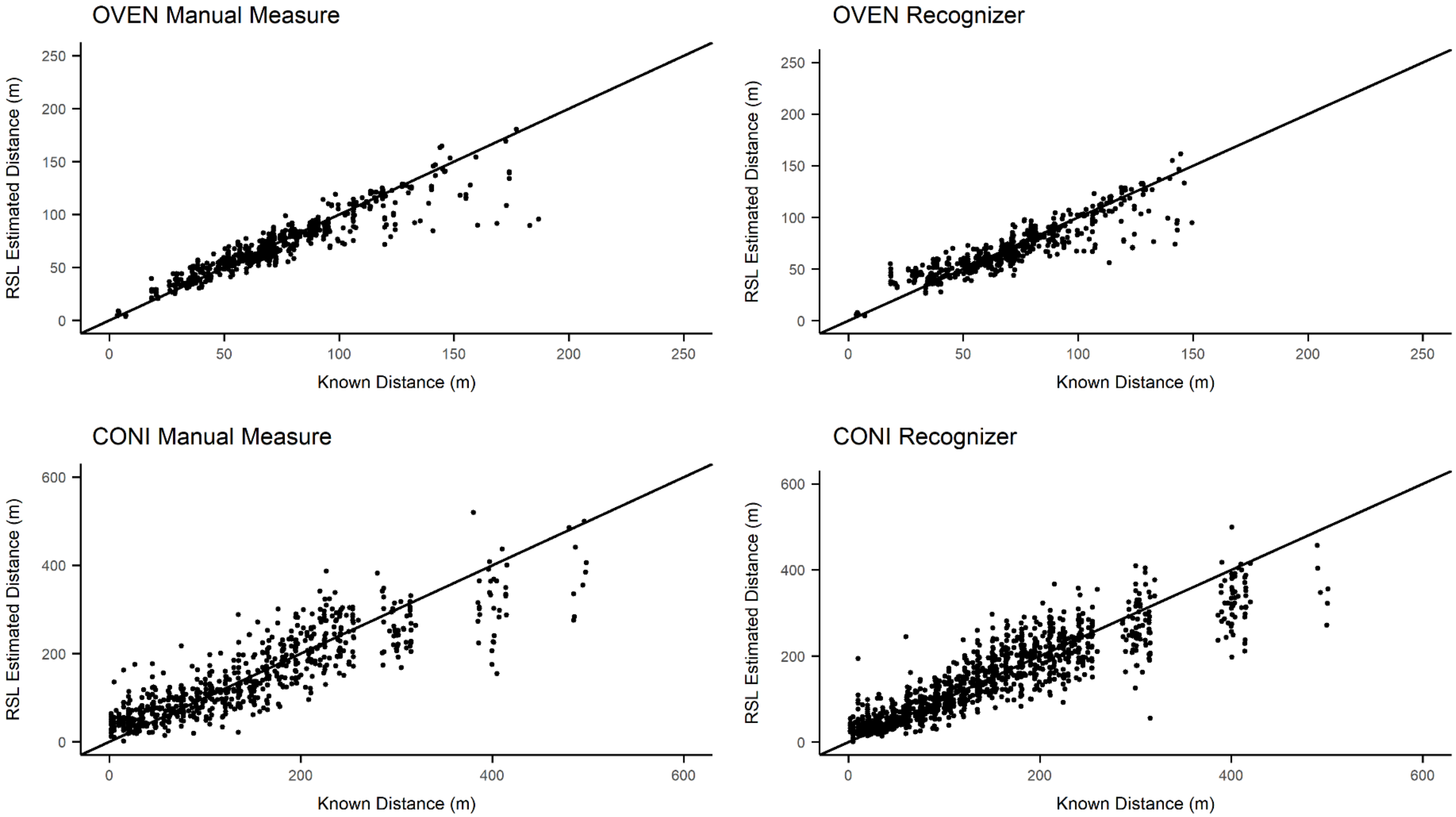

Figure 5.4. Relative sound level (RSL) estimated distance relative to known distance for Ovenbird (*Seiurus aurocapilla*; OVEN) and Common Nighthawk (*Chordeiles minor;* CONI) measured manually and with a recognizer. RSL predicted distance was predicted from generalized linear models for each species-method combination. Black line indicates no bias or error between known distance and RSL predicted distance.

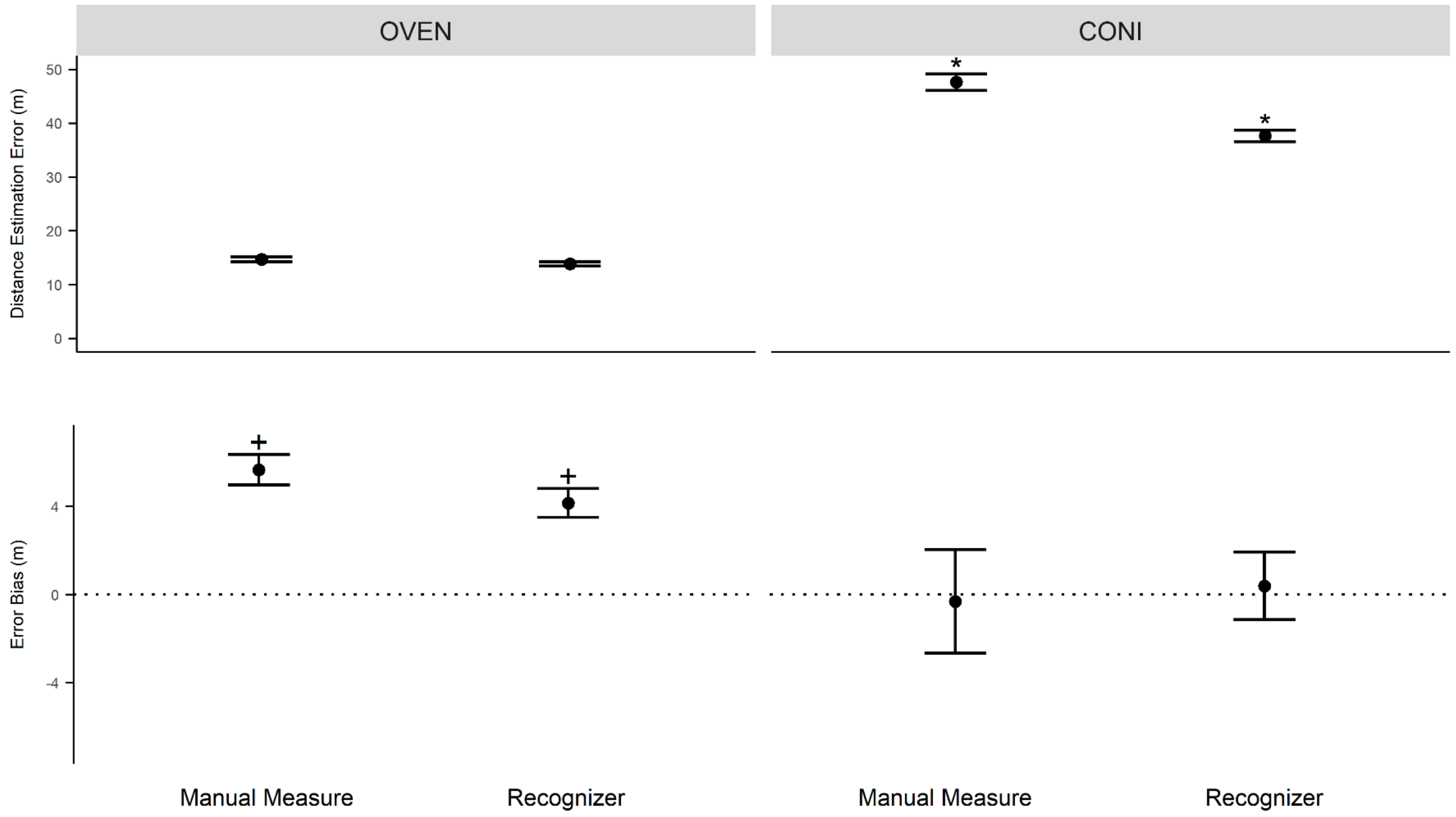

Figure 5.5. Distance estimation error and error bias of relative sound level (RSL) estimated distance for Ovenbird (*Seiurus aurocapilla*; OVEN) and Common Nighthawk (*Chordeiles minor;* CONI) measured manually and with a recognizer. Distance estimation error was calculated as the absolute value of the difference between RSL predicted distance and known distance. Error bias was calculated as the RSL predicted distance minus known distance. Known distances for both species were calculated as distance

between the autonomous recording unit (ARU) and the individual bird at the time of vocalization. Error bars represent standard error. * indicate significant differences between measurement methods for distance estimation error and + indicates significant difference (relative to zero) for error bias.

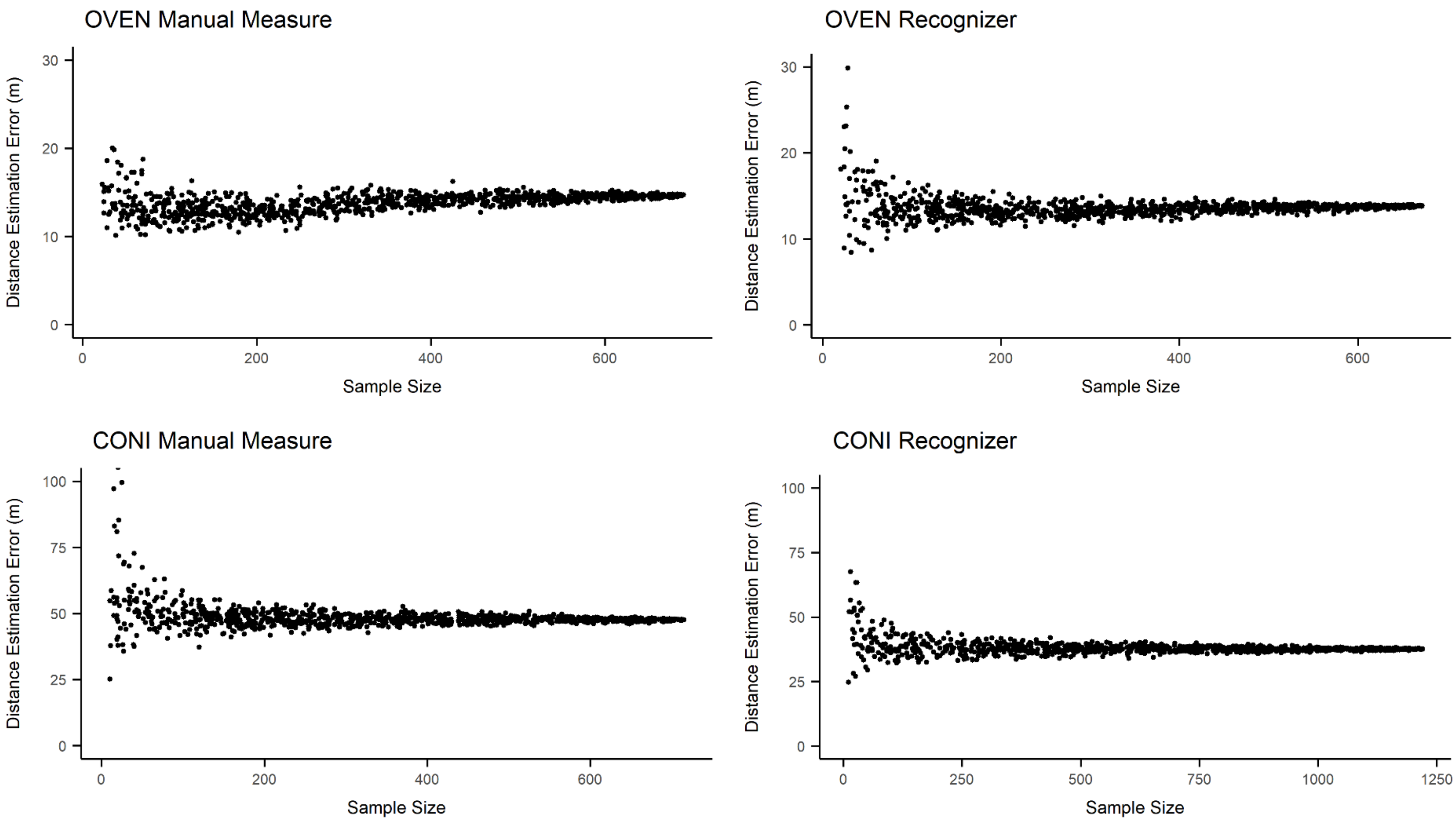

Figure 5.6. Bootstrapped distance estimation error for manual and recognizer RSL measurements of Ovenbird (*Seiurus aurocapilla*; OVEN) and Common Nighthawk (*Chordeiles minor*; CONI) recordings relative to sample size.

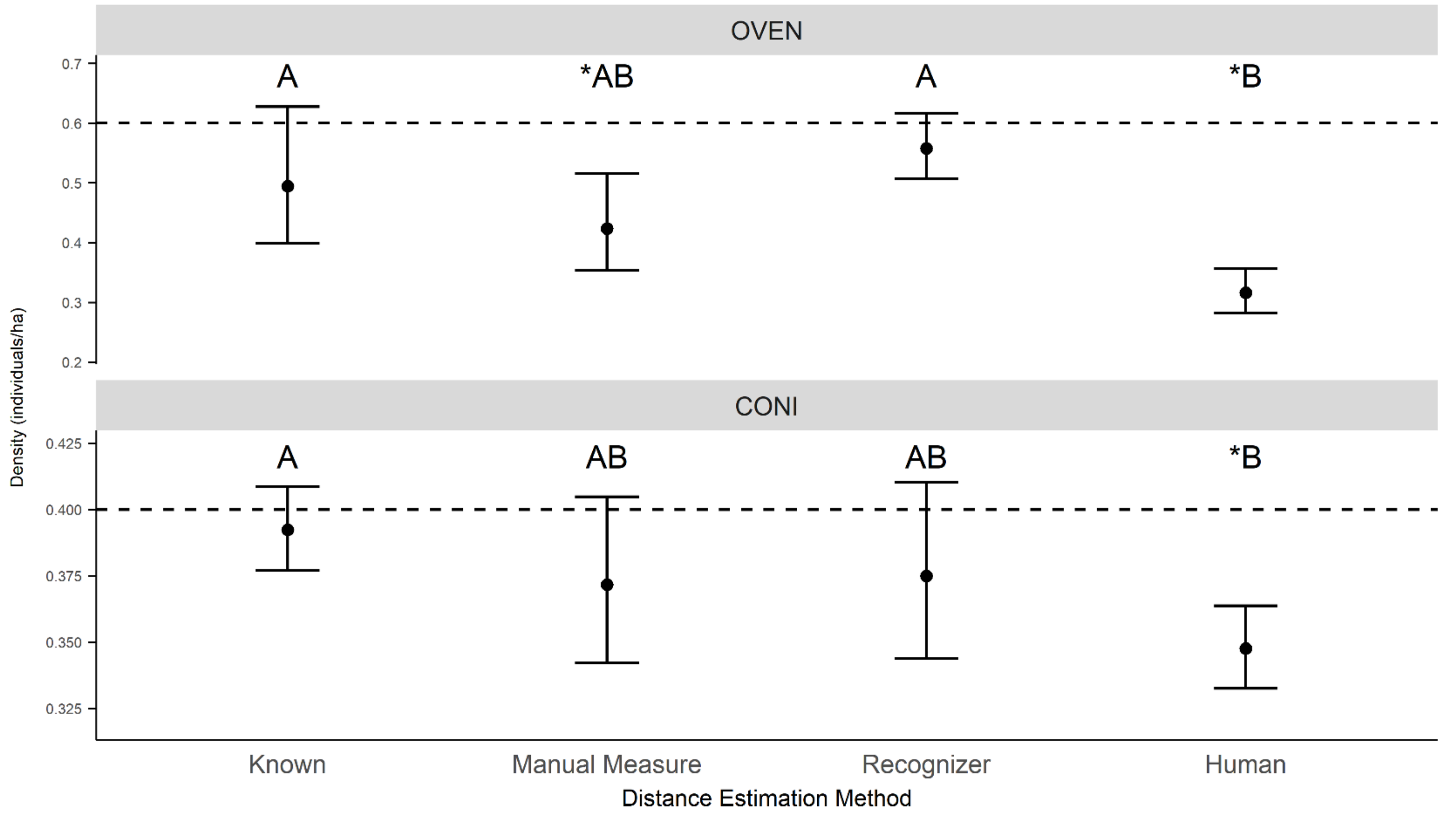

Figure 5.7. Density estimates of simulated Ovenbird (*Seiurus aurocapilla*; OVEN) and Common Nighthawk (*Chordeiles minor*; CONI) distributions using known distances, distances estimated from relative sound level (RSL) measured manually, with recognizer, and human surveyor distance estimation error. Mean error is presented with 83% confidence intervals. * indicate significant difference of density estimate from true simulation density represented by dashed line. Density estimates with different letters are significantly different.

Chapter 6. Discussion

In this thesis, I present research on factors responsible for variable detectability during avian surveys and ways to account for them, implications for ignoring detectability, and methods for estimating abundance and density from bioacoustic data. In chapter 2, I investigated differences in detectability, sound attenuation, and survey radius between roadside and traditional point counts and found that roadside surveys could result in a detection radius that is more than twice as large as a survey within interior forest. From a biological perspective, there are many variables that could influence avian surveys conducted from roadside locations. However, my findings indicated that from a sound physics perspective, the acoustic environment differs significantly and could lead to serious implications if combining roadside and traditional point count data. To address this, I presented a method to account for differences in detectability between these two environments using statistical offsets.

Continued improvement, innovation, and availability of commercially developed wildlife recording devices means that a variety of different equipment is available to researchers. However, combining data from different sources to answer larger-scale ecological questions when detectability differs between equipment is still a concern. Furthermore, integration with data collected using traditional point counts could be useful for historical analyses and trend-monitoring. In chapter 3, I examined differences in detectability and detection distance between four commercially available acoustic recording devices. I also compared these devices to detectability in human observers so that acoustic and human point count data can be standardized. I found that detectability and detection distance was highest in human observers relative to acoustic recording devices, and that significant variation between devices existed as well. The use of recording equipment introduces interference, static, and white noise into the detection process, likely lowering detectability on audio recordings relative to observations in the field. However, in this scenario, observers were only presented with a limited number of sounds and could learn to anticipate which species would be presented. Detection from audio recordings likely performs better when species are unpredictable due to the ability to double-check detections in a controlled environment. Finally, I presented a method similar to chapter 2 for standardization of bioacoustic data from multiple sources using statistical offsets. The ability to combine data from a variety of sources is of significant value when answering ecological questions about how birds interact with their environment at larger spatial scales.

In chapter 2 and 3, I presented methods for calculating statistical offsets using playback experiments for standardization of data from locations in different acoustic environments or from different sources. However, in both studies we only used 25 species, which is less useful for ecologists wishing to apply these methods to focal species not included in our experiments. In chapter 4, I similarly used sound playback experiments to quantify differences in detectability for different vegetation types and calculate statistical offsets. I used vegetation type and generalized species vocalization traits to predict offsets that could reduce bias in estimating animal abundance or density to less than 40%. I also quantified relative contributions from vegetation type, species vocalization traits, and local atmospheric conditions to determine the most important factors to account for when correcting for variable detectability. Species traits and vegetation were the most important factors and weather conditions contributed a very small amount of variation. Accounting for variation in detectability in different environments is recommended, however in acoustic monitoring this often requires pilot studies to study the relationship between sound attenuation and the environment a signal passes through for each individual species of interest. This method allows researchers to predicting offsets that account for detectability without having to conduct time consuming preliminary studies when calibration datasets already exist.

The preceding chapters recommend the use of statistical offsets to standardize variable detection probability during acoustic surveys. However, count data produced by these surveys generally provide measures of relative abundance unless additional statistical approaches are applied. Animal density is often the preferred metric when assessing wildlife populations as it is a common standard that is comparable across different study programs, regions, and datasets. In chapter 5, I presented methods to estimate animal density using point counts and conventional distance sampling (Buckland et al. 2001). By building a simple calibration dataset, I demonstrate that measurements of relative sound level (RSL) from automated recognition software can be used to estimate the distance of vocalizing birds more accurately than human observers resulting in better accuracy and precision for estimate of animal density. This method is much more efficient than using sensor grids to estimate density (Dawson and Efford 2009, Efford et al. 2009), more objective than distance estimates from human observers using audio recordings (Darras et al. 2018*b*) or in the field (Alldredge et al. 2007, Nadeau and Conway 2012), and produces a more suitable calibration dataset relative to other similar methods.

An ongoing challenge for acoustic monitoring is standardization of data and survey design. Detection probability and detection distance are influenced by numerous factors which make comparing data from different treatments, datasets, or survey designs difficult. In chapter 2, 3, and 4, I presented methods to standardize measures of relative abundance from a variety of sources by investigating differences in detection probability and survey area for variables of interest. Incorporating variable detectability is essential for avian surveys and could lead to significant error if not accounted for (Denes et al. 2015). Survey design also varies greatly in the literature (Gibb et al. 2018). Survey durations range from one minute to hours depending on the focal species and the arrangement of sensors changes depending on research objectives. Integrating data from sources where survey design differs is often complicated and require advance statistical methods (Solymos et al 2013), and in these situations measures of animal density can be preferable to relative abundance.

The results of this thesis indicate the importance of acknowledging variable detectability from sound attenuation during analysis, and the potential implications of assuming constant detectability across a range of variables studied here. Variation in detectability can mask biological patterns or lead to erroneous conclusions based on results not representative of the study system. While it is possible to reduce variation through careful selection of study design parameters, some variables, particularly those tied to research questions or objectives (i.e. surveying species in different habitats or conditions), are difficult to account for until the analysis stage. In this case, I suggest standardizing detectability through methods presented in this thesis. I also present the relative effects of different variables on detectability to assist with prioritizing the most important factors in complicated study systems. In particular, this methodology is particularly relevant to surveys or monitoring programs where locations are sampled using a single acoustic recording unit, where typical approaches for standardizing detectability in traditional surveys are no longer applicable.

Estimating animal density from acoustic recordings can be done using grids of synchronized autonomous recording units (ARUs) and simultaneous detections of individuals across these grids using spatially-explicit capture-recapture (SECR; Dawson and Efford 2009, Efford et al. 2009) or acoustic localization (Wilson and Bayne 2018) approaches. These grids provide high-resolution data on habitat associations for the focal species, however these studies usually focus on small-scale objectives as they are too equipment, labor, time, and processing intensive to answer questions at large ecological scales. Previously, estimating animal density from a single acoustic sensor was problematic because survey area, a fundamental component for estimating density, was unknown. In the past year, the findings I present in chapter 5, along with research by Sebastian-Gonzalez et al. (2018) and Darras et al. (2018), suggest that the strength of a signal on an audio recording is a reliable indicator for the distance of that signal. RSL was responsible for at least 90% of variation in distance estimation models. In combination with conventional distance sampling (Buckland et al. 2001), this method can provide results with higher accuracy than human observers and can be used to answer questions at larger scales as the number of sensors and the labor required to deploy them are no longer limiting factors.

Acoustic monitoring is becoming increasingly popular and recording equipment is also developing rapidly as demand increases. Turnover in available equipment for research programs is high as support and maintenance for older recording units is phased out. In chapter 3, I propose methods to standardize data from four of the most popular recording units at the time. However, the advancement and diversity of options currently available for acoustic monitoring means that the equipment tested may no longer be available, or better options have become available. It is unrealistic to use the methods presented in chapter 3 on every model of acoustic recorder available today. Instead, future research should investigate the effect of frequency response, dynamic range, sensitivity, and signal-to-noise ratio on detectability. Data from different recording units can then be standardized using statistical offsets predicted from these variables, which should be readily available from the manufacturer, as described in the methods for chapter 4. Modelling equipment specifications and predicting statistical offsets requires only an initial calibration study be performed and does not require collecting data for additional recording units as they are released if equipment specifications are known.

There is considerable future potential for increased automation and processing efficiency within acoustic monitoring technology. Wildlife Acoustics has tested ARUs capable of remote data uploads using cellular or satellite networks. The ability to connect these devices to an external power supply also means that ARUs could be run using solar power or other renewable sources. Without restrictions on data storage and power supply, ARUs could be deployed indefinitely for long-term monitoring programs with the added benefit of real-time data processing. Automated recognition methods are also in the early stages of development and are constantly undergoing streamlining and improvement (Knight et al. 2017, Knight and Bayne 2018). Continued advancement in the accuracy and accessibility of multi-species classifiers (Knight et al. 2019) increases the possibility for remote data collection with automated workflows that are capable of community-based monitoring. Current logistical challenges for acoustic monitoring involve the storage and interpretation of audio recordings (Shonfield and Bayne 2017). ARUs are capable of generating a high volume of data, but one of the biggest limiting steps is interpretation, which still typically involves manual listening by human observers. The development of accurate, readily accessible multi-species classifiers for interpretation of animal communities would greatly reduce the processing time required and reduce the need for storage of audio recordings awaiting processing. Furthermore, in an automated workflow, recordings could be uploaded via cellular or satellite networks and processed automatically by multi-species classifiers to generate community data at large spatial scales with little effort. If audio recordings do not need to be retained for other uses, the ability to interpret recordings automatically and in real-time would remove the need to store them completely or allow for conversion to high-compression formats to reduce storage requirements substantially.

Acoustic monitoring, like many other remote sensing tools, uses cutting edge developments in the computer sciences and in technology to address ecological and management-based objectives. While technological advancement has increased substantially with the rise in popularity of acoustic monitoring, methodological and analytical approaches that focus on traditional surveys need to be updated to deal with the challenges of acoustic data as well. Development of monitoring methods greatly increases our ability to collect a variety data, using ARUs, point counts, and through citizen-science sources such as eBird. However, integration of datasets from multiple sources requires standardization of data to be useful. Research presented in this thesis builds a foundation to facilitate the integration of avian data from multiple sources and environments by standardizing indices for relative abundance and describing methods to converting acoustic count data into more versatile forms such as animal abundance or density.

References

Abadi, M., A. Agarwal, P. Barham, E. Brevdo, Z. Chen, C. Citro, G. Corrado, A. Davis, J. Dean, M. Devin, S. Ghemawat, I. Goodfellow, A. Harp, G. Irving, M. Isard, Y. Jia, R. Jozefowicz, L. Kaiser, M. Kudler, J. Levenberg, D. Mané, R. Monga, S. Moore, D. Murray, C. Olah, M. chuster, J. Shlens, B. Steiner, I. Sutskever, K. Talwar, P. Tucker, V. Vanhoucke, V. Vasudevan, F. Viégas, O. Vinyals, P. Warden, M. Wattenberg, M. Wicke, Y. Yu, and X. Zheng. 2015. TensorFlow: Large-scale machine learning on heterogeneous systems. URL www.tensorflow.org

Alldredge, M., T. Simons, and K. Pollock. 2007. A field evaluation of distance measurement error in auditory avian point count surveys. *The Journal of Wildlife Management* 71:2759-2766.

Anderson, B. W., and R. D. Ohmart. 1977. Climatological and physical characteristics affecting avian population estimates in southwestern riparian communities using transect counts. In Importance, preservation and management of riparian habitat: a symposium (R. R. Johnson and D. A. Jones, Editors). U. S. Department of Agriculture Forest Service General Technical Report RM-43, Fort Collins, Colorado, USA. Pp. 193-200.

Anderson, D. R. 2001. The need to get the basics right in wildlife field studies. *Wildlife Society Bulletin* 29:1294–1297.

Arnold, T. W. 2010. Uninformative parameters and model selection using akaike's information criterion. *Journal of Wildlife Management* 74:1175-1178.

Aylor, D. 1972. Noise reduction by vegetation and ground. *The Journal of the Acoustical Society of America* 51:197.

Ballentine, B., J. Hyman, and S. Nowicki. 2004. Vocal performance influences female response to male bird song: An experimental test. *Behavioural Ecology* 15:163-168.

Barlow, J., P. L. Tyack, M. P. Johnson, R. W. Baird, G. S. Schorr, R. D. Andrews, and N. A. de Soto. 2013. Trackline and point detection probabilities for acoustic surveys of Cuvier's and Blainville's beaked whales. *The Journal of the Acoustical Society of America* 134:2486–2496.

Bart, J., M. Hofschen, and B. G. Peterjohn. 1995. Reliability of the Breeding Bird Survey: effects of restricting surveys to roads. *Auk* 112:758-761.

Barton, K. 2015. MuMIn: Multi-model inference. R package version 1.15.1. URL http://CRAN.R-project.org/package=MuMIn

Bates, D., M. Maechler, B. Bolker, and S. Walker. 2015. Fitting linear mixed-effects models using lme4. *Journal of Statistical Software* 67:1-48.

Berg, R. E., and D. G. Stork. 2004. The physics of sound. 3rd edition. Addison-Wesley. Boston, MA, USA.

Bioacoustics Research Program. 2014. Raven Pro: Interactive Sound Analysis Software (Version 1.5). The Cornell Lab of Ornithology, Ithaca, New York, USA.

Boersma, P., and D. Weenink. 2015. Praat: doing phonetics by computer. University of Amsterdam, Amsterdam, NL. URL http://www.fon.hum.uva.nl/praat/

Borchers, D. L., T. A. Marques, T. Gunnlaugsson, and P. E. Jupp. 2010. Estimating distance sampling detection functions when distances are measured with error. *Journal of Agricultural, Biological, and Environmental Statistics* 15:346-361.

Borchers, D. L., W. Zucchini, M. P. Heide-Jørgensen, A. Cañadas, and R. Langrock. 2013. Using hidden Markov models to deal with availability bias on line transect surveys. *Biometrics* 69:703–713.

Breusch, T. S., and A. R. Pagan. 1979. A simple test for heteroscedasticity and random coefficient variation. *Econometrica* 47:1287-1294.

Brigham, R. M., J. Ng, R. G. Poulin, and S. D. Grindal. 2011. Common Nighthawk (*Chordeiles minor*). P. G. Rodewald, editor. The Birds of North America. Cornell Lab of Ornithology, Ithaca, New York, USA. URL: https://birdsna-org /Species-Account/bna/species/comnig

Brumm, H. 2004. The impact of environmental noise on song amplitude in a territorial bird. *Journal of Animal Ecology* 73:434-440.

Brumm, H., and M. Naguib. 2009. Environmental acoustics and the evolution of bird song. *Advances in the Study of Behaviour* 40:1-33.

Bullen, R., and F. Fricke 1976. Sound propagation in a street. *Journal of Sound and Vibration* 46:33-42.

Buckland, S. T., D. R. Anderson, K. P. Burnham, and J. L. Laake. 1993. Distance sampling: estimating abundance of biological populations. Chapman & Hall, London, UK.

Buckland, S. T., D. R. Anderson, K. P. Burnham, J. L. Laake, D. L. Borchers, and L. Thomas. 2001. Introduction to distance sample: estimating abundance of biological populations, 2nd ed. Oxford University Press, New York, New York, USA.

Buckland, S. T., R. W. Summers, D. L. Borchers, and L. Thomas. 2006. Point transect sampling with traps or lures. *Journal of Applied Ecology* 43:377–384.

Buckland, S. T., E. A. Rexstad, T. A. Marques, and C. S. Oedekoven. 2015. Distance Sampling: Methods and Applications. Springer International Publishing, Switzerland.

Burnham, K. P., and D. R. Anderson. 2002. Model selection and multi-model inference: a practical information-theoretical approach, 2nd edition. Springer-Verlag. New York, NY, USA.

Camp, R. J. 2007. Measurement errors in Hawaiian forest bird surveys and their effect on density estimation. TR HCSU-005. Hawai`i Cooperative Studies Unit, University of Hawai`i, Hilo, Hawai`i, USA.

Catchpole, C. K., and P. J. B. Slater. 2008. Bird song: biological themes and variations. Second edition. Cambridge University Press, New York, New York, USA.

Cato, D. H. 1998. Simple methods of estimating source levels and locations of marine animal sounds. *The Journal of the Acoustical Society of America* 104**:**1667-1678.

Celis-Murillo, A., J. L. Deppe, and M. F. Allen. 2009. Using soundscape recordings to estimate bird species abundance, richness, and composition. *Journal of Field Ornithology* 80:64-78.

Charif, R. A., A. M. Waack, and L. M. Strickman. 2010. Raven Pro 1.4 User's Manual. Cornell Lab of Ornithology, Ithaca, NY, USA.

Clayton, N. S. 1990. Assortative mating in zebra finch subspecies, *Taeniopygia guttata guttata* and *T. g. castanotis*. *Philosophical Transactions of the Royal Society of London B* 330:351-370.

Cobos, M., F. Antonacci, A. Alexandridis, A. Mouchtaris, and B. Lee. 2017. A survey of sound source localization methods in wireless acoustic sensor networks. *Wireless Communications and Mobile Computing* 2017:3956282.

Corn, P. S., E. Muths, A. M. Kissel, and R. D. Scherer. 2011. Breeding chorus indices are weakly related to estimated abundance of boreal chorus frogs. *Copeia* 2011:365-371

Cumming, S. G., K. L. Lefevre, E. M. Bayne, T. Fontaine, F. K. A. Schmiegelow, and S. J. Song. 2010. Towards conservation of Canada's boreal forest avifauna: design and application of ecological models at continental extents. *Avian Conservation and Ecology* 5:8.

Darras, K., P. Pütz, K. Rembold, and T. Tscharntke. 2016. Measuring sound detection spaces for acoustic animal sampling and monitoring. *Biological Conservation* 201:29-37.

Darras, K., P. Batary, B. Furnas, A. Celis-Murillo, S. L. Van Wilgenburg, Y. A. Mulyani, T. Tscharntke. 2018*a*. Comparing the sampling performance of sound recorders versus point counts in bird surveys: A meta-analysis. *Journal of Applied Ecology* 55:2575-2586.

Darras, K., B. Furnas, I. Fitriawan, Y. Mulyani, and T. Tscharntke. 2018*b*. Estimating bird detection distances in sound recordings for standardizing detection ranges and distance sampling. *Methods in Ecology and Evolution* 9:1928–1938.

Dawson, D. K., and M. G. Efford. 2009. Bird population density estimated from acoustic signals. *Journal of Applied Ecology* 46:1201–1209.

Denes, F. V., L. F. Silveira, and S. R. Beissinger. 2015. Estimating abundance of unmarked animal populations: accounting for imperfect detection and other sources of zero inflation. *Methods in Ecology and Evolution* 6:543-556.

Diefenbach, D. R., M. R. Marshall, J. A. Mattice, and D. W. Brauning. 2007. Incorporating availability for detection in estimates of bird abundance. *The Auk* 124:96–106.

Droege, S. 1990. The North American Breeding Bird Survey. In Survey designs and statistical methods for the estimation of avian population trends (J.R. Sauer and S. Droege, Editors), pp. 1-4. U.S. Fish and Wildlife Service. Biological Report 90(1), Washington, DC, USA.

Efford, M. G., D. K. Dawson, and D. L. Borchers. 2009. Population density estimated from locations of individuals on a passive detector array. *Ecology* 90:2676-2682.

Emlen, J. T., and M. J. DeJong. 1981. The application of song detection threshold distance to census operations. *Studies in Avian Biology* 6:346-352.

Emlen, J. T., and M. J. DeJong. 1992. Counting birds: the problem of variable hearing abilities. *Journal of Field Ornithology* 63:26-31.

Farnsworth, G. L., K. H. Pollock, J. D. Nichols, T. R. Simons, J. E. Hines, and J. R. Sauer. 2002. A removal model for estimating detection probabilities from point-count surveys. *The Auk* 119:414-425.

Forrest, T. G. 1994. From sender to receiver: propagation and environmental effects on acoustic signals. *American Zoologist* 34:644-654.

Fricke, F. 1984. Sound attenuation in forests. *Journal of Sound and Vibration* 92:149-158.

Furnas, B. J., and R. L. Callas. 2015. Using automated recorders and occupancy models to monitor common forest birds across a large geographic region. *Journal of Wildlife Management* 79:325-337.

Gibb, R., E. Browning, P. Glover-Kapfer, and K. E. Jones. 2018. Emerging opportunities and challenges for passive acoustics in ecological assessment and monitoring. *Methods in Ecology and Evolution* 10:169-185.

Gutzwiller, K. J., and H. A. Marcum. 1997. Bird reactions to observer clothing color: implications for distance-sampling techniques. *The Journal of Wildlife Management* 61:935-947.

Harris, C. M. 1966. Absorption of sound in air versus humidity and temperature. *The Journal of the Acoustical Society of America* 40:148-159.

Haselmayer, J., and J. S. Quinn. 2000. A comparison of point counts and sound recording as bird survey methods in Amazonian southeast Peru. *The Condor* 102:887-893.

Helzner, E. P., J.A. Cauley, S. R. Pratt, S. R. Wisniewski, J. M. Zmuda, E. O. Talbott, N. Rekeneire, T. B. Harris, S. M. Rubin, E. M. Simonsick, F. A. Tylavsky, and A. B.

Newman. 2005. Race and sex differences in age-related hearing loss: the health, aging and body composition study. *Journal of the American Geriatrics Society* 53:2119-2127.

Hiby, A. R. 1985. An approach to estimating population densities of great whales from sighting surveys. *IMA Journal of Mathematics Applied in Medicine and Biology* 2:201-220.

Hill, A. P., P. Prince, E. P. Covarrubias, C. P. Doncaster, J. L. Snaddon, and A. Rogers. 2018. AudioMoth: evaluation of a smart open acoustic device for monitoring biodiversity and the environment. *Methods in Ecology and Evolution* 9:1199-1211.

Hobson, K. A., R. S. Rempel, H. Greenwood, B. Turnbull, and S. L. Van Wilgenburg. 2002. Acoustic surveys of birds using electronic recordings: new potential from an omnidirectional microphone system. *Wildlife Society Bulletin* 30:709-720.

Holland, K. R. 2001. Principles of sound radiation. Pages 1-43 *in* J. Borwick, editor. Loudspeaker and headphone handbook, 3rd ed. Focal Press, Oxford, UK.

Holmes, S. B., K. A. McIlwrick, and L. A. Venier. 2014. Using automated sound recording and analysis to detect bird species-at-risk in Southwestern Ontario woodlands. *Wildlife Society Bulletin* 38:591-598.

Hutto, R. L., S. M. Pletschet, and P. Hendricks. 1986. A fixed-radius point count method for nonbreeding and breeding season use. *The Auk* 103:593-602.

Hutto, R. L., and R. J. Stutzman. 2009. Humans versus autonomous recording units: a comparison of point-count results. *Journal of Field Ornithology* 80:387-398.

Johnson, D. H. 2008. In defence of indices: the case of bird surveys. *Journal of Wildlife Management* 72:857-868.

Jones, E., E. Oliphant, P. Peterson, et al. 2001. SciPy: Open source scientific tools for Python. URL: http://www.scipy.org/

Katz, J., S. D. Hafner, and T. Donovan. 2016. Assessment of error rates in acoustic monitoring with the R package monitoR. *Bioacoustics* 25:177-196.

Keller, C. M. E., and J. T. Scallan. 1999. Potential roadside biases due to habitat changes along Breeding Bird Survey routes. *Condor* 101:50-57.

Kepler, C. B., and J. M. Scott. 1981. Reducing bird count variability by training observers. *Studies in Avian Biology* 6:366-371.

Kéry, M., J. A. Royle, and H. Schmid. 2005. Modeling avian abundance from replicated counts using binomial mixture models. *Ecological Applications* 15:1450-1461.

Knight, E. C., K. Hannah, G. Foley, C. Scott, M. Brigham, and E. M. Bayne. 2017. Recommendations for acoustic recognizer performance assessment with application to five common automated signal recognition programs. *Avian Conservation and Ecology* 12:14.

Knight, E. C., and E. M. Bayne. 2018. Classification threshold and training data affect the quality and utility of focal species data processed with automated audio recognition software. *Bioacoustics*. DOI: 10.1080/09524622.2018.1503971.

Koloff, J., and D. J. Mennill. 2013. The responses of duetting antbirds to stereo duet playback provide support for the joint territory defence hypothesis. *Ethology* 119:462-471.

Krzywinski, M., and N. Altman. 2013. The meaning of error bars is often misinterpreted, as is the statistical significance of their overlap. *Nature Methods* 10:921-922.

Langrock, R., D. L. Borchers, and H. J. Skaug. 2013. Markov-modulated nonhomogeneous Poisson processes for unbiased estimation of marine mammal abundance. *Journal of the American Statistical Association* 108:840–851.

Lankau, H. E., E. M. Bayne, and C. S. Machtans. 2013. Ovenbird (*Seiurus aurocapilla*) territory placement near seismic lines is influenced by forest regeneration and conspecific density. *Avian Conservation and Ecology* 8:5.

Larom, D., M. Garstang, K. Payne, R. Raspet, and M. Lindeque. 1997. The influence of surface atmospheric conditions on the range and area reached by animal vocalizations. *Journal of Experimental Biology* 200:421-431.

Lawler, J. L., and R. J. O'Connor. 2004. How well do consistently monitored Breeding Bird Survey routes represent the environments of the conterminous United States? *Condor* 106:801-814.

Lein, M. R. 1981. Display behavior of Ovenbirds (*Seiurus aurocapillus*) II. Song variation and singing behavior. *The Wilson Bulletin* 93**:**21-41.

Ligges, U., S. Krey, O. Mersmann, and S. Schnackenberg. 2016. tuneR: Analysis of music. URL: http://r-forge.r-project.org/projects/tuner/.

Luczkovich, J. J., D. A. Mann, and R. A. Rountree. 2008. Passive acoustics as a tool in fisheries science. *Transactions of the American Fisheries Society* 137:533-541.

MacLaren, A. R., P. S. Crump, J. A. Royle, and M. R. J. Forstner. 2018. Observer-free experimental evaluation of habitat and distance effects on the detection of anuran and bird vocalizations. *Ecology and Evolution* 8:12991-13003.

Marques, T. A., S. T. Buckland, D. L. Borchers, D. Tosh, and R. A. McDonald. 2010. Point transect sampling along linear features. *Biometrics* 66:1247-1255.

Marten, K., and P. Marler. 1977. Sound transmission and its significance for animal vocalization: I. Temperate habitats. *Behavioral Ecology and Sociobiology* 2:271-290.

Marques, T. A., L. Thomas, S. W. Martin, D. K. Mellinger, J. A. Ward, D. J. Moretti, D. Harris, and P. L. Tyack. 2013. Estimating animal population density using passive acoustics. *Biological Reviews* 88:287–309.

Matsuoka, S. M., C. L. Mahon, C. M. Handel, P. Sólymos, E. M. Bayne, P. C. Fontaine, and C. J. Ralph. 2014. Reviving common standards in point-count surveys for broad inference across studies. *The Condor* 116:699-608.

Matyjasiak, P. 2004. Birds associate species-specific acoustic and visual cues: Recognition of heterospecific rivals by male blackcaps. *Behavioural Ecology* 16:467-471.

Maynard, D. F., K. A. Ward, S. M. Doucet, and D. J. Mennill. 2012. Calling in an acoustically competitive environment: duetting male long-tailed manakins avoid overlapping neighbours but not playback-simulated rivals. *Animal Behaviour* 84:563-573.

McDonald, M. A., and C. G. Fox. 1999. Passive acoustic methods applied to fin whale population density estimation. *The Journal of the Acoustical Society of America* 105**:**2643-2651.

McFee, B. et al. 2017. librosa 0.5.0. Zenodo. URL: https://doi.org/10. 5281/zenodo.293021

Mellinger, K. D., K. M. Stafford, S. E. Moore, R. P. Dziak, and H. Matsumoto. 2007. An overview of fixed passive acoustic observation methods for cetaceans. *Oceanography* 4:36-45.

Meyer, J., L. Dental, and F. Meunier. 2013. Speech recognition in natural background noise. *PLoS ONE* 8:e79279.

Morton, E. S. 1975. Ecological sources of selection of avian sounds. *The American Naturalist* 109:17-34.

Mosteller, F., and J. W. Tukey. 1968. Data analysis, including statistics. Pages 80-203 *in* G. Lindzey and E. Aronson, editors, Handbook of Social Psychology. Addison-Wesley, Reading, Massachusetts, USA.

Nadeau, C. P. and C. J. Conway. 2012. Field evaluation of distance-estimation error during wetland-dependent bird surveys. *Wildlife Research* 39:311-320.

Naimi, B., N. A. S. Hamm, T. A. Groen, A. K. Skidmore, and A. G. Toxopeus. 2014. Where is positional uncertainty a problem for species distribution modelling? *Ecography* 37:191-203.

Nakagawa, S., and H. Schielzeth. 2013. A general and simple method for obtaining R^2 from generalized linear mixed-effects models. *Methods in Ecology and Evolution* 4:133-142.

Nichols, J. D., J. E. Hines, J. R. Sauer, F. W. Fallon, J. E. Fallon, and P. J. Heglund. 2000. A double-observer approach for estimating detection probability and abundance from point counts. *The Auk* 117:393-408.

Nimon, K. F., and F. L. Oswald. 2013. Understanding the results of multiple linear regression: beyond standardized regression coefficients. *Organizational Research Methods* 16:650-674.

Pacifici, K., T. R. Simons, and K. H. Pollock. 2008. Effects of vegetation and background noise on the detection process in auditory avian point-count surveys. *The Auk* 125:600–607.

Padgham, M. 2004. Reverberation and frequency attenuation in forests: implications for communication in animals. *The Journal of the Acoustical Society of America* 115:402-410.

Parkins, K. L., and J. A. Clark. 2015. Green roofs provide habitat for urban bats. *Global Ecology and Conservation* 4:349-357.

Parris, K. M, and A. Schneider. 2008. Impacts of traffic noise and traffic volume on birds of roadside habitats. *Ecology and Society* 14:29.

Partners in Flight (PIF) Science Committee. 2013. Population Estimates Database, version 2013. URL: http://rmbo.org/pifpopestimates. Accessed August 19 2016.

Patricelli, G. L., M. S. Dantzker, and J. W. Bradburry. 2007. Differences in acoustic directionality among vocalizations of the male red-winged blackbird (*Agelaius pheoniceus*) are related to function in communication. *Behavioural Ecology and Sociobiology* 61:1099-1110.

Pearson, J. D., C. H. Morrell, S. Gordon-Salant, L. J. Brant, E. J. Metter, L. L. Klein, and J. L. Fozard. 1995. Gender differences in a longitudinal study of age-associated hearing loss. *The Journal of the Acoustical Society of America* 97:1196-1205.

Peek, F. W. 1972. An experimental study of the territorial function of vocal and visual display in the male red-winged blackbird. *Animal Behaviour* 20:112-118.

Petit, D. R., L. J. Petit, V. A. Saab, and T. E. Martin. 1995. Fixed-radius point counts in forests: factors influencing effectiveness and efficiency. Pages 49-56 *in* Ralph, C.J., J.R. Sauer, and S. Droege, editors. Monitoring bird populations by point counts. General Technical Report PSW-GTR-149. US Department of Agriculture, Forest Service, Pacific Southwest Research Station, Albany, NY.

Piercy, J. E., T. F. W. Embleton, and L. C. Sutherland. 1977. Review of noise propagation in the atmosphere. *The Journal of the Acoustical Society of America* 61:1403-1418.

Podos, J. 1996. Motor constraints on vocal development in a songbird. *Animal Behaviour* 51:1061-1070.

Porneluzi, P., M. A. Van Horn, and T. M. Donovan. 2011. Ovenbird (*Seiurus aurocapilla*). P. G. Rodewald, editor. The Birds of North America. Cornell Lab of Ornithology, Ithaca, New York, USA. URL: https://birdsna-org /Species-Account/bna/species/ovenbi1

R Core Team. 2015. R: A Language and Environment for Statistical Computing. R Foundation for Statistical Computing, Vienna. URL: http://www.R-project.org

R Core Team. 2017. R: A language and environment for statistical computing. R Foundation for Statistical Computing, Vienna, Austria.

Ralph, C. J., J. R. Sauer, and S. Droege. 1995. Monitoring bird populations by point counts. General Technical Report PSW-GTR-149. US Department of Agriculture, Forest Service, Pacific Southwest Research Station, Albany, NY.

Ransom, Jr., D., and W. E. Pinchak. 2003. Assessing accuracy of a laser rangefinder in estimating grassland bird density. *Wildlife Society Bulletin* 31:460-463.

Reid, M. L. 1987. Costliness and reliability in the singing vigour of Ipswich sparrows. *Animal Behaviour* 35:1735-1743.

Rempel, R. S., K. A. Hobson, G. Holborn, S. L. Van Wilgenburg, and J. Elliott. 2005. Bioacoustic monitoring of forest songbirds: interpreter variability and effects of configuration and digital processing methods in the laboratory. *Journal of Field Ornithology* 76:1-11.

Richards, D. G., and R. H. Wiley. 1980. Reverberation and amplitude fluctuations in the propagation of sound in a forest: implications for animal communication. *The American Naturalist* 115:381-399.

Richards, D. G. 1981. Environmental acoustics and censuses of singing birds. In Estimating numbers of terrestrial birds. Studies in Avian Biology 6 (C. J. Ralph and J. M. Scott, Editors). Cooper Ornithological Society, Camarillo, California, USA. Pp. 287-300.

Rigby, E. A. 2016. Simulating effects of imperfect detectability in bird surveys (Doctoral dissertation). Retrieved from the University of Minnesota Digital Conservancy, http://hdl.handle.net/11299/193439

Robin, X., N. Turck, A. Hainard, N. Tiberti, F. Lisacek, J. Sanchez, and M. Muller. 2011. pROC: an open-source package for R and S+ to analyze and compare ROC curves. *BMC Bioinformatics* 12: 77.

Rohatgi, A. 2017. WebPlotDigitizer, Version 4.0. Austin, Texas. USA. URL: https://automeris.io/WebPlotDigitizer

Rosenberg, K. V., and P. J. Blancher. 2005. Setting numerical population objectives for priority landbird species. USDA Forest Service General Technical Report PSW-GTR-191.

Rosenstock, S. S., D. R. Anderson, K. M. Giesen, T. Leukering, and M. F. Carter. 2002. Landbird counting techniques: current practices and an alternative. *The Auk* 119:46-53.

van Rossum, G. 1995. Python tutorial. Technical Report CS-R9526. Centrum voor Wiskunde en Informatica (CWI), Amsterdam, Netherlands.

Royle, J. A., and J. D. Nichols. 2003. Estimating abundance from repeated presence–absence data or point counts. *Ecology* 84:777-790.

Royle, J. A. 2018. Modelling sound attenuation in heterogeneous environments for improved bioacoustics sampling of wildlife populations. *Methods in Ecology and Evolution* 9:1939-1947.

Sandberg, U. 1987. Road traffic noise—the influence of the road surface and its characterization. *Applied Acoustics* 21:97-118.

Sandoval, L., T. Dabelsteen, and D. J. Mennill. 2015. Transmission characteristics of solo songs and duets in a neotropical thicket habitat specialist bird. *Bioacoustics* 24:289-306.

Sauer, J. R., B. G. Peterjohn, and W. A. Link. 1994. Observer differences in the North American breeding bird survey. *The Auk* 111:50-62.

Schieck, J. 1997. Biased detection of bird vocalizations affects comparisons of bird abundance among forested habitats. *Condor* 99:179–190.

Scott, J. M., F. L. Ramsey and C. B. Kepler. 1981. Distance estimation as a variable in estimating bird numbers from vocalizations. *Studies in Avian Biology* 6:334-340.

Sebastián-González, E., R. J. Camp, A. M. Tanimoto, P. M. De Oliveira, B. B. Lima, T. A. Marques, and P. J. Hart. 2018. Density estimation of sound-producing terrestrial animals using single automatic acoustic recorders and distance sampling. *Avian Conservation and Ecology* 13:7.

Shonfield, J., and E. M. Bayne. 2017. Autonomous recording units in avian ecological research: current use and future applications. *Avian Conservation and Ecology* 12:14.

Shonfield, J., S. Heemskerk, and E. M. Bayne. 2018. Utility of automated species recognition for acoustic monitoring of owls. *Journal of Raptor Research* 52:42-56.

Sillett, T. S., R. B. Chandler, J. A. Royle, M. Kéry, and S. A. Morrison. 2012. Hierarchical distance-sampling models to estimate population size and habitat-specific abundance of an island endemic. *Ecological Applications* 22:1997-2006.

Simons, T. R., M. W. Alldredge, K. H. Pollock, and J. M. Wettroth. 2007. Experimental analysis of the auditory detection process on avian point counts. *The Auk* 124:986-999.

Solymos, P., S. M. Matsuoka, E. M. Bayne, S. R. Lele, P. Fontaine, S. G. Cumming, D. Stralberg, F. K. A. Schmiegelow, and S. J. Song. 2013. Calibrating indices of avian density from non-standardized survey data: making the most of a messy situation. *Methods in Ecology and Evolution* 4:1047-1058.

Solymos, P., S. M. Matsuoka, D. Stralberg, N. K. S. Barker, and E. M. Bayne. 2018. Phylogeny and species traits predict detectability. *Ecography* 41:1595-1603.

Stimpert, A. K., S. L. DeRuiter, E. A. Falcone, J. Joseph, A. B. Douglas, D. J. Moretti, A. S. Friedlaender, J. Calambokidis, G. Gailey, P. L. Tyack, and J. A. Goldbogen. 2015. Sound production and associated behavior of tagged fin whales (*Balaenoptera physalus*) in the Southern California Bight. *Animal Biotelemetry* 3:23.

Sueur J., T. Aubin, and C. Simonis. 2008. Seewave: a free modular tool for sound analysis and synthesis. *Bioacoustics* 18:213-226.

Tarrero, A. I., M. A. Martin, J. Gonzalez, M. Machimabarrena, and F. Jacobsen. 2008. Sound propagation in forests: A comparison of experimental results and values predicted by the Nord 2000 model. *Applied Acoustics* 69:662-671.

Tegeler, A. K., M. L. Morrison, and J. M. Szewczak. 2012. Using extended-duration audio recordings to survey avian species. *Wildlife Society Bulletin* 36:21-29.

Thogmartin, W. E., F. P. Howe, F. C. James, D. H. Johnson, E. T. Reed, J. R. Sauer, and F. R. Thompson. 2006. A review of the population estimation approach of the North American landbird conservation plan. *The Auk* 123:892-904.

Thomas, L., S. T. Buckland, E. A. Rexstad, J. L. Laake, S. Strindberg, S. L. Hedley, J. R. B. Bishop, T. A. Marques, and K. P. Burnham. 2010. Distance software: design and analysis of distance sampling surveys for estimating population size. *Journal of Applied Ecology* 47:5-14.

Thomson, J. A., A. B. Cooper, D. A. Burkholder, M. R. Heithaus, and L. M. Dill. 2012. Heterogeneous patterns of availability for detection during visual surveys: spatiotemporal variation in sea turtle dive-surfacing behaviour on a feeding ground. *Methods in Ecology and Evolution* 3:378–387.

Trombulak, S.C., and C.A. Frissell. 2000. Review of ecological effects of roads on terrestrial and aquatic communities. *Conservation Biology* 14:18-30.

Turgeon, P. J., S. L. Van Wilgenburg, and K. L. Drake. 2017. Microphone variability and degradation: implications for monitoring programs employing autonomous recording units. *Avian Conservation and Ecology* 12:9.

U.S. Geological Survey. 2009. North American Breeding Bird Survey Bibliography. URL: https://www.pwrc.usgs.gov/bbs/about/bbsbib.pdf

Vanagas, G. 2004. Receiver operating characteristic curves and comparison of cardiac surgery risk stratification systems. *Interactive Cardiovascular and Thoracic Surgery* 3:319-322.

Ward, S., H. M. Lampe, and P. J. B. Slater. 2004. Singing is not energetically demanding for pied flycatchers *Ficedula hypoleuca*. *Behavioural Ecology* 15:477-484.

Wiener, F. M., and D. N. Keast. 1959. Experimental study of the propagation of sound over ground. *The Journal of the Acoustical Society of America* 31:724-733.

Wiley, R. H. 1991. Associations of song properties with habitats for territorial oscine birds of eastern North America. *American Naturalist* 138:973-993.

Wiley, R. H., and D. G. Richards. 1982. Adaptations for acoustic communication in birds: Sound transmission and signal detection. Acoustic Communication in Birds (D.E. Kroodsma, E.H. Miller, and H. Ouellet, Editors), pp. 131-181. Academic Press Inc. Waltham, MA, USA.

Wilson, S. J., and E. M. Bayne. 2018. Use of an acoustic location system to understand how presence of conspecifics and canopy cover influence Ovenbird (*Seiurus aurocapilla*) space use near reclaimed wellsites in the boreal forest of Alberta. *Avian Conservation and Ecology* 13:4.

Yang, H. S., J. Kang, and C. Cheal. 2013. Random-incidence absorption and scattering coefficients of vegetation. *Acta Acustica United With Acustica* 99:379-388.

Yip, D. A., E. M. Bayne, P. Sólymos, J. Campbell, and D. Proppe. 2017*a*. Sound attenuation in forested and roadside environments: Implications for avian point count surveys. *The Condor* 119:73-84.

Yip, D. A., L. Leston, E. M. Bayne, P. Sólymos, and A. Grover. 2017*b*. Experimentally derived detection distances from audio recordings and human observers enable integrated analysis of point count data. *Avian Conservation and Ecology* 12:11.

Appendix 1

Table 1.1 – Model selection for differences in weather between road and interior forest. Wind, temperature, and humidity all used the same models for selection. We selected top models using lowest AICc value and ΔAICc. For multiple models with ΔAICc < 2, we selected the simplest model with fewest parameters (Arnold et al. 2010). Marginal (R^2_m) and conditional (R^2_c) are listed.

Model	Parameters
global with interaction	Transect*Time + random effect: Site
global	Transect + Time + Date + random effect: Site
time, date	Time + Date + random effect: Site
transect, date	Transect + Date + random effect: Site
transect, time	Transect + Time + random effect: Site
date	Date + random effect: Site
time	Time + random effect: Site
transect	Transect + random effect: Site
null	Random effect: Site only

	Model	df	logLik	AICc	ΔAICc	AICw	R^2_m	R^2_c
Wind	transect	4	-882.220	1772.5	0	0.767	0.0986	0.4624
	null	3	-884.582	1775.5	2.70	0.199		
Humidity	transect, time	5	-2036.328	4082.8	0	0.592	0.1686	0.6978
	null	3	-2094.006	4194.1	111.29	0		
Temperature	time	4	-1350.695	2709.5	1.52	0.271	0.1551	0.7825
	null	3	-1412.013	2830.1	122.13	0		

Table 1.2 – Model selection for factors influencing relative SPL of pure tones. We selected top models using lowest AICc value and ΔAICc. For multiple models with ΔAICc < 2, we selected the simplest model with fewest parameters (Arnold et al. 2010). For each individual tone, we

subset for each frequency and removed the frequency variable from models. Marginal (R^2_m) and conditional (R^2_c) are listed.

Model	Parameters
global.interaction	Distance*transect + frequency + transect*wind + humidity
wind.interaction	Distance*transect + frequency + transect*wind
noweather.interaction	Distance*transect + frequency
global	Distance + transect + frequency + wind + humidity
wind	Distance + transect + frequency + wind
noweather	Distance + transect + frequency
frequency	Distance + frequency
null	Distance

Tone	Model	df	logLik	AICc	ΔAICc	AICw	R^2_m	R^2_c
Pooled	noweather.interaction	20	-13039.38	26119.0	0	0.951	0.7192	0.7739
	null	4	-13292.08	26592.2	473.18	0		
1000	noweather.interaction	14	-2147.507	4322.8	0	0.862	0.7291	0.8064
	null	4	-2185.518	4379.1	56.32	0		
1414	noweather.interaction	14	-2228.726	4486.1	0	0.772	0.7191	0.7953
	null	4	-2266.819	4541.7	55.60	0		
2000	noweather.interaction	14	-2277.080	4582.8	0	0.673	0.7293	0.7834
	null	4	-2316.579	4641.2	58.41	0		
2828	noweather.interaction	14	-2011.228	4051.2	0.55	0.413	0.7262	0.8131
	null	4	-2051.229	4110.5	59.89	0		
4000	noweather.interaction	14	-1857.681	3744.2	0.92	0.367	0.7173	0.8141
	null	4	-1894.656	3797.4	54.14	0		
5656	noweather.interaction	14	-1500.182	3029.4	1.54	0.295	0.7185	0.7769
	null	4	-1533.001	3074.1	46.25	0		
8000	wind.interaction	20	-780.026	1604.0	0	0.882	0.7881	0.8379
	null	1	-814.901	1638.0	33.96	0		

Table 1.3 – Model selection for factors influencing excess attenuation of pure tones. We selected top models using lowest AICc value and ΔAICc. For multiple models with ΔAICc < 2, we selected the simplest model with fewest parameters (Arnold et al. 2010). For each individual

tone, we subset for each frequency and removed the frequency variable from models. Marginal (R^2_m) and conditional (R^2_c) are listed.

Model	Parameters
global.interaction	Distance*transect + frequency + transect*wind + humidity
wind.interaction	Distance*transect + frequency + transect*wind
noweather.interaction	Distance*transect + frequency
global	Distance + transect + frequency + wind + humidity
wind	Distance + transect + frequency + wind
noweather	Distance + transect + frequency
frequency	Distance + frequency
null	Distance

Tone	Model	df	logLik	AICc	ΔAICc	AICw	R^2_m	R^2_c
Pooled	noweather.interaction	20	-13162.03	26364.3	0	0.935	0.4190	0.5275
	null	4	-13279.36	26566.7	202.44	0		
1000	noweather.interaction	14	-2147.507	4322.8	0	0.862	0.3893	0.5637
	null	4	-2192.194	4392.5	69.68	0		
1414	noweather.interaction	14	-2228.726	4486.1	0	0.772	0.3960	0.5600
	null	4	-2275.504	4559.1	72.97	0		
2000	noweather.interaction	14	-2277.080	4582.8	0	0.673	0.4986	0.5987
	null	4	-2323.311	4654.7	71.87	0		
2828	noweather.interaction	14	-2011.228	4051.2	0.55	0.413	0.4178	0.6027
	null	4	-2055.961	4120.0	69.36	0		
4000	noweather.interaction	14	-1857.681	3744.2	0.92	0.367	0.5507	0.7046
	null	4	-1903.949	3816.0	72.73	0		
5656	noweather.interaction	14	-1500.182	3029.4	1.54	0.295	0.4883	0.5944
	null	4	-1540.917	3089.9	62.09	0		
8000	wind.interaction	20	-780.026	1604.0	0	0.882	0.5720	0.6727
	null	1	-825.689	1659.6	55.54	0		

Table 1.4 – Model selection for detection by species. We selected top models using lowest AICc value and ΔAICc. For multiple models with ΔAICc < 2, we selected the simplest model with fewest parameters (Arnold et al. 2010). AUC statistics for top performing models are listed.

Model	Parameters
global	Distance + Transect:Distance + Wind:Distance + Humidity:Distance
global.observer	Distance + Transect:Distance + Wind:Distance + Humidity:Distance + Observer:Distance
wind	Distance + Transect:Distance + Wind:Distance
wind.observer	Distance + Transect:Distance + Wind:Distance + Observer:Distance
noweather	Distance + Transect:Distance
noweather.observer	Distance + Transect:Distance + Observer:Distance
null	Distance

Species	Model	df	logLik	AICc	ΔAICc	AICw	AUC
LEOW	global	8	-428.989	874.1	0	0.774	0.8845
	null	1	-479.997	962	87.85	0	
OSFL	noweather	6	-379.154	770.4	0.59	0.347	0.9482
	null	1	-408.348	818.7	48.89	0	
BHCO	global	8	-325.856	667.9	0	0.649	0.9506
	null	1	-356.978	716	48.08	0	
CORA	global	8	-395.542	807.3	0	0.631	0.9595
	null	1	-435.913	873.8	66.58	0	
GGOW	global	8	-445.007	906.2	0	0.965	0.8623
	null	1	-478.016	958	51.85	0	
BEKI	noweather	6	-256.283	524.7	0	0.546	0.9829
	null	1	-281.774	565.6	40.89	0	
TEWA	noweather	6	-249.288	510.7	1	0.223	0.9755
	null	1	-273.573	549.2	39.47	0	
PISI	noweather	6	-297.023	606.1	0	0.575	0.9762
	null	1	-336.868	675.7	69.59	0	
RBGR	noweather	6	-391.925	796	1.74	0.242	0.9633
	null	1	-432.064	866.1	71.92	0	
OVEN	global	8	-315.063	646.3	0	0.779	0.9757
	null	1	-359.52	721	74.75	0	
WAVI	noweather	6	-319.048	650.2	0	0.499	0.9795
	null	1	-350.715	703.4	53.24	0	
RBNU	global	8	-400.352	816.9	0	0.822	0.928
	null	1	-450.332	902.7	85.79	0	
CMWA	noweather	6	-232.894	477.9	0.25	0.258	0.9814
	null	1	-252.938	507.9	30.25	0	
DEJU	noweather	6	-311.332	634.8	0	0.485	0.9662
	null	1	-352.8	707.6	72.84	0	

BOOW	global	8	-441.127	898.4	0	0.752	0.9055
	null	1	-477.066	956.1	57.71	0	
BAWW	global	8	-238.445	493.1	0	0.757	0.9707
	null	1	-266.607	535.2	42.16	0	
CCSP	global	8	-293.157	602.5	0	0.838	0.9802
	null	1	-332.407	666.8	64.33	0	
NSWO	global	8	-425.371	866.9	0	0.728	0.8958
	null	1	-455.92	913.8	46.93	0	
BBWA	noweather	6	-213.717	439.5	0.05	0.395	0.9731
	null	1	-223.787	449.6	10.1	0.003	
WTSP	noweather	6	-394.838	801.8	1.58	0.263	0.9672
	null	1	-430.662	863.3	63.14	0	
BADO	global	8	-448.993	914.2	0	0.901	0.8337
	null	1	-480.858	963.7	49.56	0	
LISP	noweather	6	-329.579	671.3	1.82	0.141	0.9731
	null	1	-359.433	720.9	51.44	0	
4000Hz	noweather	6	-410.985	834.1	0	0.619	0.9522
	null	1	-434.755	871.5	37.44	0	
1414Hz	noweather	6	-450.015	912.1	0	0.863	0.8281
	null	1	-472.454	946.9	34.78	0	
1000Hz	noweather	6	-445.292	902.7	0	0.697	0.8854
	null	1	-473.595	949.2	46.51	0	
8000Hz	noweather.observer	11	-261.061	544.4	0	0.488	0.9576
	null	1	-282.809	567.6	23.19	0	
5656Hz	noweather	6	-350.718	713.5	0	0.596	0.9695
	null	1	-368.349	738.7	25.17	0	
2828Hz	global	8	-433.323	882.8	0	0.594	0.9444
	null	1	-457.328	916.7	33.84	0	
2000Hz	global	8	-443.186	902.5	0	0.988	0.7993
	null	1	-470.43	942.9	40.32	0	
WETO	global	7	-253.574	521.4	0	0.97	0.9167
	null	1	-296.63	595.3	73.91	0	
CATO	global	7	-258.735	531.7	0	0.849	0.9282
	null	1	-282.85	567.7	36.03	0	
YERA	noweather	5	-144.213	298.5	0	0.456	0.9717
	null	1	-153.026	308.1	9.52	0.004	

Table 2.1 – Model coefficients from the top selected model for each weather factor. Interior forest is the reference level for transect (factor levels: road, forest).

Factor	(intercept)	Transect	Time
Wind	0.8433	0.8931	
Humidity	82.098455	-1.646832	-0.049581
Temperature	17.293320		0.016094

Table 2.2 – Model coefficients from the top selected model predicting relative SPL for each tone. Transects are coded as EC – Edge Coniferous, ED – Edge Deciduous, FC – Forest Coniferous, FD – Forest Deciduous, and RC – Road Coniferous. Road Deciduous is the reference level for transect type. 1000Hz is the reference level for frequency.

Tone	Intercept	log(Distance)	EC	ED	FD	FC	RC
Pooled	138.5762	-13.0722	-6.1373	-7.9116	0.8934	4.3047	-4.9869

Tone	Dist:EC	Dist:ED	Dist:FC	Dist:FD	Dist:RC	1414Hz	2000Hz	2828Hz	4000Hz	5656Hz	8000Hz
Pooled	0.9381	0.5685	-2.6383	-2.1796	0.5302	-1.8855	-1.9234	-2.5307	-1.6052	-5.1473	-10.7848

Tone	Intercept	log(Distance)	EC	ED	FD	FC	RC
1000Hz	126.8015	-11.259	-1.2923	-7.0242	4.7928	15.7249	1.3262
1414Hz	119.897	-10.5146	6.9808	7.0598	17.6089	19.3498	5.309
2000Hz	138.64	-13.1234	-15.4127	-8.3396	-3.7987	-9.2298	-12.7929
2828Hz	136.9885	-13.1312	-10.1561	-9.436	4.5636	7.6209	-6.355
4000Hz	145.0618	-14.3424	-0.8352	-13.2805	-2.938	2.7846	-7.7243
5656Hz	152.393	-16.3598	-15.0276	-19.7347	-11.5844	-2.8565	-12.853
8000Hz	139.6096	-15.8022	13.2916	-6.3893	3.555	1.235	7.6346

Tone	Dist:EC	Dist:ED	Dist:FC	Dist:FD	Dist:RC	Wind	Wind:EC	Wind:ED	Wind:FC	Wind:FD	Wind:RC
1000Hz	0.3212	0.6708	-2.7762	-3.6499	-0.3151						
1414Hz	-0.7249	-1.737	-4.6825	-4.2258	-1.0584						
2000Hz	2.4383	0.2757	-2.1237	-0.4143	1.6709						
2828Hz	1.561	0.5081	-3.4959	-2.8109	0.6647						
4000Hz	-0.3323	1.3556	-2.9065	-2.5111	1.0617						
5656Hz	1.8703	2.7251	-1.0718	-1.5649	1.5521						
8000Hz	-3.1848	0.5518	-3.0787	-0.874	-1.5229	-0.34	-0.2941	0.2481	-0.4179	-1.2779	-1.6701

Table 2.3 – Model coefficients from the top selected model predicting excess attenuation for each tone. Transects are coded as EC – Edge Coniferous, ED – Edge Deciduous, FC – Forest Coniferous, FD – Forest Deciduous, and RC – Road Coniferous. Road Deciduous is the reference level for transect type. 1000Hz is the reference level for frequency.

Tone	Intercept	log(Distance)	EC	ED	FD	FC	RC
Pooled	-14.1677	4.1551	1.0258	-2.9286	-6.0306	-7.5223	1.0499

Tone	Dist:EC	Dist:ED	Dist:FC	Dist:FD	Dist:RC	1414Hz	2000Hz	2828Hz	4000Hz	5656Hz	8000Hz
Pooled	-0.6756	0.2036	3.0125	2.0958	-0.0937	-1.2580	-1.1472	1.6019	1.2816	2.5302	5.1141

Tone	Intercept	log(Distance)	EC	ED	FD	FC	RC
1000Hz	-3.9136	2.6116	-0.9206	0.3678	-19.3041	-7.8727	-2.1503
1414Hz	-3.6124	1.8433	-5.4448	-7.0191	-18.8716	-15.5865	-3.8103
2000Hz	-15.0534	4.4270	6.7456	2.0121	0.7753	-6.8923	5.1254
2828Hz	-16.7120	4.4380	7.3782	2.4371	-6.3596	-7.5808	3.0758
4000Hz	-21.3914	5.6733	-0.6565	-0.3044	-3.5388	-2.8835	3.8406
5656Hz	-28.0633	7.6801	-0.2978	7.7395	-1.1527	1.4407	0.6643
8000Hz	-24.99968	7.27556	-8.45742	0.76245	5.43475	-4.97803	-2.49632

Tone	Dist:EC	Dist:ED	Dist:FC	Dist:FD	Dist:RC	Wind	Wind:EC	Wind:ED	Wind:FC	Wind:FD	Wind:RC
1000Hz	-0.2570	-0.7074	2.7204	3.6683	0.2088						
1414Hz	0.1208	1.7255	4.7354	4.2728	0.9992						
2000Hz	-2.1235	-0.2776	2.1278	0.4785	-1.6867						
2828Hz	-1.2060	-0.4646	3.5372	2.8391	0.4770						
4000Hz	-0.3560	-1.3359	2.8623	2.4668	-0.2509						
5656Hz	-0.5366	-2.6529	0.8933	1.5897	-0.5800						
8000Hz	2.49072	-0.14919	2.81782	0.26290	0.51193	0.61736	-1.84030	-1.29307	-0.02129	-1.31768	0.74896

Table 2.4 – Model coefficients from the top selected model for each species. "x" is –distance^2. Transects are coded as EC – Edge Coniferous, ED – Edge Deciduous, FC – Forest Coniferous, FD – Forest Deciduous, and RC – Road Coniferous. Road Deciduous is the reference level for transect type. Intercept is fixed at 0 for all models. Main effects for all parameters except distance excluded from models to allow fixed intercept. MinFreq is minimum frequency of a species or tone (Hz).

Species	MinFreq	x	x:EC	x:ED	x:FC	x:FD	x:RC	x:Wind	x:Humidity
BEKI	4484	8.00E-06	-1.09E-06	9.84E-06	2.34E-05	1.99E-05	-6.16E-07		
PISI	3561	5.20E-06	-1.28E-06	2.97E-06	2.50E-05	1.28E-05	-2.03E-06		
BOOW	603	2.91E-06	2.96E-07	9.24E-07	2.06E-06	1.23E-06	-1.60E-07	-2.57E-07	-3.52E-08
NSWO	909	3.20E-06	-3.37E-07	5.47E-07	2.39E-06	9.07E-07	-6.95E-07	-4.13E-07	-2.23E-08
BBWA	7007	1.88E-05	-5.91E-06	2.16E-06	1.40E-05	2.63E-05	-1.72E-06		
TEWA	4134	9.81E-06	-1.51E-06	4.70E-06	3.10E-05	2.10E-05	-2.14E-06		
LEOW	1137	4.76E-06	4.34E-07	1.50E-07	2.02E-06	6.05E-07	6.42E-07	-3.20E-07	-6.56E-08
CMWA	6758	1.04E-05	-6.79E-07	7.42E-06	3.23E-05	2.12E-05	-3.71E-07		
BADO	420	3.38E-06	4.80E-07	3.97E-07	1.21E-06	7.33E-08	2.69E-07	-3.64E-07	-4.07E-08
WETO	1167	6.55E-06	6.33E-07	1.53E-06	2.02E-05	NA	3.48E-07	-3.54E-07	-8.04E-08
CORA	1021	5.22E-06	5.58E-07	1.24E-06	5.85E-06	2.89E-06	2.22E-07	-1.65E-07	-6.27E-08
RBNU	1027	4.70E-06	6.11E-07	1.43E-06	4.75E-06	3.04E-06	-3.03E-08	-1.18E-07	-6.24E-08
LISP	2333	3.59E-06	-4.91E-07	2.77E-06	1.35E-05	7.60E-06	-8.72E-07		
CCSP	4297	9.54E-06	3.92E-07	3.98E-06	2.00E-05	1.49E-05	1.02E-07	3.13E-07	-9.66E-08
GGOW	572	3.52E-06	2.41E-07	2.45E-07	1.73E-06	3.33E-07	3.10E-07	-2.12E-07	-4.59E-08
YERA	1327	1.24E-05	2.33E-06	1.52E-05	4.86E-05	NA	1.11E-06		
WTSP	3059	1.47E-06	-3.16E-07	9.95E-07	5.93E-06	2.99E-06	-9.18E-07		
BAWW	6353	1.30E-05	2.44E-06	6.84E-06	2.79E-05	2.81E-05	3.62E-06	1.85E-06	-1.42E-07
OSFL	1729	1.91E-06	1.70E-07	1.91E-06	7.05E-06	3.75E-06	-7.40E-07		
RBGR	1308	1.34E-06	-2.99E-07	1.68E-06	6.03E-06	4.63E-06	-5.85E-07		
WAVI	3537	3.51E-06	7.64E-07	2.60E-06	1.74E-05	1.01E-05	-4.27E-07		
CATO	1265	4.76E-06	1.48E-07	2.59E-07	1.09E-05	NA	2.16E-07	-1.10E-07	-5.44E-08
OVEN	3955	7.50E-06	2.22E-07	1.14E-06	2.27E-05	1.25E-05	-5.69E-07	3.61E-07	-7.20E-08
DEJU	2860	4.33E-06	-1.21E-06	3.89E-06	2.22E-05	9.99E-06	-1.58E-06		
BHCO	4821	7.80E-06	-1.66E-07	2.35E-06	1.32E-05	9.18E-06	-2.57E-07	1.96E-07	-7.16E-08

2000Hz	2000	2.27E-06	-6.91E-08	1.86E-07	1.66E-06	3.03E-07	-7.67E-08	-4.88E-08	-3.21E-08
4000Hz	4000	1.63E-06	-6.49E-07	6.42E-07	2.67E-06	2.49E-06	-9.66E-07		
2828Hz	2828	2.45E-06	-2.50E-07	7.46E-07	2.46E-06	1.03E-06	2.80E-07	-1.55E-07	-2.51E-08
5656Hz	5656	3.58E-06	-9.05E-07	7.94E-07	4.76E-06	6.38E-06	-8.30E-07		
8000Hz	8000	1.71E-05	-4.69E-06	-2.67E-06	-7.14E-06	6.55E-06	-7.26E-06		
1000Hz	1000	2.13E-07	-7.22E-09	3.47E-07	2.63E-06	1.20E-06	-3.49E-07		
1414Hz	1414	3.88E-07	-3.13E-07	2.00E-07	2.17E-06	3.70E-07	-5.16E-07		

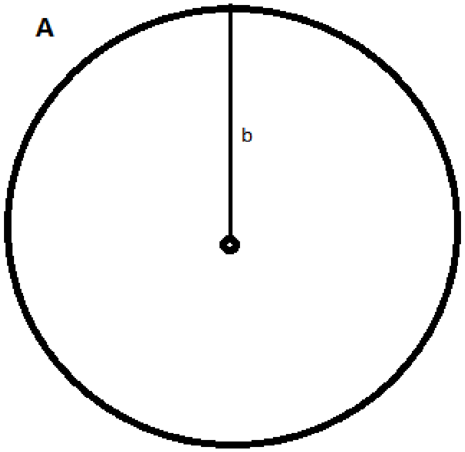
A
b

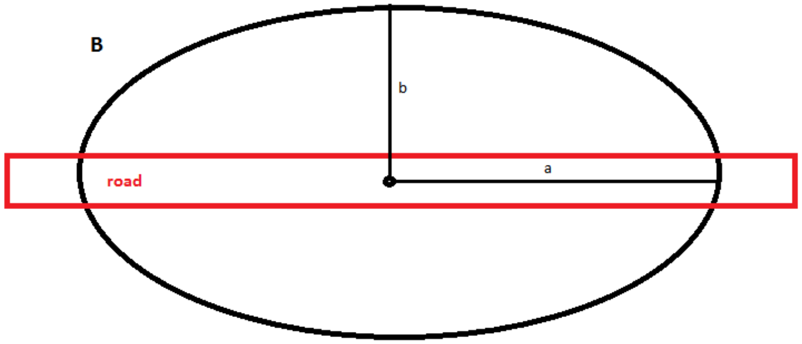
B
b
a
road

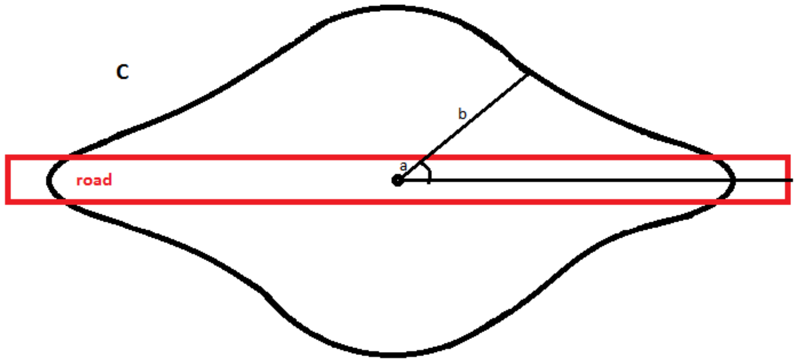

Figure 3.1 – Shapes used to estimate area surveyed for interior forests and roads/edges under two scenarios where “a” is the detection distance along roads/edges and “b” is the detection distance through the interior forest. Survey area is estimated assuming a circular detection area using the formula for area of a circle – $A_{Forest} = \pi \tau_{Forest}^2$ (**A**). The first scenario for estimating area on roads/edges assumes an elliptical detection area using the formula for area of an ellipse - $A_{Road/ForestEdge} = \pi \tau_{Forest} \tau_{Road/ForestEdge}$ (**B**). The second scenario solves for an integral that estimates area based on the proportion of sound travelling through the road corridor and interior forest at a given angle, assuming a road width of 15m (**C**) using the following:

```
#w=road width in metres
#x=forest detection distance
#y=road detection distance
#z=edge detection distance
w=15
####Calculate Road Detection Area####
  theta.not=asin(w/(2*y))
  I1=(pi-(2*theta.not))*(x^2)
  I2=w*(1-(x/y))*log((tan((pi-theta.not)/2))/(tan(theta.not/2)))
  I3=((w^2)/4)*((1-(x/y))^2)*((1/tan(theta.not))-(1/tan(pi-theta.not)))
```

```
I4=2*(theta.not)*(y^2)
A1=I1+I2+I3+I4

####Calculate Forest Detection Area####
A2=pi*x^2

####Calculate Edge Detection Area####
theta.not=asin(w/(2*y))
I1=(pi-(2*theta.not))*(x^2)
I2=w*(1-(x/z))*log((tan((pi-theta.not)/2))/(tan(theta.not/2)))
I3=((w^2)/4)*((1-(x/z))^2)*((1/tan(theta.not))-(1/tan(pi-theta.not)))
I4=2*(theta.not)*(z^2)
A3=I1+I2+I3+I4

####Calculate Correction Ratios####
C1=A1/A2
C2=A1/A3
C3=A3/A2
```

Table 3.2 – Effective detection radius (metres), area surveyed (metres^2), and correction factors for road-forest, road-edge, and edge-forest comparisons, listed in descending order of road:forest correction factor.

Scenario 1: Correction factors assuming survey area along a road or edge is elliptical

Species	Effective Detection Radius (EDR)			Area Surveyed			Correction Factor		
	ROAD	EDGE	FOREST	A:ROAD	A:EDGE	A:FOREST	Aroad:Aedge	Aroad:Aforest	Aedge:Aforest
PISI	498.73	422.81	212.09	332305.20	281719.24	141316.25	1.1796	2.3515	1.9935
WAVI	550.98	440.73	247.22	427919.25	342291.70	192002.02	1.2502	2.2287	1.7828
YERA	279.98	219.89	128.12	112695.96	88508.33	51572.23	1.2733	2.1852	1.7162
WETO	401.06	374.69	195.06	245766.94	229611.88	119532.78	1.0704	2.0561	1.9209
CMWA	328.74	290.74	166.16	171607.71	151768.63	86739.58	1.1307	1.9784	1.7497
BEKI	360.81	307.13	184.21	208802.16	177738.08	106601.20	1.1748	1.9587	1.6673
4000Hz	941.94	804.91	487.48	1442539.55	1232689.31	746551.38	1.1702	1.9323	1.6512
DEJU	396.30	360.65	215.36	268121.17	244003.06	145701.41	1.0988	1.8402	1.6747
CATO	461.52	456.14	254.05	368347.33	364053.91	202760.10	1.0118	1.8167	1.7955
8000Hz	257.68	242.79	193.82	208597.35	185193.35	118013.66	1.1264	1.7676	1.5693
OVEN	358.38	338.72	203.53	229154.10	216588.19	130144.37	1.0580	1.7608	1.6642
5656Hz	563.87	538.73	331.99	588097.28	561876.54	346255.38	1.0467	1.6984	1.6227
RBGR	561.70	507.50	339.57	599211.10	541396.31	362244.61	1.1068	1.6542	1.4946
CCSP	315.60	293.87	192.45	190810.73	177674.54	116354.55	1.0739	1.6399	1.5270
TEWA	248.23	232.53	152.77	119137.67	111602.26	73322.33	1.0675	1.6248	1.5221
BAWW	243.56	231.16	152.80	116918.51	110965.93	73351.02	1.0536	1.5940	1.5128
LISP	374.98	345.88	239.49	282132.30	260234.59	180190.44	1.0841	1.5657	1.4442
BHCO	350.30	332.75	228.59	251563.24	238963.93	164162.63	1.0527	1.5324	1.4557
WTSP	551.39	499.44	361.99	627059.67	567976.36	411670.31	1.1040	1.5232	1.3797
OSFL	498.45	434.47	329.78	516418.85	450135.04	341670.42	1.1473	1.5115	1.3175
BBWA	236.37	247.17	162.64	120771.79	126293.56	83100.53	0.9563	1.4533	1.5198
1000Hz	696.63	640.06	504.79	1104740.53	1015029.60	800506.97	1.0884	1.3801	1.2680

1414Hz	696.63	640.06	504.79	1104740.53	1015029.60	800506.97	1.0884	1.3801	1.2680
RBNU	466.44	423.13	347.41	509086.46	461822.04	379179.35	1.1023	1.3426	1.2180
CORA	435.21	407.28	333.61	456119.02	426848.18	349636.66	1.0686	1.3046	1.2208
NSWO	603.47	561.68	466.78	884955.69	823664.80	684505.80	1.0744	1.2928	1.2033
BOOW	611.79	546.92	481.19	924860.80	826790.11	727431.03	1.1186	1.2714	1.1366
2828Hz	621.70	614.98	498.63	973893.33	963365.17	781100.48	1.0109	1.2468	1.2333
2000Hz	649.01	637.34	561.63	1145119.53	1124529.99	990944.36	1.0183	1.1556	1.1348
GGOW	531.42	524.88	490.74	819286.55	809207.35	756565.03	1.0125	1.0829	1.0696
LEOW	456.52	459.69	430.46	617360.85	621652.27	582127.17	0.9931	1.0605	1.0679
BADO	557.79	532.86	529.92	928618.06	887099.52	882218.28	1.0468	1.0526	1.0055

Scenario 2: Correction factors assuming survey area is equal to proportion of distance on open road and through forest

Species	Effective Detection Radius (EDR)			Area Surveyed			Correction Factor		
	ROAD	EDGE	FOREST	A:ROAD	A:EDGE	A:FOREST	Aroad:Aedge	Aroad:Aforest	Aedge:Aforest
YERA	279.98	219.89	128.12	56197.98	54068.47	51572.23	1.0394	1.0897	1.0484
PISI	498.73	422.81	212.09	149999.73	147271.24	141316.25	1.0185	1.0614	1.0421
CMWA	328.74	290.74	166.16	91683.28	90299.43	86739.58	1.0153	1.0570	1.0410
WETO	401.06	374.69	195.06	125784.64	124810.52	119532.78	1.0078	1.0523	1.0442
BEKI	360.81	307.13	184.21	111966.36	110033.90	106601.20	1.0176	1.0503	1.0322
WAVI	550.98	440.73	247.22	201197.35	197285.18	192002.02	1.0198	1.0479	1.0275
TEWA	248.23	232.53	152.77	76234.57	75660.63	73322.33	1.0076	1.0397	1.0319
BAWW	243.56	231.16	152.80	76120.52	75666.26	73351.02	1.0060	1.0378	1.0316
DEJU	396.30	360.65	215.36	151193.60	149890.31	145701.41	1.0087	1.0377	1.0287
OVEN	358.38	338.72	203.53	134848.79	134123.65	130144.37	1.0054	1.0361	1.0306
CCSP	315.60	293.87	192.45	120101.01	119308.68	116354.55	1.0066	1.0322	1.0254
CATO	461.52	456.14	254.05	209049.21	208847.71	202760.10	1.0010	1.0310	1.0300
BBWA	236.37	247.17	162.64	85351.29	85756.42	83100.53	0.9953	1.0271	1.0320
LISP	374.98	345.88	239.49	184305.18	183256.29	180190.44	1.0057	1.0228	1.0170
BHCO	350.30	332.75	228.59	167861.10	167223.86	164162.63	1.0038	1.0225	1.0186

5656Hz	563.87	538.73	331.99	353273.58	352347.30	346255.38	1.0026	1.0203	1.0176
RBGR	561.70	507.50	339.57	368968.04	367015.80	362244.61	1.0053	1.0186	1.0132
4000Hz	941.94	804.91	487.48	760265.21	755347.31	746551.38	1.0065	1.0184	1.0118
OSFL	498.45	434.47	329.78	346780.19	344547.71	341670.42	1.0065	1.0150	1.0084
WTSP	551.39	499.44	361.99	417403.72	415558.84	411670.31	1.0044	1.0139	1.0094
RBNU	466.44	423.13	347.41	382787.08	381305.65	379179.35	1.0039	1.0095	1.0056
CORA	435.21	407.28	333.61	352718.04	351757.36	349636.66	1.0027	1.0088	1.0061
1000Hz	696.63	640.06	504.79	806305.52	804341.54	800506.97	1.0024	1.0072	1.0048
1414Hz	696.63	640.06	504.79	806305.52	804341.54	800506.97	1.0024	1.0072	1.0048
NSWO	603.47	561.68	466.78	688641.14	687215.86	684505.80	1.0021	1.0060	1.0040
BOOW	611.79	546.92	481.19	731381.70	729238.74	727431.03	1.0029	1.0054	1.0025
2828Hz	621.70	614.98	498.63	784823.07	784589.54	781100.48	1.0003	1.0048	1.0045
2000Hz	649.01	637.34	561.63	993586.63	993198.15	990944.35	1.0004	1.0027	1.0023
GGOW	531.42	524.88	490.74	757796.94	757587.32	756565.03	1.0003	1.0016	1.0014
LEOW	456.52	459.69	430.46	582917.04	583018.89	582127.17	0.9998	1.0014	1.0015
BAOW	557.79	532.86	529.92	883061.93	882303.16	882218.28	1.0009	1.0010	1.0001
8000Hz	144.30	158.40	237.55	174405.36	174502.30	177276.37	0.9994	0.9838	0.9844

Table 4 – Monte Carlo simulations to compare differences in effective detection radius for different transect and forest types for different species. 90% confidence intervals are generated from resampling of fitted values from the original model (n=1000). “***” indicates no overlap in confidence intervals, “NO DATA” indicates there was no data available to make comparison, and “NA” indicates an undefined effective detection radius calculation due to an insufficient number of non-detections. Abbreviations for letter codes are combinations of transect and forest type: R – Road, E – Edge, F – Forest, C – Conifer, and D – Deciduous.

Species	RC-RD	EC-ED	FD-FC	RC-EC	RC-ED	RD-EC	RD-ED	EC-FC	EC-FD	ED-FC	ED-FD	RC-FC	RC-FD	RD-FC	RD-FD
BBWA								***	***		***		***		***
BEKI		***			***		***	***	***			***	***	***	***
CMWA								***	***	***		***	***	***	***
DEJU		***			***		***	***	***	***		***	***	***	***
LISP		***			***			***	***	***		***	***	***	***
OSFL					***		***	***	***	***		***	***	***	***
PISI		***			***			***	***	***	***	***	***	***	***
RBGR		***			***		***	***	***	***		***	***	***	***
TEWA					***			***	***	***		***	***	***	***
WAVI					***			***	***	***	***	***	***	***	***
WTSP	NA			NA	NA			***	***	***		NA	NA	***	***
YERA			NO DATA				***	***	NO DATA		NO DATA	***	NO DATA	***	NO DATA
BAWW								***	***			***	***	***	***
BHCO								***	***	***		***	***	***	***
CCSP								***	***	***		***	***	***	***
CORA								***		***		***		***	
OVEN								***	***	***	***	***	***	***	***
RBNU								***				***		***	

CATO			NO DATA					***	NO DATA	***	NO DATA	***	NO DATA	***	NO DATA
WETO			NO DATA					***	NO DATA	***	NO DATA	***	NO DATA	***	NO DATA
NSWO															
BOOW															
GGOW															
LEOW															
BADO															
1000Hz	NA	NA	***	NA	NA	NA	NA	NA	NA	NA	NA	NA	NA	NA	NA
1414Hz	NA	NA	NA	NA	NA	NA	NA	NA	NA	NA	NA	NA	NA	NA	NA
2000Hz		NA		NA		NA		NA	NA						
2828Hz															
4000Hz	NA	***		NA	NA			***	***			NA	NA	***	***
5656Hz								***	***		***	***	***	***	***
8000Hz													***		

Appendix 2

Table 1. Detection radius, detection area, and correction factors calculated for EDR for different songs and tones detected by four brands of autonomous recording units (ARUs), from listening trials conducted at 20 transects near Calling Lake and Lac La Biche, Alberta, Canada in 2014. Correction factors are relative to human observers in the field and are calculated using a ratio of ARU to Field Observer detection areas. Values less than 1 indicate a smaller detection area relative to human observers and values greater than 1 indicate greater detection area relative to human observers. Correction factors can be applied to ARU data to standardize survey areas with those of observers in the field. "NA" indicates EDR values that could not be solved by our models due to uncertainty caused by insufficient non-detections.

Sound	Habitat	Effective Detection Radius (m) ± 90% CI					Effective Detection Area (m^2)					EDR Correction Factor				
		Human	RiverForks	SM2	SM3	Zoom	Human	RiverForks	SM2	SM3	Zoom	Human	RiverForks	SM2	SM3	Zoom
1000Hz	Conifer	612 ± 118	586 ± 106	549 ± 91	553 ± 87	540 ± 84	1175276	1077627	946839	961247	915295	1.0000	0.9169	0.8056	0.8179	0.7788
1000Hz	Deciduous	676 ± 141	642 ± 119	594 ± 105	600 ± 105	583 ± 98	1436767	1293480	1109522	1129359	1066455	1.0000	0.9003	0.7722	0.7860	0.7423
1000Hz	Road	1078 ± 611	952 ± 376	815 ± 254	829 ± 245	786 ± 223	3650033	2848426	2086584	2157865	1939301	1.0000	0.7804	0.5717	0.5912	0.5313
1414Hz	Conifer	601 ± 110	568 ± 94	536 ± 86	545 ± 85	529 ± 82	1135418	1014684	902944	934322	879387	1.0000	0.8937	0.7953	0.8229	0.7745
1414Hz	Deciduous	658 ± 127	615 ± 113	575 ± 93	587 ± 100	566 ± 91	1359334	1189839	1039059	1080828	1007986	1.0000	0.8753	0.7644	0.7951	0.7415
1414Hz	Road	NA	903 ± 323	788 ± 224	818 ± 237	766 ± 200	NA	2560424	1951144	2103814	1844379	NA	NA	NA	NA	NA
2000Hz	Conifer	567 ± 105	553 ± 92	531 ± 86	551 ± 92	533 ± 85	1010637	961422	887345	952392	893324	1.0000	0.9513	0.8780	0.9424	0.8839
2000Hz	Deciduous	680 ± 142	656 ± 128	621 ± 115	652 ± 126	624 ± 115	1452730	1353163	1210887	1335343	1222048	1.0000	0.9315	0.8335	0.9192	0.8412

2000Hz	Road	1223 ± 0	1099 ± 610	953 ± 396	1079 ± 537	964 ± 406	4698534	3795315	2854582	3658388	2917393	1.0000	0.8078	0.6075	0.7786	0.6209
2828Hz	Conifer	566 ± 98	570 ± 96	536 ± 85	571 ± 96	549 ± 89	1005770	1019704	903720	1022910	948115	1.0000	1.0139	0.8985	1.0170	0.9427
2828Hz	Deciduous	707 ± 150	715 ± 146	652 ± 121	717 ± 150	676 ± 130	1570691	1604941	1335227	1612896	1434465	1.0000	1.0218	0.8501	1.0269	0.9133
2828Hz	Road	NA	NA	NA	NA	NA	NA	NA	NA	NA	NA	NA	NA	NA	NA	NA
4000Hz	Conifer	450 ± 74	451 ± 74	439 ± 72	458 ± 76	432 ± 68	635063	639295	604230	658029	587147	1.0000	1.0067	0.9514	1.0362	0.9245
4000Hz	Deciduous	495 ± 85	497 ± 84	481 ± 81	506 ± 93	473 ± 73	771104	777352	726114	805228	701584	1.0000	1.0081	0.9417	1.0443	0.9098
4000Hz	Road	1308 ± 783	1346 ± 679	1093 ± 465	NA	1006 ± 326	5370930	5689426	3751783	NA	3177717	1.0000	1.0593	0.6985	NA	0.5917
5656Hz	Conifer	358 ± 62	351 ± 60	333 ± 52	361 ± 63	348 ± 57	403523	387750	347486	408884	381134	1.0000	0.9609	0.8611	1.0133	0.9445
5656Hz	Deciduous	301 ± 52	297 ± 49	285 ± 45	302 ± 52	295 ± 47	284257	276339	255260	286907	272962	1.0000	0.9721	0.8980	1.0093	0.9603
5656Hz	Road	743 ± 210	686 ± 168	571 ± 135	765 ± 207	664 ± 161	1734810	1476581	1024515	1838439	1385027	1.0000	0.8511	0.5906	1.0597	0.7984
8000Hz	Conifer	219 ± 46	203 ± 37	150 ± 26	198 ± 34	184 ± 30	150853	129882	70873	123612	106319	1.0000	0.8610	0.4698	0.8194	0.7048
8000Hz	Deciduous	173 ± 41	165 ± 35	132 ± 24	162 ± 33	154 ± 29	93671	85135	55077	82396	74337	1.0000	0.9089	0.5880	0.8796	0.7936
8000Hz	Road	439 ± 111	342 ± 77	187 ± 45	320 ± 74	268 ± 61	605363	367344	109498	321258	225806	1.0000	0.6068	0.1809	0.5307	0.3730
BADO	Conifer	550 ± 117	476 ± 81	459 ± 77	464 ± 74	407 ± 56	951248	711751	660835	676513	519872	1.0000	0.7482	0.6947	0.7112	0.5465
BADO	Deciduous	658 ± 166	541 ± 100	516 ± 88	524 ± 90	445 ± 64	1362132	919221	836029	861281	622494	1.0000	0.6748	0.6138	0.6323	0.4570
BADO	Road	842 ± 360	630 ± 155	591 ± 134	603 ± 133	491 ± 88	2229825	1246571	1098354	1142356	757137	1.0000	0.5590	0.4926	0.5123	0.3396
BAWW	Conifer	238 ± 50	206 ± 35	201 ± 33	221 ± 42	201 ± 35	178608	132841	127386	153547	127431	1.0000	0.7438	0.7132	0.8597	0.7135
BAWW	Deciduous	213 ± 43	189 ± 33	185 ± 31	200 ± 36	185 ± 32	142657	111873	107979	126205	108011	1.0000	0.7842	0.7569	0.8847	0.7571
BAWW	Road	515 ± 126	319 ± 71	304 ± 67	388 ± 89	304 ± 70	834320	319744	289867	473396	290097	1.0000	0.3832	0.3474	0.5674	0.3477
BEKI	Conifer	294 ± 50	286 ± 46	257 ± 39	297 ± 51	287 ± 46	272203	256849	207309	277682	258925	1.0000	0.9436	0.7616	1.0201	0.9512
BEKI	Deciduous	224 ± 39	221 ± 38	206 ± 31	226 ± 42	221 ± 37	158083	152779	133765	159915	153511	1.0000	0.9664	0.8462	1.0116	0.9711
BEKI	Road	619 ± 160	550 ± 123	401 ± 84	647 ± 156	559 ± 125	1202325	951184	504616	1317122	980290	1.0000	0.7911	0.4197	1.0955	0.8153
BHCO	Conifer	341 ± 58	333 ± 54	293 ± 42	339 ± 58	334 ± 55	366090	348880	269548	361559	350184	1.0000	0.9530	0.7363	0.9876	0.9566
BHCO	Deciduous	318 ± 54	312 ± 50	278 ± 41	317 ± 52	312 ± 51	318681	305559	242938	315242	306559	1.0000	0.9588	0.7623	0.9892	0.9620
BHCO	Road	811 ± 241	717 ± 178	467 ± 102	784 ± 209	724 ± 180	2067520	1617024	683986	1930874	1645432	1.0000	0.7821	0.3308	0.9339	0.7958

BLWA	Conifer	220 ± 40	209 ± 36	199 ± 32	214 ± 37	209 ± 36	151680	137797	124066	144512	137427	1.0000	0.9085	0.8179	0.9527	0.9060
BLWA	Deciduous	197 ± 36	189 ± 33	181 ± 29	193 ± 33	189 ± 32	121478	112408	103100	116837	112162	1.0000	0.9253	0.8487	0.9618	0.9233
BLWA	Road	517 ± 136	414 ± 94	346 ± 80	458 ± 108	412 ± 93	838861	538708	376011	658290	533089	1.0000	0.6422	0.4482	0.7847	0.6355
BOOW	Conifer	593 ± 127	548 ± 105	536 ± 99	529 ± 90	473 ± 74	1106172	944125	903878	879743	702424	1.0000	0.8535	0.8171	0.7953	0.6350
BOOW	Deciduous	665 ± 156	603 ± 117	588 ± 115	578 ± 106	507 ± 76	1389224	1142871	1084420	1049866	806810	1.0000	0.8227	0.7806	0.7557	0.5808
BOOW	Road	NA	827 ± 287	788 ± 259	766 ± 220	620 ± 133	NA	2150999	1952887	1843612	1205750	NA	NA	NA	NA	NA
CATO	Conifer	369 ± 54	360 ± 52	345 ± 47	358 ± 52	346 ± 48	428512	407623	372931	402582	375217	1.0000	0.9513	0.8703	0.9395	0.8756
CATO	Deciduous	453 ± 79	437 ± 70	409 ± 61	433 ± 70	411 ± 60	644911	598735	526759	587920	531331	1.0000	0.9284	0.8168	0.9116	0.8239
CATO	Road	527 ± 110	501 ± 100	461 ± 82	495 ± 99	464 ± 86	871521	789262	668798	770577	676186	1.0000	0.9056	0.7674	0.8842	0.7759
CCSP	Conifer	323 ± 56	304 ± 50	288 ± 45	313 ± 56	306 ± 49	327909	290576	259790	308570	293834	1.0000	0.8861	0.7923	0.9410	0.8961
CCSP	Deciduous	221 ± 38	215 ± 35	208 ± 33	218 ± 37	215 ± 36	153281	144597	136545	148918	145399	1.0000	0.9433	0.8908	0.9715	0.9486
CCSP	Road	717 ± 192	561 ± 129	474 ± 104	627 ± 153	572 ± 135	1615921	989455	704981	1234604	1028273	1.0000	0.6123	0.4363	0.7640	0.6363
CMWA	Conifer	204 ± 58	171 ± 37	143 ± 29	178 ± 42	163 ± 35	130129	92195	64544	99939	83796	1.0000	0.7085	0.4960	0.7680	0.6439
CMWA	Deciduous	183 ± 50	159 ± 34	136 ± 25	164 ± 36	152 ± 31	105434	79073	57826	84702	72813	1.0000	0.7500	0.5485	0.8034	0.6906
CMWA	Road	NA	272 ± 101	189 ± 53	303 ± 128	243 ± 80	NA	232105	111667	288352	185335	NA	NA	NA	NA	NA
CORA	Conifer	339 ± 52	336 ± 51	324 ± 45	335 ± 49	324 ± 46	360271	355630	329144	351526	328965	1.0000	0.9871	0.9136	0.9757	0.9131
CORA	Deciduous	402 ± 64	398 ± 62	377 ± 55	395 ± 61	377 ± 54	506688	497556	447208	489560	446878	1.0000	0.9820	0.8826	0.9662	0.8820
CORA	Road	617 ± 162	604 ± 149	538 ± 117	593 ± 141	538 ± 112	1195481	1145859	909937	1104322	908571	1.0000	0.9585	0.7611	0.9237	0.7600
DEJU	Conifer	338 ± 58	325 ± 53	305 ± 47	332 ± 56	323 ± 51	359372	331614	291619	345693	328565	1.0000	0.9228	0.8115	0.9619	0.9143
DEJU	Deciduous	272 ± 48	265 ± 44	253 ± 39	268 ± 47	264 ± 44	231936	220049	201693	226161	218702	1.0000	0.9487	0.8696	0.9751	0.9429
DEJU	Road	857 ± 266	691 ± 166	543 ± 124	765 ± 205	677 ± 168	2306824	1500568	925935	1839584	1440084	1.0000	0.6505	0.4014	0.7975	0.6243
GGOW	Conifer	451 ± 81	406 ± 62	417 ± 68	410 ± 61	370 ± 48	640105	517272	545437	528611	430366	1.0000	0.8081	0.8521	0.8258	0.6723
GGOW	Deciduous	552 ± 113	474 ± 76	492 ± 86	482 ± 78	420 ± 59	958741	707208	760929	728575	554202	1.0000	0.7376	0.7937	0.7599	0.5781
GGOW	Road	754 ± 288	585 ± 131	619 ± 163	598 ± 144	491 ± 88	1787139	1074656	1203800	1124781	757050	1.0000	0.6013	0.6736	0.6294	0.4236
LEOW	Conifer	439 ± 79	375 ± 52	376 ± 53	384 ± 56	350 ± 46	604238	442240	444761	463471	384757	1.0000	0.7319	0.7361	0.7670	0.6368

LEOW	Deciduous	604 ± 142	464 ± 78	466 ± 76	481 ± 81	419 ± 61	1147801	676832	682755	727862	550874	1.0000	0.5897	0.5948	0.6341	0.4799
LEOW	Road	761 ± 298	525 ± 110	528 ± 109	550 ± 121	462 ± 81	1818378	864916	874612	950033	669342	1.0000	0.4757	0.4810	0.5225	0.3681
LISP	Conifer	340 ± 56	335 ± 55	311 ± 46	335 ± 54	331 ± 53	362661	353478	303974	353358	344209	1.0000	0.9747	0.8382	0.9743	0.9491
LISP	Deciduous	315 ± 55	312 ± 51	292 ± 44	312 ± 51	308 ± 51	312364	305527	267827	305438	298578	1.0000	0.9781	0.8574	0.9778	0.9559
LISP	Road	883 ± 291	815 ± 222	582 ± 133	814 ± 227	757 ± 199	2450595	2084615	1063347	2080457	1798947	1.0000	0.8507	0.4339	0.8490	0.7341
NSWO	Conifer	514 ± 101	520 ± 101	492 ± 86	490 ± 85	461 ± 75	831479	848211	759484	755817	666715	1.0000	1.0201	0.9134	0.9090	0.8018
NSWO	Deciduous	654 ± 150	664 ± 155	609 ± 125	606 ± 120	553 ± 98	1342154	1386295	1164038	1155446	959430	1.0000	1.0329	0.8673	0.8609	0.7148
NSWO	Road	NA	1019 ± 570	846 ± 344	840 ± 304	712 ± 200	NA	3261993	2250769	2218867	1593628	NA	NA	NA	NA	NA
OSFL	Conifer	360 ± 57	356 ± 56	337 ± 49	359 ± 57	350 ± 54	407639	399089	357836	403974	385462	1.0000	0.9790	0.8778	0.9910	0.9456
OSFL	Deciduous	385 ± 66	381 ± 63	358 ± 55	383 ± 65	373 ± 62	466053	454911	402075	461269	437290	1.0000	0.9761	0.8627	0.9897	0.9383
OSFL	Road	672 ± 237	649 ± 204	552 ± 139	662 ± 216	614 ± 182	1419791	1321209	956249	1376306	1182781	1.0000	0.9306	0.6735	0.9694	0.8331
OVEN	Conifer	325 ± 52	315 ± 47	298 ± 43	319 ± 49	313 ± 46	331061	311820	278854	319042	308335	1.0000	0.9419	0.8423	0.9637	0.9314
OVEN	Deciduous	268 ± 46	262 ± 43	252 ± 39	264 ± 43	261 ± 41	225414	216326	199929	219777	214643	1.0000	0.9597	0.8869	0.9750	0.9522
OVEN	Road	810 ± 241	688 ± 167	550 ± 131	729 ± 201	670 ± 165	2059789	1488393	951477	1668686	1412204	1.0000	0.7226	0.4619	0.8101	0.6856
PISI	Conifer	309 ± 54	296 ± 48	281 ± 44	305 ± 52	298 ± 48	299449	275404	248338	292895	278887	1.0000	0.9197	0.8293	0.9781	0.9313
PISI	Deciduous	251 ± 44	244 ± 41	236 ± 36	249 ± 43	245 ± 43	198113	187294	174370	195222	188899	1.0000	0.9454	0.8802	0.9854	0.9535
PISI	Road	690 ± 184	576 ± 134	484 ± 105	654 ± 157	590 ± 138	1494823	1041080	737311	1344611	1092670	1.0000	0.6965	0.4932	0.8995	0.7310
RBGR	Conifer	352 ± 54	355 ± 53	337 ± 48	357 ± 55	345 ± 49	388454	396463	357506	399853	372913	1.0000	1.0206	0.9203	1.0293	0.9600
RBGR	Deciduous	460 ± 82	468 ± 82	429 ± 67	472 ± 80	445 ± 72	665431	689281	579496	699595	621090	1.0000	1.0358	0.8709	1.0513	0.9334
RBGR	Road	724 ± 246	757 ± 265	619 ± 161	772 ± 271	667 ± 191	1646605	1800795	1204587	1872936	1399394	1.0000	1.0936	0.7316	1.1375	0.8499
RBNU	Conifer	384 ± 54	383 ± 53	367 ± 49	385 ± 55	372 ± 52	462807	462006	422414	464594	435349	1.0000	0.9983	0.9127	1.0039	0.9407
RBNU	Deciduous	457 ± 71	457 ± 71	429 ± 62	459 ± 70	438 ± 63	657096	655483	578549	660704	603090	1.0000	0.9975	0.8805	1.0055	0.9178
RBNU	Road	686 ± 200	685 ± 189	601 ± 143	691 ± 189	626 ± 146	1480552	1472391	1133737	1498995	1231977	1.0000	0.9945	0.7658	1.0125	0.8321
TEWA	Conifer	242 ± 44	227 ± 36	205 ± 30	237 ± 41	232 ± 37	184312	161263	131965	176926	168614	1.0000	0.8749	0.7160	0.9599	0.9148
TEWA	Deciduous	200 ± 39	191 ± 34	177 ± 28	197 ± 37	194 ± 36	125623	114471	98887	122147	118127	1.0000	0.9112	0.7872	0.9723	0.9403

TEWA	Road	625 ± 159	447 ± 98	328 ± 71	553 ± 138	491 ± 115	1227152	628779	337030	960241	757566	1.0000	0.5124	0.2746	0.7825	0.6173
WAVI	Conifer	325 ± 54	319 ± 52	299 ± 44	324 ± 51	318 ± 50	330968	320161	280277	329029	317975	1.0000	0.9673	0.8468	0.9941	0.9607
WAVI	Deciduous	283 ± 48	280 ± 48	266 ± 42	283 ± 47	279 ± 47	252295	245966	221726	251166	244673	1.0000	0.9749	0.8788	0.9955	0.9698
WAVI	Road	787 ± 239	719 ± 181	548 ± 125	774 ± 219	707 ± 172	1946153	1623847	943138	1880981	1569126	1.0000	0.8344	0.4846	0.9665	0.8063
WETO	Conifer	340 ± 47	327 ± 44	312 ± 40	326 ± 43	306 ± 37	364208	335585	305270	333213	293587	1.0000	0.9214	0.8382	0.9149	0.8061
WETO	Deciduous	386 ± 57	367 ± 53	346 ± 47	365 ± 51	337 ± 44	468266	421989	375143	418246	357653	1.0000	0.9012	0.8011	0.8932	0.7638
WETO	Road	449 ± 84	419 ± 75	388 ± 61	417 ± 73	377 ± 59	633332	551529	474144	545152	446545	1.0000	0.8708	0.7487	0.8608	0.7051
WTSP	Conifer	398 ± 65	394 ± 64	379 ± 57	404 ± 70	394 ± 64	497421	488406	450744	512106	487937	1.0000	0.9819	0.9062	1.0295	0.9809
WTSP	Deciduous	427 ± 67	423 ± 66	404 ± 61	434 ± 70	422 ± 66	572980	561051	511915	592552	560432	1.0000	0.9792	0.8934	1.0342	0.9781
WTSP	Road	721 ± 239	700 ± 218	623 ± 169	758 ± 289	699 ± 214	1634891	1541379	1219736	1805002	1536714	1.0000	0.9428	0.7461	1.1041	0.9399
YERA	Conifer	212 ± 44	568 ± 41	536 ± 28	207 ± 43	203 ± 39	140596	1014684	902944	134210	129845	1.0000	7.2170	6.4223	0.9546	0.9235
YERA	Deciduous	188 ± 39	183 ± 37	158 ± 27	185 ± 37	182 ± 35	111247	105054	78683	107211	104407	1.0000	0.9443	0.7073	0.9637	0.9385
YERA	Road	442 ± 119	384 ± 92	244 ± 55	402 ± 108	379 ± 98	614773	463702	187026	508896	451357	1.0000	0.7543	0.3042	0.8278	0.7342

Table 2. Detection radius, detection area, and correction factors calculated for MDD of different songs and tones detected by four brands of autonomous recording units (ARUs), from listening trials conducted at 20 transects near Calling Lake and Lac La Biche, Alberta, Canada in 2014. Correction factors are relative to human observers in the field and are calculated using a ratio of ARU to Field Observer detection areas. Values less than 1 indicate a smaller detection area relative to human observers and values greater than 1 indicate greater detection area relative to human observers. Correction factors can be applied to ARU data to standardize survey areas with those of observers in the field.

Sound	Habitat	Maximum Detection Distance (m)					Maximum Detection Area (m^2)					MDD Correction Factor				
		Human	RiverForks	SM2	SM3	Zoom	Human	RiverForks	SM2	SM3	Zoom	Human	RiverForks	SM2	SM3	Zoom
1000Hz	Conifer	913	813	763	563	513	2615867	2073942	1826542	994020	825159	1.0000	0.7928	0.6983	0.3800	0.3154
1000Hz	Deciduous	913	763	763	713	713	2615867	1826542	1826542	1594849	1594849	1.0000	0.6983	0.6983	0.6097	0.6097
1000Hz	Road	1113	1113	913	1013	1013	3888212	3888212	2615867	3220623	3220623	1.0000	1.0000	0.6728	0.8283	0.8283
1414Hz	Conifer	913	763	763	563	463	2615867	1826542	1826542	994020	672006	1.0000	0.6983	0.6983	0.3800	0.2569
1414Hz	Deciduous	813	763	713	713	713	2073942	1826542	1594849	1594849	1594849	1.0000	0.8807	0.7690	0.7690	0.7690
1414Hz	Road	1113	1113	913	1013	1013	3888212	3888212	2615867	3220623	3220623	1.0000	1.0000	0.6728	0.8283	0.8283
2000Hz	Conifer	513	663	613	563	463	825159	1378865	1178588	994020	672006	1.0000	1.6710	1.4283	1.2046	0.8144
2000Hz	Deciduous	763	713	613	713	713	1826542	1594849	1178588	1594849	1594849	1.0000	0.8732	0.6453	0.8732	0.8732
2000Hz	Road	1113	1013	913	1013	913	3888212	3220623	2615867	3220623	2615867	1.0000	0.8283	0.6728	0.8283	0.6728
2828Hz	Conifer	513	613	363	513	413	825159	1178588	412825	825159	534562	1.0000	1.4283	0.5003	1.0000	0.6478
2828Hz	Deciduous	713	763	513	663	663	1594849	1826542	825159	1378865	1378865	1.0000	1.1453	0.5174	0.8646	0.8646
2828Hz	Road	913	1013	813	1013	913	2615867	3220623	2073942	3220623	2615867	1.0000	1.2312	0.7928	1.2312	1.0000
4000Hz	Conifer	413	388	363	388	363	534562	471730	412825	471730	412825	1.0000	0.8825	0.7723	0.8825	0.7723
4000Hz	Deciduous	513	513	388	513	413	825159	825159	471730	825159	534562	1.0000	1.0000	0.5717	1.0000	0.6478
4000Hz	Road	763	813	763	813	713	1826542	2073942	1826542	2073942	1594849	1.0000	1.1354	1.0000	1.1354	0.8732
5656Hz	Conifer	413	313	288	313	313	534562	306796	259672	306796	306796	1.0000	0.5739	0.4858	0.5739	0.5739
5656Hz	Deciduous	338	288	213	363	363	357847	259672	141863	412825	412825	1.0000	0.7257	0.3964	1.1536	1.1536
5656Hz	Road	563	563	513	613	563	994020	994020	825159	1178588	994020	1.0000	1.0000	0.8301	1.1857	1.0000
8000Hz	Conifer	238	188	163	188	188	177205	110447	82958	110447	110447	1.0000	0.6233	0.4681	0.6233	0.6233
8000Hz	Deciduous	188	188	113	163	138	110447	110447	39761	82958	59396	1.0000	1.0000	0.3600	0.7511	0.5378
8000Hz	Road	363	338	188	313	288	412825	357847	110447	306796	259672	1.0000	0.8668	0.2675	0.7432	0.6290
BADO	Conifer	813	463	388	463	363	2073942	672006	471730	672006	412825	1.0000	0.3240	0.2275	0.3240	0.1991
BADO	Deciduous	913	1013	763	513	338	2615867	3220623	1826542	825159	357847	1.0000	1.2312	0.6983	0.3154	0.1368
BADO	Road	1113	763	763	763	663	3888212	1826542	1826542	1826542	1378865	1.0000	0.4698	0.4698	0.4698	0.3546
BAWW	Conifer	263	163	138	213	238	216475	82958	59396	141863	177205	1.0000	0.3832	0.2744	0.6553	0.8186
BAWW	Deciduous	213	213	188	213	163	141863	141863	110447	141863	82958	1.0000	1.0000	0.7785	1.0000	0.5848
BAWW	Road	413	313	313	338	288	534562	306796	306796	357847	259672	1.0000	0.5739	0.5739	0.6694	0.4858

BEKI	Conifer	313	288	238	263	288	306796	259672	177205	216475	259672	1.0000	0.8464	0.5776	0.7056	0.8464
BEKI	Deciduous	263	263	213	213	188	216475	216475	141863	141863	110447	1.0000	1.0000	0.6553	0.6553	0.5102
BEKI	Road	513	463	388	563	513	825159	672006	471730	994020	825159	1.0000	0.8144	0.5717	1.2046	1.0000
BHCO	Conifer	338	313	263	313	313	357847	306796	216475	306796	306796	1.0000	0.8573	0.6049	0.8573	0.8573
BHCO	Deciduous	388	313	213	313	413	471730	306796	141863	306796	534562	1.0000	0.6504	0.3007	0.6504	1.1332
BHCO	Road	663	613	413	663	613	1378865	1178588	534562	1378865	1178588	1.0000	0.8548	0.3877	1.0000	0.8548
BLWA	Conifer	213	238	163	213	238	141863	177205	82958	141863	177205	1.0000	1.2491	0.5848	1.0000	1.2491
BLWA	Deciduous	263	188	138	213	138	216475	110447	59396	141863	59396	1.0000	0.5102	0.2744	0.6553	0.2744
BLWA	Road	463	363	338	388	388	672006	412825	357847	471730	471730	1.0000	0.6143	0.5325	0.7020	0.7020
BOOW	Conifer	813	613	463	563	413	2073942	1178588	672006	994020	534562	1.0000	0.5683	0.3240	0.4793	0.2578
BOOW	Deciduous	763	713	763	563	363	1826542	1594849	1826542	994020	412825	1.0000	0.8732	1.0000	0.5442	0.2260
BOOW	Road	1113	913	813	913	763	3888212	2615867	2073942	2615867	1826542	1.0000	0.6728	0.5334	0.6728	0.4698
CATO	Conifer	413	463	288	338	338	534562	672006	259672	357847	357847	1.0000	1.2571	0.4858	0.6694	0.6694
CATO	Deciduous	663	563	463	563	563	1378865	994020	672006	994020	994020	1.0000	0.7209	0.4874	0.7209	0.7209
CATO	Road	913	813	763	763	663	2615867	2073942	1826542	1826542	1378865	1.0000	0.7928	0.6983	0.6983	0.5271
CCSP	Conifer	338	313	238	288	313	357847	306796	177205	259672	306796	1.0000	0.8573	0.4952	0.7257	0.8573
CCSP	Deciduous	213	213	213	238	188	141863	141863	141863	177205	110447	1.0000	1.0000	1.0000	1.2491	0.7785
CCSP	Road	563	463	413	513	513	994020	672006	534562	825159	825159	1.0000	0.6760	0.5378	0.8301	0.8301
CMWA	Conifer	213	138	113	163	188	141863	59396	39761	82958	110447	1.0000	0.4187	0.2803	0.5848	0.7785
CMWA	Deciduous	213	188	113	113	88	141863	110447	39761	39761	24053	1.0000	0.7785	0.2803	0.2803	0.1696
CMWA	Road	413	263	213	288	263	534562	216475	141863	259672	216475	1.0000	0.4050	0.2654	0.4858	0.4050
CORA	Conifer	363	363	288	313	288	412825	412825	259672	306796	259672	1.0000	1.0000	0.6290	0.7432	0.6290
CORA	Deciduous	663	463	338	413	363	1378865	672006	357847	534562	412825	1.0000	0.4874	0.2595	0.3877	0.2994
CORA	Road	813	813	713	813	713	2073942	2073942	1594849	2073942	1594849	1.0000	1.0000	0.7690	1.0000	0.7690
DEJU	Conifer	388	313	238	313	313	471730	306796	177205	306796	306796	1.0000	0.6504	0.3757	0.6504	0.6504
DEJU	Deciduous	363	288	213	238	263	412825	259672	141863	177205	216475	1.0000	0.6290	0.3436	0.4293	0.5244
DEJU	Road	613	613	463	663	563	1178588	1178588	672006	1378865	994020	1.0000	1.0000	0.5702	1.1699	0.8434
GGOW	Conifer	513	463	463	413	388	825159	672006	672006	534562	471730	1.0000	0.8144	0.8144	0.6478	0.5717
GGOW	Deciduous	763	663	713	463	338	1826542	1378865	1594849	672006	357847	1.0000	0.7549	0.8732	0.3679	0.1959
GGOW	Road	1113	763	813	813	663	3888212	1826542	2073942	2073942	1378865	1.0000	0.4698	0.5334	0.5334	0.3546
LEOW	Conifer	613	338	288	463	338	1178588	357847	259672	672006	357847	1.0000	0.3036	0.2203	0.5702	0.3036
LEOW	Deciduous	913	763	763	388	338	2615867	1826542	1826542	471730	357847	1.0000	0.6983	0.6983	0.1803	0.1368
LEOW	Road	1113	713	763	813	663	3888212	1594849	1826542	2073942	1378865	1.0000	0.4102	0.4698	0.5334	0.3546
LISP	Conifer	338	313	263	313	313	357847	306796	216475	306796	306796	1.0000	0.8573	0.6049	0.8573	0.8573
LISP	Deciduous	363	313	213	363	413	412825	306796	141863	412825	534562	1.0000	0.7432	0.3436	1.0000	1.2949
LISP	Road	663	663	513	663	663	1378865	1378865	825159	1378865	1378865	1.0000	1.0000	0.5984	1.0000	1.0000
NSWO	Conifer	463	813	388	413	388	672006	2073942	471730	534562	471730	1.0000	3.0862	0.7020	0.7955	0.7020
NSWO	Deciduous	763	913	663	563	613	1826542	2615867	1378865	994020	1178588	1.0000	1.4321	0.7549	0.5442	0.6453
NSWO	Road	1013	913	813	813	763	3220623	2615867	2073942	2073942	1826542	1.0000	0.8122	0.6440	0.6440	0.5671
OSFL	Conifer	363	338	288	338	338	412825	357847	259672	357847	357847	1.0000	0.8668	0.6290	0.8668	0.8668
OSFL	Deciduous	563	513	288	463	388	994020	825159	259672	672006	471730	1.0000	0.8301	0.2612	0.6760	0.4746
OSFL	Road	713	713	613	763	713	1594849	1594849	1178588	1826542	1594849	1.0000	1.0000	0.7390	1.1453	1.0000
OVEN	Conifer	338	313	263	313	313	357847	306796	216475	306796	306796	1.0000	0.8573	0.6049	0.8573	0.8573
OVEN	Deciduous	413	238	213	238	213	534562	177205	141863	177205	141863	1.0000	0.3315	0.2654	0.3315	0.2654
OVEN	Road	613	613	513	663	563	1178588	1178588	825159	1378865	994020	1.0000	1.0000	0.7001	1.1699	0.8434
PISI	Conifer	338	288	213	288	288	357847	259672	141863	259672	259672	1.0000	0.7257	0.3964	0.7257	0.7257
PISI	Deciduous	363	288	213	213	213	412825	259672	141863	141863	141863	1.0000	0.6290	0.3436	0.3436	0.3436

PISI	Road	563	513	413	563	513	994020	825159	534562	994020	825159	1.0000	0.8301	0.5378	1.0000	0.8301
RBGR	Conifer	363	363	288	338	338	412825	412825	259672	357847	357847	1.0000	1.0000	0.6290	0.8668	0.8668
RBGR	Deciduous	513	613	388	563	513	825159	1178588	471730	994020	825159	1.0000	1.4283	0.5717	1.2046	1.0000
RBGR	Road	813	813	713	913	763	2073942	2073942	1594849	2615867	1826542	1.0000	1.0000	0.7690	1.2613	0.8807
RBNU	Conifer	413	388	313	388	338	534562	471730	306796	471730	357847	1.0000	0.8825	0.5739	0.8825	0.6694
RBNU	Deciduous	663	563	338	563	513	1378865	994020	357847	994020	825159	1.0000	0.7209	0.2595	0.7209	0.5984
RBNU	Road	813	813	763	813	763	2073942	2073942	1826542	2073942	1826542	1.0000	1.0000	0.8807	1.0000	0.8807
TEWA	Conifer	288	238	138	238	238	259672	177205	59396	177205	177205	1.0000	0.6824	0.2287	0.6824	0.6824
TEWA	Deciduous	238	213	138	213	163	177205	141863	59396	141863	82958	1.0000	0.8006	0.3352	0.8006	0.4681
TEWA	Road	513	388	338	513	413	825159	471730	357847	825159	534562	1.0000	0.5717	0.4337	1.0000	0.6478
WAVI	Conifer	313	313	263	313	313	306796	306796	216475	306796	306796	1.0000	1.0000	0.7056	1.0000	1.0000
WAVI	Deciduous	313	363	238	263	263	306796	412825	177205	216475	216475	1.0000	1.3456	0.5776	0.7056	0.7056
WAVI	Road	613	613	513	663	563	1178588	1178588	825159	1378865	994020	1.0000	1.0000	0.7001	1.1699	0.8434
WETO	Conifer	513	413	288	338	313	825159	534562	259672	357847	306796	1.0000	0.6478	0.3147	0.4337	0.3718
WETO	Deciduous	463	563	363	463	363	672006	994020	412825	672006	412825	1.0000	1.4792	0.6143	1.0000	0.6143
WETO	Road	1013	763	713	813	663	3220623	1826542	1594849	2073942	1378865	1.0000	0.5671	0.4952	0.6440	0.4281
WTSP	Conifer	413	388	313	388	388	534562	471730	306796	471730	471730	1.0000	0.8825	0.5739	0.8825	0.8825
WTSP	Deciduous	613	613	338	463	463	1178588	1178588	357847	672006	672006	1.0000	1.0000	0.3036	0.5702	0.5702
WTSP	Road	813	763	713	813	763	2073942	1826542	1594849	2073942	1826542	1.0000	0.8807	0.7690	1.0000	0.8807
YERA	Conifer	238	213	138	163	188	177205	141863	59396	82958	110447	1.0000	0.8006	0.3352	0.4681	0.6233
YERA	Deciduous	213	138	138	188	213	141863	59396	59396	110447	141863	1.0000	0.4187	0.4187	0.7785	1.0000
YERA	Road	413	388	313	413	363	534562	471730	306796	534562	412825	1.0000	0.8825	0.5739	1.0000	0.7723

Table 3. Effective detection radius (EDR) for SM2 recorders at different sound pressure levels (SPL) in open and closed habitat for different songs and tones. Data were collected from listening trials conducted along 20 transects in the Blackfoot-Cooking Lake Natural Area near Edmonton, Alberta, Canada in 2014. "NA" values indicate undefined EDR due to an insufficient number of non-detections at that SPL for that species.

	Sound Pressure Level ± 90% CI (m)																					
	Closed Habitat											Open Habitat										
Sound	40dB	45dB	50dB	55dB	60dB	65dB	70dB	75dB	80dB	85dB	90dB	40dB	45dB	50dB	55dB	60dB	65dB	70dB	75dB	80dB	85dB	90dB
1000Hz	71 ± 25	75 ± 26	93 ± 35	123 ± 62	NA	NA	NA	NA	NA	NA	NA	95 ± 61	105 ± 76	NA	NA	NA	NA	NA	NA	NA	NA	NA
1414Hz	38 ± 17	57 ± 22	66 ± 19	82 ± 29	81 ± 28	NA	NA	NA	NA	NA	NA	44 ± 26	86 ± 73	NA	NA	NA	NA	NA	NA	NA	NA	NA
2000Hz	62 ± 19	75 ± 22	89 ± 31	92 ± 32	110 ± 62	107 ± 56	NA	NA	NA	NA	NA	87 ± 53	NA	NA	NA	NA	NA	NA	NA	NA	NA	NA
2828Hz	47 ± 14	53 ± 15	58 ± 18	58 ± 18	61 ± 22	NA	NA	NA	NA	NA	NA	79 ± 49	NA	NA	NA	NA	NA	NA	NA	NA	NA	NA
4000Hz	58 ± 22	67 ± 20	71 ± 23	85 ± 41	NA	NA	96 ± 60	NA	NA	NA	NA	84 ± 70	NA	NA	NA	NA	NA	NA	NA	NA	NA	NA
5656Hz	46 ± 11	44 ± 12	49 ± 12	54 ± 12	57 ± 17	78 ± 43	58 ± 19	60 ± 20	NA	NA	NA	83 ± 48	72 ± 42	NA	NA	NA	NA	NA	NA	NA	NA	NA
8000Hz	48 ± 20	29 ± 26	29 ± 25	12 ± 1	53 ± 24	47 ± 22	59 ± 23	72 ± 26	64 ± 24	86 ± 36	91 ± 40	56 ± 31	31 ± 29	30 ± 27	12 ± 1	64 ± 38	54 ± 33	76 ± 45	109 ± 76	87 ± 48	NA	NA
BADO	12 ± 1	44 ± 21	64 ± 27	86 ± 37	121 ± 68	NA	NA	NA	NA	NA	NA	12 ± 1	47 ± 25	72 ± 39	110 ± 79	NA	NA	NA	NA	NA	NA	NA
BAWW	12 ± 1	29 ± 25	46 ± 16	49 ± 18	56 ± 15	60 ± 16	67 ± 19	69 ± 21	71 ± 22	NA	89 ± 44	12 ± 1	32 ± 33	63 ± 38	71 ± 49	98 ± 63	NA	NA	NA	NA	NA	NA
BEKI	12 ± 1	34 ± 14	12 ± 1	39 ± 13	39 ± 13	49 ± 13	53 ± 17	53 ± 16	55 ± 19	83 ± 59	NA	12 ± 1	45 ± 30	12 ± 1	60 ± 40	59 ± 38	NA	NA	NA	NA	NA	NA
BHCO	45 ± 13	45 ± 15	51 ± 14	58 ± 13	60 ± 15	66 ± 23	73 ± 30	74 ± 28	90 ± 50	NA	NA	64 ± 36	66 ± 41	93 ± 69	NA	NA	NA	NA	NA	NA	NA	NA
BLWA	12 ± 1	12 ± 1	28 ± 23	54 ± 15	59 ± 18	63 ± 16	74 ± 22	76 ± 26	83 ± 33	80 ± 31	83 ± 34	12 ± 1	12 ± 1	30 ± 28	79 ± 43	97 ± 72	117 ± 90	NA	NA	NA	NA	NA
BOOW	58 ± 24	63 ± 23	81 ± 29	109 ± 48	NA	NA	NA	NA	NA	NA	NA	69 ± 41	79 ± 45	NA	NA	NA	NA	NA	NA	NA	NA	NA
CATO	10 ± 1	30 ± 26	52 ± 22	62 ± 19	77 ± 23	82 ± 27	109 ± 57	114 ± 72	NA	NA	NA	11 ± 1	32 ± 31	68 ± 46	93 ± 58	NA	NA	NA	NA	NA	NA	NA
CCSP	12 ± 1	33 ± 28	37 ± 14	51 ± 13	55 ± 14	60 ± 19	59 ± 18	84 ± 47	61 ± 19	NA	NA	12 ± 1	41 ± 42	48 ± 32	NA	NA	NA	NA	NA	NA	NA	NA
CMWA	38 ± 16	12 ± 1	12 ± 1	38 ± 17	34 ± 14	39 ± 16	44 ± 17	53 ± 18	57 ± 21	57 ± 23	63 ± 28	44 ± 26	12 ± 1	12 ± 1	45 ± 28	38 ± 21	47 ± 27	56 ± 33	79 ± 57	NA	NA	NA

CORA	12 ± 1	35 ± 30	53 ± 15	60 ± 16	65 ± 17	70 ± 21	79 ± 31	106 ± 74	NA	NA	NA	12 ± 1	40 ± 42	83 ± 53	NA	NA	NA	NA	NA	NA	NA	NA
DEJU	12 ± 1	37 ± 14	46 ± 11	51 ± 11	55 ± 14	57 ± 16	66 ± 26	96 ± 56	74 ± 44	NA	NA	12 ± 1	50 ± 35	83 ± 49	NA	NA	NA	NA	NA	NA	NA	NA
GGOW	12 ± 1	34 ± 31	55 ± 24	73 ± 23	93 ± 39	97 ± 38	120 ± 76	NA	NA	NA	NA	12 ± 1	37 ± 36	66 ± 42	113 ± 83	NA	NA	NA	NA	NA	NA	NA
LEOW	12 ± 1	34 ± 31	51 ± 26	59 ± 34	102 ± 60	NA	NA	NA	NA	NA	NA	12 ± 1	35 ± 32	52 ± 28	61 ± 40	114 ± 93	NA	NA	NA	NA	NA	NA
LISP	12 ± 1	33 ± 28	34 ± 30	54 ± 13	63 ± 18	68 ± 21	81 ± 44	72 ± 25	94 ± 57	101 ± 80	NA	12 ± 1	39 ± 40	40 ± 43	100 ± 66	NA	NA	NA	NA	NA	NA	NA
NSWO	34 ± 29	47 ± 20	60 ± 19	84 ± 26	97 ± 39	NA	117 ± 79	104 ± 45	NA	NA	NA	37 ± 35	57 ± 34	86 ± 54	NA	NA	NA	NA	NA	NA	NA	NA
OSFL	39 ± 18	56 ± 18	68 ± 19	75 ± 20	85 ± 31	85 ± 26	94 ± 43	NA	NA	NA	NA	44 ± 27	77 ± 45	124 ± 118	NA	NA	NA	NA	NA	NA	NA	NA
OVEN	12 ± 1	34 ± 12	42 ± 12	46 ± 11	49 ± 14	49 ± 13	52 ± 16	60 ± 27	NA	NA	NA	12 ± 1	47 ± 29	78 ± 57	NA	NA	NA	NA	NA	NA	NA	NA
PISI	12 ± 1	32 ± 12	40 ± 11	47 ± 12	51 ± 14	51 ± 13	54 ± 16	56 ± 19	91 ± 63	NA	NA	12 ± 1	40 ± 24	64 ± 38	114 ± 104	NA	NA	NA	NA	NA	NA	NA
RBGR	12 ± 1	37 ± 15	58 ± 17	28 ± 23	67 ± 19	78 ± 27	74 ± 25	111 ± 81	NA	NA	NA	12 ± 1	43 ± 24	103 ± 88	31 ± 29	NA	NA	NA	NA	NA	NA	NA
RBNU	30 ± 23	37 ± 14	48 ± 12	50 ± 12	53 ± 16	61 ± 32	62 ± 27	NA	NA	NA	NA	36 ± 36	52 ± 40	NA	NA	NA	NA	NA	NA	NA	NA	NA
TEWA	11 ± 1	11 ± 1	11 ± 1	11 ± 1	48 ± 16	52 ± 15	57 ± 17	60 ± 19	67 ± 29	69 ± 30	NA	12 ± 1	11 ± 1	12 ± 1	12 ± 1	76 ± 51	97 ± 68	NA	NA	NA	NA	NA
WAVI	12 ± 1	33 ± 28	44 ± 18	29 ± 25	62 ± 17	68 ± 19	72 ± 22	76 ± 28	NA	NA	NA	12 ± 1	37 ± 39	56 ± 41	32 ± 32	NA	NA	NA	NA	NA	NA	NA
WETO	29 ± 24	29 ± 25	49 ± 17	57 ± 18	62 ± 20	66 ± 23	73 ± 29	NA	NA	NA	NA	31 ± 30	32 ± 30	64 ± 34	85 ± 55	NA	NA	NA	NA	NA	NA	NA
WTSP	38 ± 14	47 ± 12	48 ± 12	52 ± 15	62 ± 27	55 ± 19	NA	NA	NA	NA	NA	56 ± 41	NA	NA	NA	NA	NA	NA	NA	NA	NA	NA
YERA	29 ± 25	11 ± 1	11 ± 1	11 ± 1	34 ± 31	37 ± 16	59 ± 21	63 ± 20	79 ± 42	77 ± 37	80 ± 40	32 ± 31	11 ± 1	12 ± 1	12 ± 1	40 ± 44	43 ± 28	NA	NA	NA	NA	NA

Appendix 3

Table 1. Model coefficients for generalized linear models for the effects of distance, vegetation type, sound characteristics, and atmospheric conditions on the probability of detecting a sound, with all species pooled.

Variable	β	Standard Error	z	p
Intercept	-2.696	0.140	-19.285	0.000
Distance	-4.723	0.122	-38.680	0.000
Conifer Forest	0.957	0.134	7.158	0.000
Deciduous Forest	1.493	0.102	14.660	0.000
Graminoid Fen	3.779	0.125	30.121	0.000
Forest Edge	3.289	0.090	36.499	0.000
Grassland	3.339	0.111	30.219	0.000
Road	3.764	0.090	41.594	0.000
Wind	-0.007	0.083	-0.085	0.932
Minimum Frequency	-0.798	0.123	-6.483	0.000
Bandwidth	-1.166	0.124	-9.434	0.000
Humidity	0.164	0.024	6.883	0.000
Temperature	-0.172	0.029	-5.900	0.000
Distance*Conifer Forest	-0.503	0.189	-2.656	0.008
Distance*Deciduous Forest	1.345	0.149	9.054	0.000
Distance*Graminoid Fen	1.618	0.168	9.652	0.000
Distance*Forest Edge	1.850	0.137	13.481	0.000
Distance*Grassland	1.812	0.147	12.303	0.000
Distance*Road	1.939	0.135	14.318	0.000
Wind*Conifer Forest	1.126	0.142	7.926	0.000
Wind*Deciduous Forest	0.103	0.114	0.905	0.366
Wind*Graminoid Fen	-0.784	0.117	-6.706	0.000
Wind*Forest Edge	-0.473	0.096	-4.921	0.000
Wind*Grassland	-0.094	0.087	-1.074	0.283
Wind*Road	0.214	0.097	2.199	0.028
Minimum Frequency*Conifer Forest	-0.219	0.068	-3.237	0.001
Minimum Frequency*Deciduous Forest	-0.152	0.061	-2.519	0.012
Minimum Frequency*Graminoid Fen	0.068	0.078	0.870	0.385
Minimum Frequency*Forest Edge	-0.235	0.059	-3.978	0.000
Minimum Frequency*Grassland	-0.359	0.067	-5.335	0.000
Minimum Frequency*Road	-0.307	0.058	-5.255	0.000
Bandwidth*Conifer Forest	-0.217	0.072	-2.993	0.003
Bandwidth*Deciduous Forest	-0.089	0.064	-1.392	0.164

Bandwidth*Graminoid Fen	0.172	0.081	2.112	0.035
Bandwidth*Forest Edge	-0.242	0.063	-3.809	0.000
Bandwidth*Grassland	-0.076	0.070	-1.079	0.280
Bandwidth*Road	-0.239	0.062	-3.822	0.000

Table 2. Top performing model for each species estimating the effect of distance, vegetation type, and atmospheric conditions on the probability of detection. We selected models based on small sample size corrected AIC.

Species	Model
1000 Hz	Distance*Vegetation + Wind*Vegetation + Temp
1414 Hz	Distance*Vegetation + Wind*Vegetation + Humidity
2000 Hz	Distance*Vegetation + Wind*Vegetation + Humidity
2828 Hz	Distance*Vegetation + Wind*Vegetation + Temp
4000 Hz	Distance*Vegetation + Wind*Vegetation
5656 Hz	Distance*Vegetation + Wind*Vegetation + Humidity + Temp
Barred owl	Distance*Vegetation + Wind*Vegetation + Temp
Bay-breasted warbler	Distance*Vegetation
Belted kingfisher	Distance*Vegetation + Wind*Vegetation
Black-and-white warbler	Distance*Vegetation + Wind*Vegetation + Humidity + Temp
Boreal owl	Distance*Vegetation + Wind*Vegetation + Humidity + Temp
Brown-headed cowbird	Distance*Vegetation + Wind*Vegetation
Canadian toad	Distance*Vegetation + Wind + Temp
Cape-may warbler	Distance*Vegetation + Wind*Vegetation
Clay-coloured sparrow	Distance*Vegetation + Wind*Vegetation
Common raven	Distance*Vegetation + Wind*Vegetation + Humidity
Dark-eyed junco	Distance*Vegetation + Wind*Vegetation
Great gray owl	Distance*Vegetation + Wind*Vegetation + Temp
Lincoln's sparrow	Distance*Vegetation
Long-eared owl	Distance*Vegetation + Wind*Vegetation + Humidity + Temp
Northern saw-whet owl	Distance*Vegetation + Wind*Vegetation + Temp
Olive-sided flycatcher	Distance*Vegetation + Wind*Vegetation
Ovenbird	Distance*Vegetation + Humidity
Pine siskin	Distance*Vegetation + Temp + Humidity
Red-breasted nuthatch	Distance*Vegetation + Wind*Vegetation + Humidity
Rose-breasted grosbeak	Distance*Vegetation + Wind*Vegetation
Tennessee warbler	Distance*Vegetation + Wind*Vegetation
Warbling vireo	Distance*Vegetation + Wind*Vegetation
Western toad	Distance*Vegetation + Wind*Vegetation + Temp
White-throated sparrow	Distance*Vegetation + Wind*Vegetation + Humidity + Temp
Yellow rail	Distance*Vegetation + Temp

Table 3. Model coefficients for generalized linear models for the effects of distance, vegetation type, and atmospheric conditions on the probability of detecting a sound, for each species.

Variable	Intercept	Distance	Distance*Conifer Forest	Distance*Deciduous Forest	Distance*Forest Edge	Distance*Graminoid Fen	Distance*Grassland	Distance*Road
1000 Hz	6.950	-0.008	-0.002	0.002	0.003	0.001	0.004	0.003
1414 Hz	2.627	-0.008	-0.006	0.002	0.003	-0.001	0.002	0.003
2000 Hz	1.608	-0.007	-0.003	0.003	0.001	-0.003	0.002	0.002
2828 Hz	5.531	-0.010	0.000	0.002	0.002	0.001	-0.001	0.003
4000 Hz	3.312	-0.013	0.000	0.000	0.004	-0.002	0.000	0.003
5656 Hz	2.831	-0.032	0.017	0.016	0.019	0.019	0.007	0.018
Barred owl	5.035	-0.007	0.000	0.003	0.002	0.002	0.004	0.003
Black-and-white warbler	1.955	-0.045	-0.006	-0.020	0.023	0.025	0.021	0.025
Bay-breasted warbler	13.254	-0.118	0.087	0.071	0.098	0.105	0.074	0.095
Belted kingfisher	12.804	-0.075	0.031	0.043	0.057	0.061	0.055	0.059
Brown-headed cowbird	12.742	-0.070	0.048	0.049	0.057	0.060	0.056	0.059
Boreal owl	4.402	-0.010	-0.003	0.002	0.006	0.005	0.006	0.006
Canadian toad	7.137	-0.013	-0.008	-0.002	0.006	0.005	0.005	0.005
Clay-coloured sparrow	13.321	-0.077	0.038	0.037	0.058	0.063	0.059	0.064
Cape-may warbler	9.646	-0.059	-0.023	0.009	0.034	0.043	0.035	0.037
Common raven	2.886	-0.022	-0.005	0.011	0.014	0.015	0.018	0.016
Dark-eyed junco	9.096	-0.051	-0.004	0.025	0.037	0.038	0.031	0.038
Great gray owl	5.761	-0.009	-0.002	0.004	0.004	0.002	0.004	0.004
Long-eared owl	3.687	-0.006	-0.005	0.001	0.001	0.001	0.002	0.001
Lincoln's sparrow	14.717	-0.078	0.050	0.054	0.066	0.067	0.062	0.065
Northern saw-whet owl	5.086	-0.011	-0.009	0.004	0.004	0.006	0.005	0.004

Olive-sided flycatcher	6.140	-0.027	0.011	0.013	0.016	0.015	0.015	0.018
Ovenbird	8.929	-0.056	0.029	0.021	0.044	0.044	0.040	0.046
Pine siskin	4.816	-0.044	0.005	0.014	0.029	0.031	0.025	0.029
Rose-breasted grosbeak	5.779	-0.023	0.000	0.010	0.013	0.011	0.015	0.016
Red-breasted nuthatch	2.119	-0.014	-0.011	0.003	0.006	-0.003	0.005	0.008
Tennessee warbler	7.327	-0.048	0.008	0.031	0.030	0.037	0.033	0.032
Warbling vireo	9.660	-0.052	0.025	0.025	0.032	0.040	0.036	0.040
Western toad	7.931	-0.014	-0.012	0.002	0.008	0.005	0.007	0.009
White-throated sparrow	1.705	-0.021	-0.007	0.005	0.011	0.008	0.002	0.013
Yellow rail	10.364	-0.069	0.019	0.010	0.042	0.047	0.053	0.053

Variable	Conifer Forest	Wind*Conifer Forest	Deciduous Forest	Wind*Deciduous Forest	Forest Edge	Wind*Forest Edge	Graminoid Fen	Wind*Graminoid Fen
1000 Hz	-0.154	2.124	-0.177	0.147	0.487	0.351	2.859	0.356
1414 Hz	1.243	2.812	-1.467	0.574	0.076	0.406	1.774	0.380
2000 Hz	1.419	1.661	-0.737	0.233	2.729	-0.010	4.080	-0.044
2828 Hz	-0.510	1.306	-1.038	0.386	1.956	-0.287	2.775	-0.250
4000 Hz	0.566	0.981	0.805	0.016	2.632	-0.521	6.435	-0.671
5656 Hz	-2.469	-0.583	-2.722	-0.330	0.126	-1.035	1.531	-1.564
Barred owl	0.249	1.434	-0.193	0.269	0.746	0.442	2.093	-0.121
Black-and-white warbler	2.270	-1.860	4.426	-0.691	0.382	-1.328	2.354	-1.563
Bay-breasted warbler	-9.486		-7.425		-9.014		-10.946	
Belted kingfisher	-4.629	-1.232	-7.645	0.292	-7.416	-0.031	-5.896	-0.347
Brown-headed cowbird	-7.874	-0.244	-8.043	-0.328	-6.776	-0.775	-6.335	-0.994
Boreal owl	0.847	2.607	0.456	-0.009	-1.684	0.539	0.217	0.331
Canadian toad	2.120		1.784		0.315		1.019	

Clay-coloured sparrow	-5.460	-0.822	-5.144	-0.192	-5.501	-1.117	-4.337	-1.527
Cape-may warbler	2.875	-1.544	-1.699	0.496	-2.608	-0.131	-3.849	-0.105
Common raven	1.871	2.700	-1.295	-0.009	0.280	-0.324	-0.138	-0.497
Dark-eyed junco	1.142	-1.082	-3.483	-0.501	-2.508	-1.078	-3.044	-0.913
Great gray owl	0.628	2.246	-0.641	0.351	0.185	0.488	2.601	-0.177
Long-eared owl	1.313	1.870	0.211	0.445	1.009	0.652	0.679	0.327
Lincoln's sparrow	-8.387		-9.293		-10.129		-9.906	
Northern saw-whet owl	2.564	3.603	-0.236	0.055	1.136	0.100	0.554	0.003
Olive-sided flycatcher	-1.831	0.517	-1.989	-0.287	-0.171	-0.560	1.294	-0.494
Ovenbird	-4.716		-2.732		-5.582		-4.917	
Pine siskin	-0.832		-1.975		-2.746		-3.354	
Rose-breasted grosbeak	0.672	1.208	-1.732	-0.267	0.984	-0.710	2.207	-0.719
Red-breasted nuthatch	3.780	3.163	0.284	-0.087	1.685	-0.514	9.133	-1.039
Tennessee warbler	-0.972	-1.227	-4.324	-0.037	-1.858	-0.541	-2.769	-0.530
Warbling vireo	-3.866	-0.097	-3.555	-0.271	-1.613	-0.462	-2.584	-0.840
Western toad	1.462	2.433	0.704	-0.949	-0.719	0.067	3.590	-0.525
White-throated sparrow	2.936	0.651	-0.745	-0.316	0.370	-1.058	3.449	-1.397
Yellow rail	-2.208		-1.322		-3.404		-3.281	

Variable	**Grassland**	**Wind*Grassland**	**Road**	**Wind*Road**	**Humidity**	**Temperature**	**Wind**
1000 Hz	-1.301	0.534	0.851	0.615		-0.100	-0.599
1414 Hz	0.872	0.380	-0.210	0.613	0.041		-0.475
2000 Hz	1.742	-0.019	1.602	0.226	0.034		-0.035
2828 Hz	3.308	-0.133	0.391	0.246		-0.048	0.050
4000 Hz	3.589	-0.287	3.669	-0.373			0.314
5656 Hz	5.735	-0.942	0.134	-0.681	0.024	0.086	0.782
Barred owl	-0.423	0.183	0.859	0.532		-0.083	-0.259

Black-and-white warbler	0.866	-0.843	-0.837	-0.669	0.039	0.085	0.811
Bay-breasted warbler	-6.765		-8.451				
Belted kingfisher	-6.041	0.117	-8.257	0.439			-0.204
Brown-headed cowbird	-6.551	-0.395	-8.289	-0.373			0.366
Boreal owl	-0.965	0.379	-0.408	0.474	0.022	-0.051	-0.420
Canadian toad	1.038		1.316			-0.117	-0.130
Clay-coloured sparrow	-6.778	-0.533	-8.280	-0.370			0.496
Cape-may warbler	-3.710	0.376	-3.876	0.501			-0.437
Common raven	-1.501	-0.200	-1.287	0.137	0.038		0.067
Dark-eyed junco	-0.634	-0.558	-3.679	-0.360			0.469
Great gray owl	-1.314	0.411	0.458	0.463		-0.087	-0.413
Long-eared owl	-0.864	0.455	0.976	0.838	0.017	-0.076	-0.543
Lincoln's sparrow	-7.735		-8.781				
Northern saw-whet owl	0.168	0.185	0.751	0.490		-0.062	-0.186
Olive-sided flycatcher	0.781	-0.243	-1.178	-0.059			0.278
Ovenbird	-3.222		-5.903		0.025		
Pine siskin	0.208		-1.817		0.027	0.064	
Rose-breasted grosbeak	-0.237	-0.316	-0.311	-0.332			0.301
Red-breasted nuthatch	3.510	-0.441	0.849	-0.290	0.022		0.395
Tennessee warbler	-2.908	-0.026	-2.749	0.044			0.048
Warbling vireo	-3.743	0.004	-4.829	0.095			0.151
Western toad	-0.612	0.197	-1.084	0.424		-0.144	-0.281
White-throated sparrow	6.467	-1.033	0.119	-0.941	0.039	0.065	1.001
Yellow rail	-5.503		-5.099			-0.068	

Table 4. Commonality coefficients and % total variation reporting unique variation explained by each predictor variable and shared variation for combinations of independent predictors.

Variables	Coefficient	% Total Variation
Distance	0.342	0.653
Vegetation	0.044	0.083
Wind	0.001	0.001
Minimum Frequency	0.034	0.066
Bandwidth	0.053	0.101
Humidity	0.001	0.002
Temperature	0.000	0.000
Distance,Vegetation	0.010	0.019
Distance,Wind	0.006	0.011
Vegetation,Wind	0.001	0.001
Distance,Minimum Frequency	0.000	0.000
Vegetation,Minimum Frequency	0.000	0.001
Wind,Minimum Frequency	0.000	0.000
Distance,Bandwidth	0.000	0.000
Vegetation,Bandwidth	0.000	0.000
Wind,Bandwidth	0.000	0.000
Minimum Frequency,Bandwidth	-0.010	-0.020
Distance,Humidity	0.017	0.032
Vegetation,Humidity	0.000	-0.001
Wind,Humidity	0.000	0.000
Minimum Frequency,Humidity	0.000	0.000
Bandwidth,Humidity	0.000	0.000
Distance,Temperature	0.000	0.000
Vegetation,Temperature	0.002	0.004
Wind,Temperature	0.000	0.000
Minimum Frequency,Temperature	0.000	0.000
Bandwidth,Temperature	0.000	0.000
Humidity,Temperature	0.003	0.006
Distance,Vegetation,Wind	-0.007	-0.014
Distance,Vegetation,Minimum Frequency	0.000	0.000
Distance,Wind,Minimum Frequency	0.000	0.000
Vegetation,Wind,Minimum Frequency	0.000	0.000
Distance,Vegetation,Bandwidth	0.000	0.000
Distance,Wind,Bandwidth	0.000	0.000
Vegetation,Wind,Bandwidth	0.000	0.000
Distance,Minimum Frequency,Bandwidth	0.000	0.000
Vegetation,Minimum Frequency,Bandwidth	0.000	0.000

Wind,Minimum Frequency,Bandwidth	0.000	0.000
Distance,Vegetation,Humidity	-0.001	-0.001
Distance,Wind,Humidity	0.002	0.003
Vegetation,Wind,Humidity	0.000	-0.001
Distance,Minimum Frequency,Humidity	0.000	0.000
Vegetation,Minimum Frequency,Humidity	0.000	0.000
Wind,Minimum Frequency,Humidity	0.000	0.000
Distance,Bandwidth,Humidity	0.000	0.000
Vegetation,Bandwidth,Humidity	0.000	0.000
Wind,Bandwidth,Humidity	0.000	0.000
Minimum Frequency,Bandwidth,Humidity	0.000	0.000
Distance,Vegetation,Temperature	0.001	0.002
Distance,Wind,Temperature	0.000	0.000
Vegetation,Wind,Temperature	0.002	0.004
Distance,Minimum Frequency,Temperature	0.000	0.000
Vegetation,Minimum Frequency,Temperature	0.000	0.000
Wind,Minimum Frequency,Temperature	0.000	0.000
Distance,Bandwidth,Temperature	0.000	0.000
Vegetation,Bandwidth,Temperature	0.000	0.000
Wind,Bandwidth,Temperature	0.000	0.000
Minimum Frequency,Bandwidth,Temperature	0.000	0.000
Distance,Humidity,Temperature	0.021	0.040
Vegetation,Humidity,Temperature	0.002	0.003
Wind,Humidity,Temperature	0.000	0.000
Minimum Frequency,Humidity,Temperature	0.000	0.000
Bandwidth,Humidity,Temperature	0.000	0.000
Distance,Vegetation,Wind,Minimum Frequency	0.000	0.000
Distance,Vegetation,Wind,Bandwidth	0.000	0.000
Distance,Vegetation,Minimum Frequency,Bandwidth	0.000	0.000
Distance,Wind,Minimum Frequency,Bandwidth	0.000	0.000
Vegetation,Wind,Minimum Frequency,Bandwidth	0.000	0.000
Distance,Vegetation,Wind,Humidity	0.000	-0.001
Distance,Vegetation,Minimum Frequency,Humidity	0.000	0.000
Distance,Wind,Minimum Frequency,Humidity	0.000	0.000
Vegetation,Wind,Minimum Frequency,Humidity	0.000	0.000
Distance,Vegetation,Bandwidth,Humidity	0.000	0.000
Distance,Wind,Bandwidth,Humidity	0.000	0.000
Vegetation,Wind,Bandwidth,Humidity	0.000	0.000
Distance,Minimum Frequency,Bandwidth,Humidity	0.000	0.000
Vegetation,Minimum Frequency,Bandwidth,Humidity	0.000	0.000
Wind,Minimum Frequency,Bandwidth,Humidity	0.000	0.000
Distance,Vegetation,Wind,Temperature	-0.001	-0.003
Distance,Vegetation,Minimum Frequency,Temperature	0.000	0.000

Distance,Wind,Minimum Frequency,Temperature	0.000	0.000
Vegetation,Wind,Minimum Frequency,Temperature	0.000	0.000
Distance,Vegetation,Bandwidth,Temperature	0.000	0.000
Distance,Wind,Bandwidth,Temperature	0.000	0.000
Vegetation,Wind,Bandwidth,Temperature	0.000	0.000
Distance,Minimum Frequency,Bandwidth,Temperature	0.000	0.000
Vegetation,Minimum Frequency,Bandwidth,Temperature	0.000	0.000
Wind,Minimum Frequency,Bandwidth,Temperature	0.000	0.000
Distance,Vegetation,Humidity,Temperature	0.005	0.009
Distance,Wind,Humidity,Temperature	-0.001	-0.002
Vegetation,Wind,Humidity,Temperature	0.001	0.001
Distance,Minimum Frequency,Humidity,Temperature	0.000	0.000
Vegetation,Minimum Frequency,Humidity,Temperature	0.000	0.000
Wind,Minimum Frequency,Humidity,Temperature	0.000	0.000
Distance,Bandwidth,Humidity,Temperature	0.000	0.000
Vegetation,Bandwidth,Humidity,Temperature	0.000	0.000
Wind,Bandwidth,Humidity,Temperature	0.000	0.000
Minimum Frequency,Bandwidth,Humidity,Temperature	0.000	0.000
Distance,Vegetation,Wind,Minimum Frequency,Bandwidth	0.000	0.000
Distance,Vegetation,Wind,Minimum Frequency,Humidity	0.000	0.000
Distance,Vegetation,Wind,Bandwidth,Humidity	0.000	0.000
Distance,Vegetation,Minimum Frequency,Bandwidth,Humidity	0.000	0.000
Distance,Wind,Minimum Frequency,Bandwidth,Humidity	0.000	0.000
Vegetation,Wind,Minimum Frequency,Bandwidth,Humidity	0.000	0.000
Distance,Vegetation,Wind,Minimum Frequency,Temperature	0.000	0.000
Distance,Vegetation,Wind,Bandwidth,Temperature	0.000	0.000
Distance,Vegetation,Minimum Frequency,Bandwidth,Temperature	0.000	0.000
Distance,Wind,Minimum Frequency,Bandwidth,Temperature	0.000	0.000
Vegetation,Wind,Minimum Frequency,Bandwidth,Temperature	0.000	0.000
Distance,Vegetation,Wind,Humidity,Temperature	0.000	-0.001
Distance,Vegetation,Minimum Frequency,Humidity,Temperature	0.000	0.000
Distance,Wind,Minimum Frequency,Humidity,Temperature	0.000	0.000
Vegetation,Wind,Minimum Frequency,Humidity,Temperature	0.000	0.000
Distance,Vegetation,Bandwidth,Humidity,Temperature	0.000	0.000
Distance,Wind,Bandwidth,Humidity,Temperature	0.000	0.000
Vegetation,Wind,Bandwidth,Humidity,Temperature	0.000	0.000
Distance,Minimum Frequency,Bandwidth,Humidity,Temperature	0.000	0.000
Vegetation,Minimum Frequency,Bandwidth,Humidity,Temperature	0.000	0.000
Wind,Minimum Frequency,Bandwidth,Humidity,Temperature	0.000	0.000
Distance,Vegetation,Wind,Minimum Frequency,Bandwidth,Humidity	0.000	0.000
Distance,Vegetation,Wind,Minimum Frequency,Bandwidth,Temperature	0.000	0.000
Distance,Vegetation,Wind,Minimum Frequency,Humidity,Temperature	0.000	0.000
Distance,Vegetation,Wind,Bandwidth,Humidity,Temperature	0.000	0.000

Distance,Vegetation,Minimum Frequency,Bandwidth,Humidity,Temperature	0.000	0.000
Distance,Wind,Minimum Frequency,Bandwidth,Humidity,Temperature	0.000	0.000
Vegetation,Wind,Minimum Frequency,Bandwidth,Humidity,Temperature	0.000	0.000
Distance,Vegetation,Wind,Minimum Frequency,Bandwidth,Humidity,Temperature	0.000	0.000

Appendix 4

Appendix 4.1 – Detailed calibration data collection materials & methods

Ovenbird

See Wilson and Bayne 2018.

Common Nighthawk

We collected acoustic recordings of Common Nighthawks (*Chordeiles minor*) with known locations by attracting male Common Nighthawks to the beginning of a transect of ARUs using conspecific broadcast calls. An observer stood at the beginning of the transect and recorded the time stamp, height, horizontal distance, and bearing of every vocalization from the target individual. We subsequently excluded all detections greater than 20 m in horizontal distance from the observer to minimize any observer bias in distance estimation. We collected recordings at eight transects between July 13 and July 20, 2016, starting at 1 hour before sunset and ending at sunset, when Common Nighthawks are most active. Each transect consisted of 15 ARUs placed at standardized distances along a linear feature (Fig. 3) and we played an airhorn at the start of the recording period from the beginning of the transect. Following acoustic data collection, we clipped each of the recordings at the airhorn to synchronize them. Next, we visually confirmed the timestamp of each vocalization of the target individual and identified any vocalizations that were masked by the broadcast call. We then used the seewave package (Sueur, Aubin & Simonis 2008) in R to clip each unmasked detection from each of the 17 recordings along the transect as 0.7 s clips for further RSL measurement.

Site Selection

We selected transects within a study area north of Fort McMurray, Alberta, Canada where Common Nighthawks are known to be abundant. The study area was at the southern extent of the Athabasca Plain jack pine (*Pinus banksia*) forest that was burned in 2011. The resultant vegetation was a forested matrix containing a mix of clear cuts, jack pine forest, fallen burned pines, and standing burned snags, with regenerating jack pine saplings distributed throughout. The study area was accessible by vehicle on non-paved roads, and was subject to other anthropogenic influence including clearcuts, water and transmission lines, and open-pit bitumen mines.

We determined the starting point for each transect (n = 8) by observing territorial male Common Nighthawks and selecting those that responded aggressively to conspecific broadcast calls of vocalizations and mechanical wingboom sounds. Reconnaissance was conducted along non-paved roads within the study area.

Acoustic Data Collection

We collected recordings of Common Nighthawks with known distances by attracting the territorial male Common Nighthawk to the first ARU at each transect with the same conspecific broadcast call of vocalizations and mechanical wingboom sounds. Each transect comprised 15 ARUs placed at standardized distances along a non-paved road. Along each transect, we placed the ARUs at 0 m, 30 m, 60 m, 90 m, 120 m, 150 m, 180 m, 210 m, 240 m, 300 m, 400 m, 500 m, 600 m, 700 m, and 800 m from the broadcast call. We confirmed the distances between ARUs to the nearest metre by seeking agreement between a hand-held GPS and a laser range-finder. We used Song Meter SM4 ARUs (Wildlife Acoustics Inc.) to collect the recordings and time-synchronized each unit to ± 1 s with a Garmin GPS extension. Recordings had a 48 kHz sampling rate and a 16 bit depth.

We collected hour-long recordings starting at 30 minutes before sunset and ending 30 minutes after sunset, when Common Nighthawks are most vocally active. We played an airhorn at the beginning of the recording session to ensure the recordings could be synced for analysis. A single observer was stationed at the beginning of the transect to observe each vocalization of the target individual because there were other Common Nighthawks vocalizing during the recording session at each transect. The observer collected observations of each vocalization that the target nighthawk emitted within 20 horizontal metres of the broadcast call. The observer time-stamped each observed vocalization using the ClikTrack app on an iPhone 5 so that we could identify that vocalization within the recordings during processing. The observer also estimated the vertical and horizontal distance of the target nighthawk for each observed vocalization so that we could correct the known distances of each recording for the position of the target individual. The observer calibrated their vertical distance estimations at the beginning of each recording session by measuring the vertical height to the target Common Nighthawk with a laser-range finder. The observer similarly calibrated their horizontal distance estimations by measuring the horizontal height to various objects in the nearby area with a laser-range finder. All observations were collected by a single observer.

Acoustic Localization

We collected acoustic recordings of Common Nighthawks with known locations by attracting male Common Nighthawks to the beginning of a transect of ARUs using conspecific broadcast calls. An observer stood at the beginning of the transect and recorded the time stamp, height, horizontal distance, and bearing of every vocalization from the target individual relative to the first ARU (0 m). We subsequently excluded all detections greater than 20 m in horizontal distance from the observer to minimize any observer bias in distance estimation. We collected recordings at eight transects between July 13 and July 20, 2016, starting at 1 hour before sunset and ending at sunset, when Common Nighthawks are most active. Each transect consisted of 15 ARUs placed at standardized distances along a linear feature (Fig. 3) and we played an airhorn at the start of the recording period from the beginning of the transect. Following acoustic data collection, we clipped each of the recordings at the airhorn to synchronize them and remove the time it took for sound to travel to each ARU. Next, we visually confirmed the timestamp of each vocalization of the target individual and identified any vocalizations that were masked by the broadcast call. In total, we selected 100 vocalizations for localization. We then used the seewave package (Sueur, Aubin & Simonis 2008) in R to clip each unmasked detection from the full length recording to a 0.7 s long clip. Finally, we corrected the distance of each clip for the position of the target bird by calculating the Euclidean distance between the bird’s location and the ARU. The resultant dataset comprised 1500 0.7 s clips of Common Nighthawk calls at a known distance with approximately 5-10 m of human surveyor error.

References

Sueur J., T. Aubin, and C. Simonis. 2008. Seewave: a free modular tool for sound analysis and synthesis. *Bioacoustics*. 18: 213-226. doi: 10.1080/09524622.2008.9753600

Appendix 4.2 – Detailed recognizer training and automated relative sound level (RSL) estimation

We down-sampled audio files to 22050 Hz for efficient processing and high-pass filtered the files to remove low frequency noise. We then calculated spectrograms using the short-time Fourier transform (STFT) and converted sound power to decibel (dB) units. We extracted a time series of sound power estimates from the spectrograms by taking the maxima along the first axis, resulting in a single value for each column in a given spectrogram. We then down-sampled the time series by max-pooling (segmenting the time series into non-overlapping blocks and retaining the max value in each block) to match the sampling rate of the CNN recognizer output. Each detection made by the recognizer therefore had an associated estimate of the local sound power. We conducted RSL analysis in Python (van Rossum 1995) version 3.5, using librosa (McFee et al. 2017) for audio loading and spectrogram generation, and scipy (Jones et al. 2001) for signal filtering.

Automated audio processing parameters

Audio sample rate: 22050 Hz

Audio filtering: high-pass 4th-order digital Butterworth filter, cutoff frequency 1 kHz

STFT: FFT window size 128 samples, 50% window overlap, blackman window function

Max-pooling block size: 16

Score threshold: 0.01

References

Jones, E., T. Oliphant, P. Peterson, et al. SciPy: Open source scientific tools for Python. 2001. URL http://www.scipy.org/. [Online; accessed 2017-06-14]

McFee, B., M. McVicar, O. Nieto, S. Balke, C. Thome, D. Liang, E. Battenberg, … H. Lee. 2017. “librosa 0.5.0”, Zenodo. Available at https://doi.org/10. 5281/zenodo.293021.

van Rossum, G. 1995. Python tutorial, Technical Report CS-R9526, Centrum voor Wiskunde en Informatica (CWI), Amsterdam.

Appendix 4.3 - Model selection for GLMs predicting distance.

Table 3.1. Candidate model parameters. RSL refers to relative sound level, Vertical to the vertical height of the individual (m), and Sunset to the time after sunset (min).

Dataset	Model	Parameters
OVEN Manual	Null	$RSL + RSL^2$
	Log	log(RSL)
	R+T	$RSL + RSL^2$ + Time
OVEN Recognizer	Null	$RSL + RSL^2$
	R+Sc	$RSL + RSL^2$ + Score
	R+Sc+T	$RSL + RSL^2$ + Score + Time
	R+T	$RSL + RSL^2$ + Time
CONI Manual	R+V+Snt	$RSL + RSL^2$ + Vertical + Sunset
	R+V	$RSL + RSL^2$ + Vertical
	R+Snt	$RSL + RSL^2$ + Sunset
	Log	log(RSL)
	Null	$RSL + RSL^2$
CONI Recognizer	Null	$RSL + RSL^2$
	R+ Sc	$RSL + RSL^2$ + Score
	R+V	$RSL + RSL^2$ + Vertical
	R+Snt	$RSL + RSL^2$ + Sunset
	R+Sc+V	$RSL + RSL^2$ + Score + Vertical
	R+Sc+Snt	$RSL + RSL^2$ + Score + Sunset
	R+V+Snt	$RSL + RSL^2$ + Vertical + Sunset
	R+Sc+V+Sn	$RSL + RSL^2$ + Score + Vertical + Sunset

Table 3.2. Model selection output. Models selected for use in analysis are in bold.

Dataset	Model	df	logLik	AIC_c	ΔAIC_c	AIC_w

OVEN Manual	R+T	6	-2692.95	5398.00	0.00	0.947
	Null	5	-2696.85	5403.80	5.77	0.053
	Log	4	-2849.48	5707.00	308.99	0.00
OVEN Recognizer	R+Sc+T	7	-2722.65	5459.50	0.00	1.00
	R+Sc	6	-2735.81	5483.70	24.27	0.00
	R+T	6	-2867.39	5746.90	287.44	0.00
	Null	5	-2872.95	5756.00	296.52	0.00
CONI Manual	R+V+Snt	6	-3971.70	7955.50	0.00	1.00
	R+V	5	-3987.71	7985.50	29.98	0.00
	R+Snt	5	-3992.58	7995.20	39.71	0.00
	Null	4	-4004.96	8018.00	62.44	0.00
	Log	3	-4043.15	8092.30	136.80	0.00
CONI Recognizer	R+Sc+Snt	6	-6576.14	13164.40	0.00	0.69
	R+Sc+V+Snt	7	-6575.95	13166.00	1.64	0.31
	R+Sc+V	6	-6583.59	13179.20	14.89	0.00
	R+Sc	5	-6587.49	13185.00	20.68	0.00
	R+Snt	5	-6592.29	13194.60	30.27	0.00
	R+V+Snt	6	-6592.04	13196.20	31.79	0.00
	R+V	5	-6597.81	13205.70	41.30	0.00
	Null	4	-6601.08	13210.20	45.84	0.00

Appendix 4.4 - Commonality analysis

Table 4.1. Results of commonality analysis. Total refers to partitioned contribution to total R^2 of model.

Dataset	Variables	Coefficient	Total
OVEN Manual	RSL	0.660	0.934
	Time	0.006	0.009
	RSL, Time	0.040	0.057
OVEN Recognizer	RSL	0.084	0.136
	Score	0.152	0.245
	Time	0.017	0.027
	RSL, Score	0.353	0.570
	RSL, Time	0.011	0.018
	Score, Time	-0.006	-0.010
	RSL, Score, Time	0.008	0.013
CONI Manual	RSL	0.639	0.990
	Sunset	0.023	0.036
	Vertical	0.017	0.026
	RSL, Sunset	-0.021	-0.032
	RSL, Vertical	-0.013	-0.021
	Sunset, Vertical	0.003	0.004
	RSL, Sunset, Vertical	-0.002	-0.004
CONI Recognizer	RSL	0.715	0.997
	Vertical	0.004	0.010
	RSL, Vertical	-0.002	-0.003

Appendix 4.5 - Intraclass correlation coefficients (ICC) for selecting random effects in GLMs

Table 5.1. Intraclass correlation coefficients (ICC) for selecting random effects in GLMs. Random effects included in final models highlighted in bold.

Species	Method	Transect	Station	Individual
OVEN	manual	-	**0.723**	0.104
	recognizer	-	**0.637**	0.074
CONI	manual	0.014	-	-
	recognizer	0.014	-	-

Appendix 4.6 - Distance sampling model selection.

Table 6.1. Candidate distance sampling models for OVEN known distances. Selected model is in bold.

Detection Function	Adjustment Term	AIC
Half Normal	**None**	**2891.977**
Uniform	Cosine	2892.099
Hazard Rate	Cosine	2895.905
Hazard Rate	Polynomial	2895.905

Table 6.2. Candidate distance sampling models for OVEN manual measurements. Selected model is in bold.

Detection Function	Adjustment Term	AIC_c
Half Normal	**Cosine**	**4022.527**
Half Normal	Polynomial	4024.205
Uniform	Cosine	4023.195
Hazard Rate	Cosine	4026.08
Hazard Rate	Polynomial	4025.2

Table 6.3. Candidate distance sampling models for OVEN recognizer measurements. Selected model is in bold.

Detection Function	Adjustment Term	AIC_c
Half Normal	**Cosine**	**4103.783**
Half Normal	Polynomial	4111.829
Uniform	Cosine	4105.862

Hazard Rate	Cosine	4107.048
Hazard Rate	Polynomial	4105.116

Table 6.4. Candidate distance sampling models for OVEN human error predicted distances. Selected model is in bold.

Detection Function	Adjustment Term	AIC
Half Normal	**None**	**2819.015**
Uniform	Cosine	2846.84
Hazard Rate	Cosine	2821.145
Hazard Rate	Polynomial	2824.815

Table 6.5. Candidate distance sampling models for CONI known distances. Selected model is in bold.

Detection Function	Adjustment Term	AIC
Half Normal	**None**	**20956.791**
Uniform	Cosine	20976.499
Hazard Rate	Cosine	20958.961
Hazard Rate	Polynomial	20960.614

Table 6.6. Candidate distance sampling models for CONI manual measurements. Selected model is in bold.

Detection Function	Adjustment Term	AIC_c
Half Normal	Cosine	32166.021
Half Normal	Polynomial	32172.993

Uniform	Cosine	32167.368
Hazard Rate	**Cosine**	**32165.481**
Hazard Rate	Polynomial	32169.966

Table 6.7. Candidate distance sampling models for CONI recognizer measurements. Selected model is in bold.

Detection Function	Adjustment Term	AIC_c
Half Normal	Cosine	29059.706
Half Normal	Polynomial	29059.861
Uniform	Cosine	29060.213
Hazard Rate	**Cosine**	**29059.564**
Hazard Rate	Polynomial	29060.834

Table 6.8. Candidate distance sampling models for CONI human error predicted distances. Selected model is in bold.

Detection Function	Adjustment Term	AIC
Half Normal	**None**	**18179.814**
Uniform	Cosine	18231.291
Hazard Rate	Cosine	18246.8
Hazard Rate	Polynomial	18192.598

Appendix 4.7 - Model Coefficients for GLMs predicting distance.

Table 7.1. Model coefficients (± SE) from the top selected model for each dataset. RSL refers to relative sound level, Vertical to vertical height (m), and Sunset to time after sunset (min).

Model	Intercept	RSL	RSL^2	Score	Vertical	Time	Sunset
OVEN Manual	4.394 ± 0.039	-0.354 ± 0.010	-0.091 ± 0.006			-0.016 ± 0.006	
OVEN CNN	4.299 ± 0.042	-0.147 ± 0.009	-0.047 ± 0.006	-0.168 ± 0.009		-0.039 ± 0.007	
CONI Manual	4.924 ± 0.022	-0.724 ± 0.035	-0.150 ± 0.022		0.093 ± 0.014		-0.084 ± 0.014
CONI CNN	4.841 ± 0.015	-0.749 ± 0.023	-0.100 ± 0.012	0.047 ± 0.008			0.042 ± 0.009

Appendix 4.8 - Distance estimation error and post-hoc comparisons.

Table 8.1. One sample t-tests to test for significant deviation of error from zero.

Species/Method	One sample t-test (Error Bias)				One sample t-test (Absolute)			
	t	df	p	cohen’s *d*	t	df	p	cohen’s *d*
OVEN Manual	8.140	690	1.84E-15	0.310	31.548	690	2.20E-16	1.200
OVEN Recognizer	6.324	672	4.66E-10	0.244	33.4247	672	2.20E-16	1.288
CONI Manual	-0.133	715	0.894	-0.005	30.935	715	2.20E-16	1.167
CONI Recognizer	0.252	1222	0.801	0.007	35.503	1222	2.20E-16	0.985

Table 8.2. Two sample t-tests to test for significant differences between RSL measurement methods.

Species/Method	Two-sample t-test (Absolute)				Two-sample t-test (Error Bias)			
	t	df	p	cohen’s *d*	t	df	p	cohen’s *d*
OVEN Manual OVEN Recognizer	1.346	1347.8	0.179	0.073	-1.572	1359.5	0.116	0.085
CONI Manual CONI Recognizer	5.339	1417.4	1.09E-07	0.253	-0.250	1315.9	0.803	0.012